

Comparative Study On Optimum Shear Wall Contribution in Design at Eighteen Storeyed Reinforce Concrete Residential Building

Kyaw Naing⁽¹⁾, Sunday Aung⁽²⁾

⁽¹⁾Technological University (Lashio), Myanmar

⁽²⁾Technological University (Lashio), Myanmar

Email: kyawnaing.civil@gmail.com, usundayaung@gmail.com

ABSTRACT: Multistorey buildings are the symbols of a modernized living standard because of the population growth. South East Asia including Myanmar is situated in secondary seismic belt. Therefore, it is necessary to pay special attention to the effect of earthquake in designing the high-rise building.

Shear walls are very common in high-rise reinforced concrete building. In this study, comparative study of shear wall contribution for eighteen-storeyed reinforced concrete building are present. It belongs to seismic zone 2A. This is why, seismic forces are essentially considered in the design of this building and shear walls are also considered to resist seismic forces.

Structural analysis is done by using ETABS software. Load consideration is based on UBC-1997. All necessary load combinations are considered in shear walls analysis and frame analysis. In addition to this study gravity load and lateral load are considered. Design of structural elements are calculated by using the provision of American Concrete Institute (ACI 318-99) code.

The selected building with seven different locations of shear walls are analyzed and checked for stability. Then eccentricity required steel area and allowable values for torsional irregularity, overturning and sliding are compared to point out the best location of shear wall. Design results are checked for safety, economy and serviceability by checking in P- Δ effect, storey drift, structural irregularity, sliding and overturning.

KEYWORDS: Gravity load and lateral load, ETABS Software, Eighteen-Storey Building, Planar Shear Wall, Regular Shape, ACI 318-99, UBC-97.

1. INTRODUCTION

According to social and economical demands, presently, Yangon, needs various types of tall buildings. These buildings are the solutions to the problem of living population growth. Because they form distinctive landmarks, tall buildings are frequently developed in central business zone as prestige symbols for corporate organization. The feasibility and desirability of high-rise structure have always depended on the available materials, the level of construction technology, and the state of development of the services necessary for the use of the building. It is important to ensure adequate stiffness to resist lateral forces induced by wind or seismic or blast effects. These forces can develop high

stresses, and produce, way moment or vibration. Concrete walls, which have high in-plane stiffness placed at convenient locations, are often economically used to provide the necessary resistance to horizontal forces. This type of wall is called a shear wall.

To obtain the required stiffness and strength to withstand lateral load in high-rise building, shear walls are normally included some frames of the building. They are continuous down to the base to which they are rigidly attached to form vertical cantilever. The positions of shear walls within a building are dictated by functional requirements. They may or may not suit structural planning. Building sites, architectural interests may lead, on the other hand, to positions of walls that one undesirable from a structural point of view. Hence, structural designers will often be in the position desirable locations for shear wall in order to optimize lateral force resistance. Shear wall are efficient, both in terms of construction cost and effectiveness in minimizing earthquake damage in structural and non- structural

2. THEORETICAL BACKGROUND

2.1 Scope of the Study

The scope of the study is defined as follows:

1. The proposed building is eighteen storied R.C.C building in seismic zone 2A.
2. Only planar shear walls are considered
3. Structural analysis and design are to be done by ETABS.
4. Load consideration is based on UBC Code (1997).
5. Structural elements are designed according to ACI-318-99.

2.2 Material Properties of the Structure

Material properties used in this structure are; weight per unit volume (R.C); $w = 150 \text{ lb/ft}^3$, concrete strength $f_c' = 3 \text{ ksi}$; reinforced yield strength = 50 ksi, Poisson's ratio = 0.175.

2.3 Loading

- | | |
|--------------------------|--------------------------|
| (1) Dead load | |
| Unit weight of concrete | = 150 lb/ft ³ |
| 4½" thick wall weight | = 55 lb/ft ² |
| 9" thick wall weight | = 100 lb/ft ² |
| Ceiling weight | = 25 lb/ft ² |
| Floor finishing | = 10 lb/ft ² |
| (2) Live load | |
| Live load on residential | = 40 lb/ft ² |

- Live load on roof = 20 lb/ft²
- (3) Wind load
 - Exposure type = Type C
 - Basic wind velocity = 80 mph
 - Important factor = 1
 - Windward coefficient = 0.8
 - Leeward coefficient = 0.5
- (4) Earthquake load
 - Seismic zone = zone 2A (Yangon)
 - Zone factor (Z) = 0.15
 - Soil type = S_D
 - Importance factor (I) = 1.0
 - Response modification factor (R) = 6.5
 - Seismic coefficient (C_a) = 0.22 N_a
 - Seismic coefficient (C_v) = 0.32 N_v
 - Near source factor (N_a) = 1.0
 - Near source factor (N_v) = 1.0
 - seismic source type = A

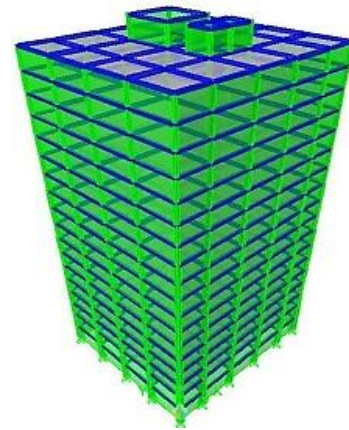


Fig 2. Three-Dimensional Proposed Building

3. ANALYSIS AND DESIGN

The selected structure is eighteen-storeyed reinforced concrete building. The building is located in Seismic Zone 2A. It is analyzed to meet the requirements of the Uniform Building Code (UBC), 1997. The building is symmetric about both principal plan axes. In this building, dual system is used for resistance to gravity and lateral loads.

3.1 Modeling of Non- Shear Wall Structure

An eighteen- storeyed R.C building is chosen for the analysis. The height of the base and story 2 are 12 feet. Other stories are 10 feet high. Total height is 194 feet. The building is located in the UBC seismic Zone 2A. It is analyzed by the using ETABS software. After analyzing structure, storey drift of the structure must be checked. Some storey drift are exceed the drift limitation value. Hence the structure is not stable and shear wall must be provided for the structure. Floor plan and three-dimensional proposed building of the selected model are shown in Fig. 1 and Fig. 2. Check for storey drift is as shown in Table 1.

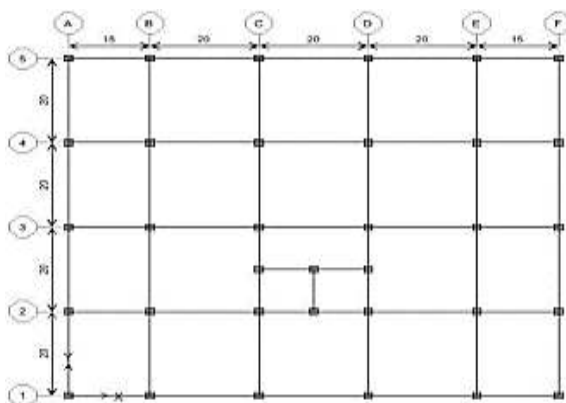


Fig 1. Plan of the selected model

Table 1. Check for Storey Drift of Non-Shear Wall Structure

Storey	Height (in)	Drift ratio X	Drift ratio Y	Δ _{sx} (in)	Δ _{sv} (in)	Δ _{mx} (in)	Δ _{my} (in)	Δ _{limit} (in)
roof	120	0.0012	0.0011	0.1520	0.1359	0.9046	0.8089	2.4
18	120	0.0014	0.0013	0.1686	0.1552	1.0031	0.9239	2.4
17	120	0.0014	0.0013	0.1686	0.1552	1.0031	0.9239	2.4
16	120	0.0019	0.0018	0.2389	0.2251	1.4215	1.3394	2.4
15	120	0.0009	0.0019	0.2518	0.2371	1.4986	1.4108	2.4
14	120	0.0035	0.0022	0.2825	0.2665	1.6807	1.5857	2.4
13	120	0.0026	0.0025	0.3149	0.2977	1.8735	1.7744	2.4
12	120	0.0027	0.0025	0.3271	0.3091	1.9463	1.8393	2.4
11	120	0.0029	0.0027	0.3540	0.3349	2.1063	1.9928	2.4
10	120	0.0031	0.0030	0.3823	0.3624	2.2748	2.1562	2.4
9	120	0.0032	0.0031	0.3942	0.3736	2.3455	2.2224	2.4
8	120	0.0034	0.0032	0.4172	0.3955	2.4826	2.3534	2.4
7	120	0.0036	0.0034	0.4398	0.4165	2.6168	2.4783	2.4
6	120	0.0037	0.0035	0.4446	0.4201	2.6454	2.4997	2.4
5	120	0.0037	0.0035	0.4446	0.4229	2.6454	2.5162	2.4
4	120	0.0038	0.0035	0.4522	0.4308	2.6904	2.5633	2.4
3	120	0.0037	0.0035	0.4446	0.4229	2.6454	2.5162	2.4
2	144	0.0034	0.0032	0.4809	0.4589	2.8617	2.7306	2.88
1	144	0.0016	0.0015	0.2321	0.2231	1.3812	1.3272	2.88

3.2 Member Sizes of Structure

- Column (up to 1st floor) - 26"×26"
- (1st floor to 4th floor) - 24" × 24"
- (4th floor to 7th floor) - 22" × 22"
- (7th floor to 10th floor) - 20" × 20"
- (10th floor to 13th floor) - 18" × 18"
- (13th floor to 16th floor) - 16" × 16"
- (16th floor to Roof floor) - 14" × 14"

Beam sizes – 10"×16", 10"×18",
12" ×18", 12" ×20"

Slab thickness - 4"

3.3 Modeling of Shear Wall Structure

In this study, the models are constructed with different contributions shear wall are used. The cross-sectional dimensions of beams, columns and slabs are the same with the previous non-shear wall structure except that of the beams connecting to the shear walls. The cross sections of the beams connecting to the shear walls are

taken as 12"×24". The material properties, loading and other data for wind and seismic forces are the same as the non-shear wall structure. The thickness of shear walls are:

- Shear walls (up to 1st floor) - 22"
- (1st floor to 4th floor) - 20"
- (4th floor to 7th floor) - 18"
- (7th floor to 10th floor) - 16"
- (10th floor to 13th floor) - 14"
- (13th floor to 16th floor) - 12"
- (16th floor to Roof floor) - 10"

3.4 Locations of Shear Wall Contribution

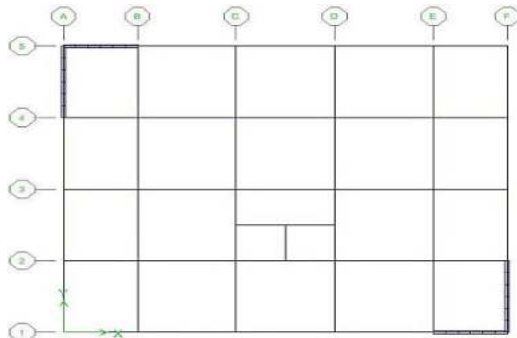


Fig 3. Model-1

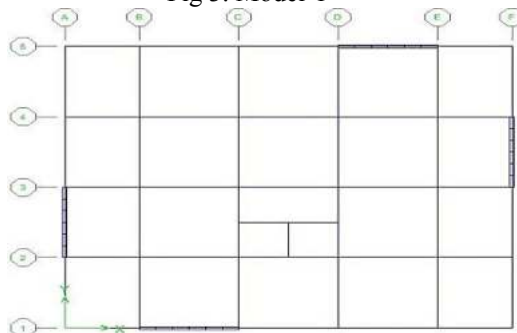


Fig 4. Model-2

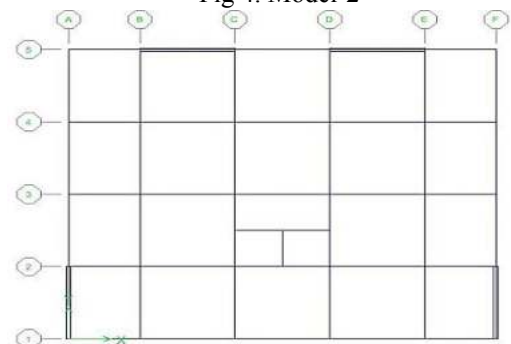


Fig 5. Model-3

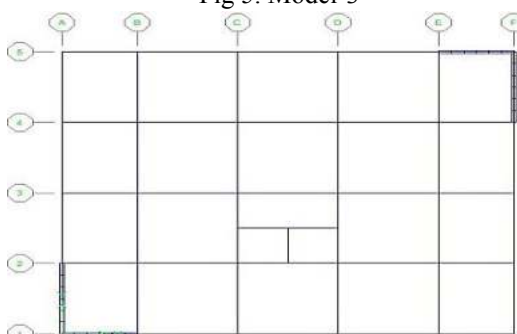


Fig 6. Model-4

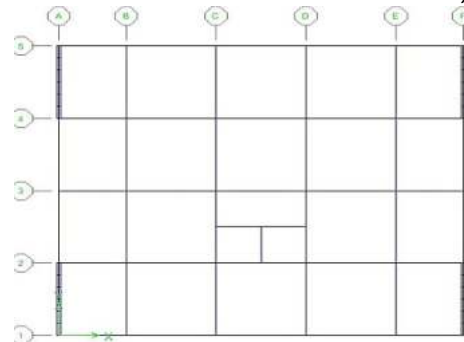


Fig 7. Model-5

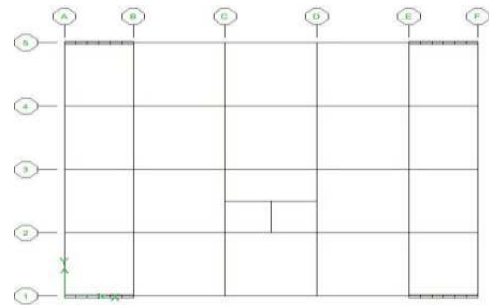


Fig 8. Model-6

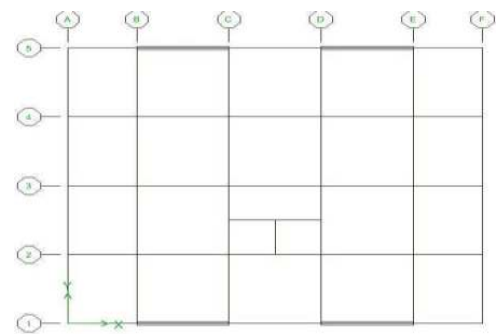


Fig 9. Model-7

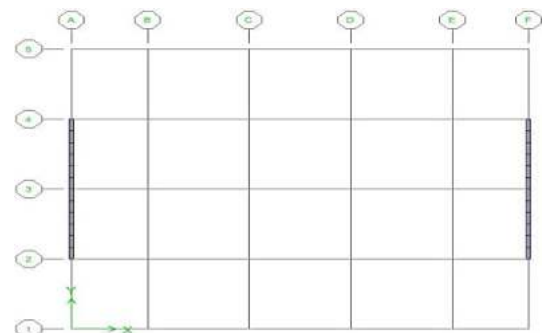


Fig 10. Model-8

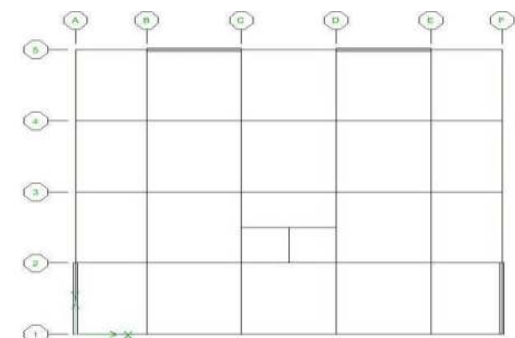


Fig 11. Model-9

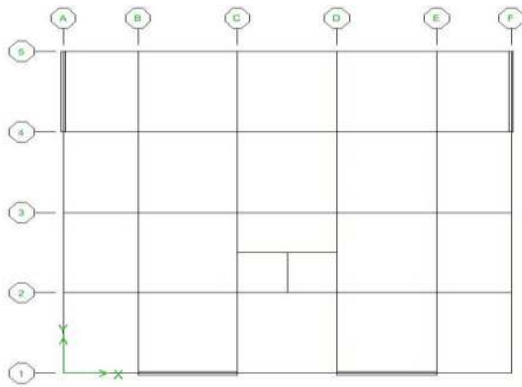


Fig 12. Model-10

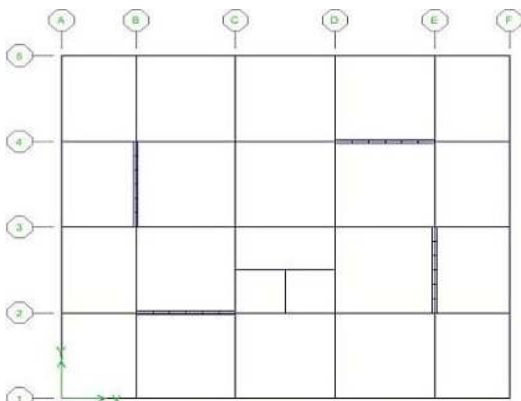


Fig 13. Model-11

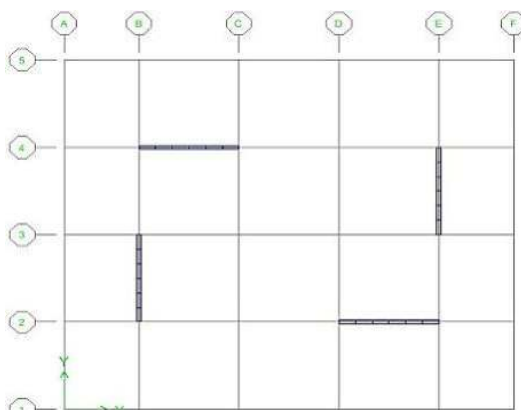


Fig 14. Model-12

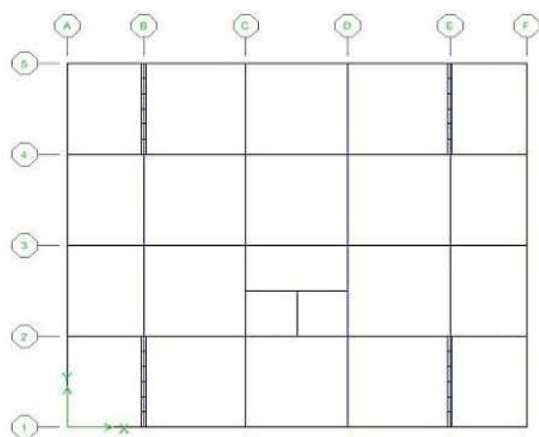


Fig 15. Model-13

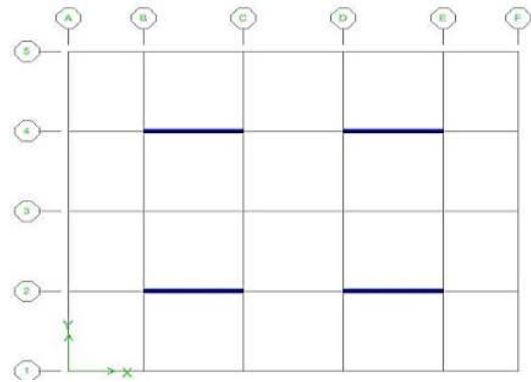


Fig 16. Model-14

4. CHECK FOR STABILITY OF STRUCTURE

A. Overturning Moment

The safety factor for both X and Y direction have greater than 1.5. Therefore, the structure is capable of resisting overturning effect.

B. Sliding

The ratio of the Resistance to friction to sliding force is called factor of safety for sliding. For these proposed building, the factor of safety for sliding is greater than that of 1.5. Therefore, there is no sliding occur in the structure. Sliding and overturning moment is occurred in model-(7) & (10) because the factor of safety is less than 1.5.

C. Storey Drift

The storey drifts are checked in order to determine whether the structure is stable or not by using UBC- 97 formula.

$$\Delta_M = 0.7 RDs < \Delta_{Limit} \text{ where,}$$

Δ_M = Maximum storey drift

Δ_S = Storey drift obtained from the analysis

R = Response modification factor = 8.5

Δ_{Limit} = Storey drift limitation

= 2.0% of storey height for T>0.7 sec

D. Torsional Irregularity

The maximum drift at one end of the structure transverse to its axis is not more than 1.2 times the average storey drifts of both ends.

The selected building with fourteen different locations of planar shear walls are analyzed and checked for stability. From those checking, model (1), (2), (3), (4), (5), (6), (8), (9), (11), (12), (13) and (14) are selected as the desirable models for storey drift of shear walls. The comparative studies on results for these models are shown in Table 2.

Table 2(A). Check for Storey Drift of Model (1), (2) & (3)

Storey	Model (1)		Model (2)		Model (3)	
	Δ_{MX} (in)	Δ_{MY} (in)	Δ_{MX} (in)	Δ_{MY} (in)	Δ_{MX} (in)	Δ_{MY} (in)
roof	1.460	1.1788	1.3823	1.1531	1.3980	1.2023
18	1.522	1.2216	1.4301	1.1980	1.4929	1.2516
17	1.599	1.270	1.4651	1.2337	1.586	1.2980
16	1.662	1.3080	1.4715	1.2423	1.6350	1.3187
15	1.677	1.3159	1.4851	1.2587	1.6957	1.3458

14	1.711	1.3337	1.4922	1.2694	1.7421	1.3637
13	1.738	1.3473	1.382	1.1531	1.7464	1.356
12	1.732	1.3394	1.4786	1.2623	1.7671	1.356
11	1.747	1.3444	1.4751	1.2644	1.78	1.3508
10	1.756	1.3451	1.4644	1.2609	1.7635	1.3272
9	1.735	1.3273	1.4358	1.2409	1.7642	1.310
8	1.722	1.3130	1.4101	1.2237	1.7564	1.2873
7	1.690	1.2823	1.3673	1.192	1.7228	1.2466
6	1.615	1.2216	1.2980	1.1359	1.6943	1.2066
5	1.523	1.1445	1.2145	1.066	1.6443	1.1502
4	1.380	1.0310	1.0974	0.9674	1.556	1.0695
3	1.173	0.872	0.9396	0.8325	1.4494	0.9767
2	1.059	0.7788	0.8747	0.7788	1.2973	0.8560
1	0.463	0.3392	0.4489	0.4018	0.0570	0.4635

Table 2(B). Check for Storey Drift of Model (4), (5) & (6)

Storey	Model (4)		Model (5)		Model (6)	
	Δ_{MX} (in)	Δ_{MY} (in)	Δ_{MX} (in)	Δ_{MY} (in)	Δ_{MX} (in)	Δ_{MY} (in)
roof	1.3573	1.4666	1.30519	1.41729	1.54938	1.14097
18	1.3823	1.4894	1.35803	1.46727	1.59936	1.16739
17	1.4144	1.5180	1.38302	1.49012	1.66005	1.19809
16	1.4366	1.5365	1.41515	1.51868	1.70646	1.21879
15	1.4323	1.5272	1.43728	1.53653	1.71074	1.21737
14	1.4359	1.5265	1.43228	1.52796	1.73145	1.22308
13	1.4316	1.5173	1.43585	1.52653	1.74501	1.22308
12	1.4080	1.4894	1.43157	1.51725	1.73002	1.20594
11	1.3930	1.4687	1.36945	1.44014	1.73145	1.19666
10	1.3695	1.4394	1.32804	1.39230	1.72573	1.18024
9	1.3280	1.3923	1.28734	1.34589	1.6936	1.14668
8	1.2881	1.3452	1.22951	1.28092	1.66719	1.11526
7	1.2302	1.2802	1.14954	1.19095	1.62006	1.06743
6	1.1495	1.1902	1.05672	1.08671	1.53438	0.99674
5	1.0581	1.0853	0.93320	0.95248	1.43014	0.91463
4	0.9339	0.9518	0.77398	0.78611	1.28234	0.8061
3	0.7747	0.7854	0.67516	0.68287	1.08099	0.6683
2	0.6752	0.6820	0.28960	0.29645	0.96475	0.58519
1	0.2896	0.2965	1.68961	1.78728	0.42068	0.25704

Table 2(C). Check for Storey Drift of Model (8), (9) &(11)

Storey	Model (8)		Model (9)		Model (11)	
	Δ_{MX} (in)	Δ_{MY} (in)	Δ_{MX} (in)	Δ_{MY} (in)	Δ_{MX} (in)	Δ_{MY} (in)
roof	1.31161	1.1224	1.3366	1.11455	1.16881	1.1374
18	1.35588	1.14811	1.37873	1.15453	1.2395	1.20594
17	1.40443	1.17738	1.42514	1.1988	1.31376	1.27734
16	1.44228	1.19809	1.46084	1.2345	1.35874	1.31875
15	1.4487	1.19809	1.46655	1.24307	1.40586	1.36445
14	1.4637	1.2038	1.47869	1.25878	1.44156	1.39872
13	1.47155	1.20309	1.4844	1.26949	1.44727	1.40443
12	1.4587	1.18666	1.46941	1.26163	1.46084	1.41657
11	1.45656	1.17524	1.46441	1.26306	1.46798	1.423

10	1.44799	1.15596	1.45156	1.25806	1.45513	1.40943
9	1.42014	1.12098	1.42014	1.23664	1.45156	1.40586
8	1.39444	1.08599	1.39015	1.21594	1.44228	1.39658
7	1.35088	1.0353	1.3423	1.17952	1.41372	1.36873
6	1.27734	0.96318	1.2652	1.11598	1.38658	1.34232
5	1.18809	0.87964	1.17167	1.03672	1.3416	1.29876
4	1.06029	0.7704	1.04172	0.92534	1.26735	1.22736
3	0.8875	0.63403	0.871	0.77754	1.17738	1.13811
2	0.78225	0.55006	0.76512	0.68629	1.04958	1.01388
1	0.33586	0.23904	0.32986	0.29473	0.8775	0.85037

Table 2(D). Check for Storey Drift of Model (12), (13) & (14)

Storey	Model (12)		Model (13)		Model (14)	
	Δ_{MX} (in)	Δ_{MY} (in)	Δ_{MX} (in)	Δ_{MY} (in)	Δ_{MX} (in)	Δ_{MY} (in)
roof	1.20237	1.2038	1.34089	1.26664	1.44871	1.43157
18	1.27306	1.27163	1.36160	1.40015	1.52939	1.52082
17	1.34589	1.34089	1.37445	1.51582	1.55366	1.54795
16	1.38873	1.38016	1.37017	1.49369	1.56509	1.56080
15	1.43656	1.423	1.36731	1.57294	1.57294	1.57009
14	1.47155	1.4537	1.35660	1.64863	1.59865	1.60364
13	1.47726	1.45513	1.33304	1.45656	1.61007	1.62007
12	1.49011	1.46298	1.31019	1.68575	1.61364	1.62863
11	1.49511	1.46441	1.27877	1.73716	1.59365	1.61435
10	1.48083	1.44727	1.23308	1.73216	1.58365	1.60864
9	1.47512	1.43942	1.18310	1.82927	1.56509	1.59508
8	1.46298	1.42585	1.11670	1.92209	1.44871	1.43157
7	1.43228	1.39444	1.03030	1.93851	1.52939	1.52082
6	1.40301	1.36516	0.93106	1.96493	1.55366	1.54795
5	1.35517	1.31804	0.80539	1.99777	1.56509	1.56080
4	1.27877	1.24378	0.65688	1.95993	1.57294	1.57009
3	1.18524	1.15168	0.56634	2.11116	1.59865	1.60364
2	1.05457	1.02459	0.23819	1.02473	1.61007	1.62007
1	0.8825	0.85751	1.64420	2.39733	1.61364	1.62863

Table 3. Check for Torsional Irregularity, Overturning and Sliding

Model	Torsional Irregularity		Overturning			Sliding		
	Actual value	Allowable value	Actual Value		Safety Factor	Actual Value		Safety Factor
			X dire;	Y dire;		X dire;	Y dire;	
1	1.09	1.2	16.8	10.46	1.5	7.98	7.68	1.5
2	1.11	1.2	15	10.81	1.5	6.9	7.66	1.5
3	1.13	1.2	16.33	10.58	1.5	7.65	7.22	1.5
4	1.05	1.2	15.49	10.22	1.5	6.98	7.02	1.5
5	1.05	1.2	15.38	10.23	1.5	6.98	7.02	1.5
6	1.14	1.2	16.2	10.02	1.5	7.48	6.96	1.5
7	1.21	1.2	-	-	1.5	-	-	1.5
8	1.1	1.2	13.77	8.9	1.5	6.36	6.46	1.5
9	1.1	1.2	14.94	10.8	1.5	6.89	7.68	1.5
10	1.21	1.2	-	-	1.5	-	-	1.5
11	1.05	1.2	14.94	10.38	1.5	6.85	7.4	1.5
12	1	1.2	14.9	10.77	1.5	6.87	7.56	1.5
13	1.14	1.2	15.32	19.9	1.5	6.72	10.21	1.5
14	1	1.2	15.24	11.65	1.5	6.9	8.3	1.5

Check for P-Δ Effect (Model 4)

P-Δ effect must be considered wherever the ratio of secondary moments to primary moments exceed 10 %.

$$\theta_x = \frac{P_x \Delta_{sx}}{V_x h_x}$$

- where, θ_x = stability coefficient for story x
- P_x = total vertical load (unfactored) on all columns in story x
- Δ_{sx} = story drift due to design base shear
- V_x = design shear in story x
- h_x = height of story x
- P-Δ effect must be considered when $\theta_x > 0.1$

CHECK,

RFL, $P_x = 1993.994 \times 32.2 = 64206.6$ kips
 (P_x From ETABS)
 $V_x = 2321.68$ kips (V_x From ETABS)
 $\Delta_{sx} = 0.000043 \times 10 \times 12 = 0.00516$ in
 (Δ_{sx} From ETABS)

$$\theta_x = \frac{64206.6 \times 0.00516}{2321.68 \times 120}$$

$$\theta_x = 0.0012 \times 10^{-3} < 0.1$$

Therefore, P - Δ effect must not be considered.

Table 4. Comparison of Required Steel Area

Model	Required Steel area for columns (in ²)	Required Steel area for shear wall (in ²)	Total required steel area (in ²)
1	7352.55	209.54	7562.09
2	8215.029	234.43	8449.45
3	8373.384	225.10	8595.48
4	6786.32	335.69	7122.01
5	7073.255	347.90	7421.155
6	7500.285	225.10	7725.385
8	7269.228	349.86	7619.088
9	7687.479	209.54	7897.019
11	7388.59	355.27	7743.86
12	7282.088	355.27	7637.358
13	7916.642	209.54	8126.182
14	6815.125	347.90	7163.025

5. REASONS FOR SELECTION THE BEST CONTRIBUTION OF SHEAR WALL

First, non-shear wall structure is use to analyze and design. After that, check for the structure is stability or not. The proposed building is not stable, so the shear wall should be provided.

In this study planar shear walls are provided for each model changing their locations fourteen times. After the analysis and design, the necessary checking are made for each model in order to determine whether the locations of shear walls are acceptable or not for the selected building.

From this study, model-4 has minimum steel requirement. The required steel area for columns and shear walls of each model is calculated and compared to find the most suitable location of shear wall from the

economical point of view. From these checking model-4 is suitable for shear wall location.

6. CONCLUSIONS

The analysis and design of the selected building was done by using ETABS software. In addition to wind load, seismic analysis procedure, P-Δ effect was also considered in the analysis load consideration was based on UBC code (1997) and structural elements were designed according to ACI- 318- 99. In making the structural analysis using software, it is necessary to give the cross-sectional dimension of the members. The beam sections are 10"×16", 10"×18", 12"×18", 12"×20". Since beam members nearest to the shear wall carries greater magnitude of bending moment, the cross sections of the beams connecting to the shear walls were taken as 12"×24". If necessary, the assumed cross sections were modified and the analysis was repeated until to reach the final acceptable results. During the analysis of structure, the cross sections of columns, beams and shear wall were modified until they were uniform for all models for the comparative study on required steel area for columns and shear walls. After the analysis and design procedure were done, the necessary checking were made for each model in order to determine whether the locations of shear walls were acceptable or not for the selected building.

ACKNOWLEDGEMENT

The author is very thankful to Dr. Tin San, Pro-rector, Technological University (Lashio), for his motivation, his all supports and guidance. Then, the author would like to express grateful thanks to his all teachers for their suggestions and valuable discussions. The author also wishes to thanks his friends for their helps and advices on this paper. Finally, the author likes to express grateful thanks to his parents for their supports, kindness and unconditional love.

REFERENCES

- [1] Authur H. Nilson, 1997, Design of Concrete Structures, McGraw- Hill Companies, Inc.
- [2] Smith, B.s and Coull, A. 1991. Tall Building Structure: Analysis and Design, John Wiley & Sons, Inc.
- [3] American Concrete Institute 1999. Building Code Requirements for Structural Concrete (ACI 318-99). U.S.A.
- [4] Uniform Building Code. 1997. Volume 2. Structural Engineering Design Provisions. U.S.A. International Conference of Building Officials.

Evaluation of Non–Revenue Water for Mandalay City

Thu Thu Win⁽¹⁾, Nwe Nwe Win⁽²⁾, Thinn Thinn Soe⁽³⁾

^(1,2,3)Department of Civil Engineering, Technological University (Mandalay), Myanmar

Email: thuthuttw@gmail.com

ABSTRACT: The purpose of the study is to evaluate the non-revenue water for Mandalay city. It deals the condition of existing water supply system and assessment of non-revenue water (NRW) of the study area. Existing water supply network data is obtained from Mandalay city development committee (MCDC). Causes of physical losses and meter error are known by field survey. Required pressure data is measured by pressure sensor using with WIND FLUID software. All data described above are recorded in Q.GIS software. Free Water balance software (WB-Easy Calc V.5.15) is used to evaluate non-revenue water including water losses of the study area. Water losses are further divided into physical losses and commercial losses. The calculation of physical losses was based on unavoidable annual real losses (UARL). The highest value of NRW is 79.5% in Aung Myay Thar Zan and lowest NRW is Chan Mya Thar Si, 10.3%.

KEYWORDS: *non-revenue water, water losses.*

1. INTRODUCTION

Even though the Earth is composed largely of water, fresh water comprises only three percent of the total water available to humans. Of that only 0.06 percent is easily accessible mostly in rivers, lakes, wells, and natural springs. So fresh water scarcity becomes an important problem to be solved. Water shortage or water scarcity is the inadequacy of satisfactory water assets that can meet the water requests for a specific area. The main causes of water scarcity are environmental change, water overuse and expanded contamination. Mandalay is in the dry zone at central Myanmar and faces water crises every April, May and June. Some townships in Mandalay are affected by water shortage during summer. Water supply from water resources is not proportionate with the increasing population and caused a shortage. Therefore we should be aware of the wasting of fresh water. Mandalay City has 1.46 million populations and city area is 53 square kilometers, it has 96 wards, 179 village and 6 townships. For current water supply situation, total production is 1,36,363.64 m³/d, surface water(10%)13,636.36m³/d and ground water (90%) 1,22,727.27 m³/d, 46 Nos. of production tube well, 11 Nos of booster pumping station and 2 Nos. of surface water treatment plant are used. This system can serve only 70 % of population. This shows that some fresh water has been wasted. Therefore, it is important to manage water sustainability in water supply system. NRW is defined as

the difference between a systemic input volume and the billed authorized consumption. This study focused on non-revenue water reduction.

2. EXISTING NETWORK CONDITION FOR MANDALAY

Mandalay city has four supply townships: Aung Myay Thar Zan, Chan Aye Thar Zan, Mahar Aung Myay and Chan Mya Thar Si. Mandalay locates between E. long 96° 06' and N. lat 21° 59'. Mandalay city is composed of six townships. The total area is about 53 square kilometers and study area is around 44 square kilometers. In Mandalay, unbilled authorized consumption is about 14368m³/day for high way gates, markets, fire hydrants, gardens and monasteries. System of Mandalay water supply is intermittent system. The supplied area is divided into four zones each zone is situated in each township. In the study area, there are 90000 registered meters. Among them, 1141 meters are closed because of lack of duty and housekeepers. In the existing supply, the main source is ground water. In each system, the functioning is similar, pumped water is stored into storage reservoirs. From these tanks, water is further supplied using Booster Pumping Stations (BPS). The only elevated point is Mandalay Hill where a reservoir is located (distribution by gravity). The distribution network of study area is shown in Fig 1.

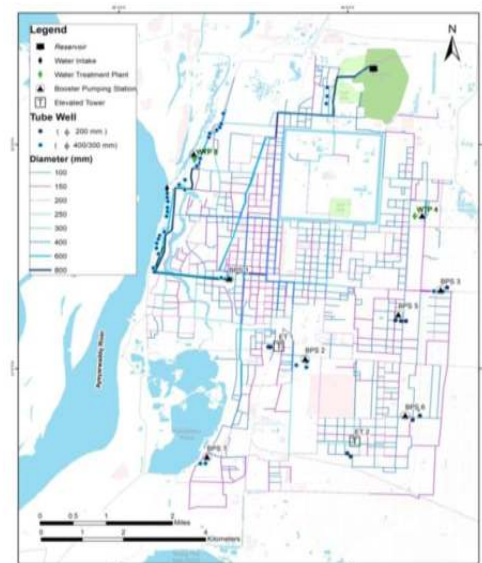


Fig 1. Water distribution network of Mandalay

The characteristics of the distribution pipe diameters and lengths, and distribution network plan data are from Mandalay city development committee. The field survey was carried out to find the causes of NRW. The whole network of study area is the recorded in Q-GIS software. Required pressure data is collected by using pressure sensors with the help of WIND FLUID software. The system input volume, pipe size and length, number of service connections, average length of customer’s meter to secondary pipe line, bill metered consumption, unbilled consumption and authorized consumption are used as input data to WB Easy Calc software Version 5.15 which is used to calculate water balance of the area. Unavoidable annual real issues for each zone are calculated in water balance software and they are represented as physical losses of the studied area.

3.1 Q-GIS software

This study combines application of Geographic Information System (GIS) as a framework for managing and integrating data by Quantum GIS i.e (Q-GIS). The geographic Information System (GIS) is taken as an aid to visualize the sources and feeders and conceptualize the entire distribution network. Q-GIS plays a good role in finding solution to lay the best possible network and can show the simulation of water distribution network including tank, adding nodes and pipe. Q-GIS version 2.14.3 – Essen software is used in this study.

3.2 Water Pressure Sensor

Pressure sensors can be used in systems to measure other variables such as fluid flow, speed, water level and altitude. They are transducers, generating and electrical signal in proportional to the pressure they measure. Water pressure sensors G1/41.2 MPa, as shown in Fig 2 are used to collect pressure data in this study. By joining these sensors with computer, Wind Fluid Software can give the required daily pressure. Fig 2 shows water pressure sensor and Fig 3 shows joining it with meter.



Fig 2. Water pressure sensor



Fig 3. Water pressure sensor joining with meter

3.3 WB-Easy Calc Software

WB-Easy Calc software can be used to carry out a water balance audit. It can be used for intermittent water supply system. It calculates the NRW percent and describes the physical losses and commercial losses differently for day, month and year. The required data are system input volume, billed consumption, customer, unbilled consumption, unauthorized consumption, customer meter inaccuracies and data handling error, network data (pipe lengths, diameter, number of service connection, number of meter and average length of service connections to property boundary), pressure, supply hour and final data. The software format is excel format and not allowed to edit the form. Equation (1) is used in the WB-Easy Calc software version 5.15 is described as below:

Unavoidable Annual Real losses (UARL),

$$UARL(L/day)=(18Lm+0.8Nc+25Lp)P \quad (1)$$

Where,

Lm = Length of mains in km

Nc = Number of service connections

Lp = Total length in km of underground connection pipes(between in the edge of the street and customer meters)

P = Average operating pressure in m (head)

Water balance results for Aung Myay Thar Zan township for 365 days periods using WB-Easy Calc software version 5.15 for are shown in Figure 4 as an example. The results for other three townships can also be shown.

Water Balance in m3 for a period of 365 Days			
System Input Volume 42,941 (m3) Error Margin(+/-) 0.0%	Authorized Consumption 14,259 (m3) Error Margin(+/-) 0.0%	Billed Metered Consumption 8,704 (m3)	Revenue Water 8,704 (m3)
		Billed Unmetered Consumption 0 (m3)	
		Unbilled Metered Consumption 5,475 (m3) Error Margin(+/-) 0.0%	
		Unbilled Unmetered Consumption 0 (m3) Error Margin(+/-) 0.0%	
		Unauthorized Consumption 0 (m3) Error Margin(+/-) 0.0%	
		Apparent Losses 89 (m3) Error Margin(+/-) 0.0%	Customer Meter Inaccuracies and Data Handling Errors 89 (m3) Error Margin(+/-) 0.0%
	Water Losses 28,682 (m3) Error Margin(+/-) 0.0%	Real Losses 28,593 (m3) Error Margin(+/-) 0.0%	

Fig 4. Water balance results for 365 days

The system input volume is obtained from Water and Sanitation Department, Mandalay Development Committee (MCDC). Billed consumption and unbilled authorized consumption are known by field survey. No. of service connection in each zone are recorded in Q-GIS software. Meter errors are known by inquiring by local people Pressure head is recorded by using pressure sensor. Water supply system is intermittent system in all zones. The supply hour is 6 hours. Maximum system input volume is in Mahar Aung Myay. Maximum consumption is in Aung Myay Thar Zan according population. Maximum meter error is in Mahar Aung Myay is due to their age and careless of local people. The required input data per day for each zone are summarized in Table 1.

4.RESULTS AND DISCUSSION

According to the results, the highest NRW is occurred at Aung Myay Thar Zan, zone 1 and the lowest is at Chan Mya Thar Si, zone 4. Field survey was done for all zones to find the causes of losses. The causes were occurred due to leakage at pipe to pipe connections and pipe bursts locating near main road. For pressurized system, the physical losses are calculated based on UARL. UARL is directly proportion to average pressure head which was expressed in equation (1). The lowest NRW rate is found at zone 4 because the pressure head is relatively low and NRW rate is realistic and sustainable level for developing countries (a range of 15%-20%). At zone 1, there is 137m³ meter error and 5496m³ authorized consumptions and there have losses at economic level but some leakages are due to unstable pressure and pipe burst due to vibration of pipe during pumping. The amount of NRW at zone 2 and zone 3 are the second highest amount of all values. According to field survey, the losses are mostly found in Mayga Giri ward. These are caused due to external affects such as construction of culvert, drainage, firing the rubbish carelessly. According to the result and field survey, zone 3 was 67.8% NRW losses and it was slightly higher than zone 2 because the pipe size at zone 3 is larger than the pipe size of other zone. The larger the pipe size, the higher amount of leakage of the line. All about the described losses are physical losses and shown in Fig 5, 6 and 7.

Table 1. Input data for WB-Easy Calc software

Zone-1(Aung Myay Thar Zan)	
System input volume (m ³ /day)	42941
Billed consumption (m ³ /day)	8784
No. of service connection	2040
Unbilled authorized consumption (m ³ /day)	5475
Meter error	137
Pressure head (m)	0.89
Supply system	Intermittent
Supply hour per day	6 hr
Zone-2 (Chan Aye Thar Zan)	
System input volume (m ³ /day)	44836
Billed consumption (m ³ /day)	13909
No. of service connection	2122
Unbilled authorized consumption (m ³ /day)	2928
Meter error	218
Pressure head (m)	1.11
Supply system	Intermittent
Supply hour per day	6 hr
Zone-3 (Mahar Aung Myay)	
System input volume (m ³ /day)	48415
Billed consumption (m ³ /day)	7724
No. of service connection	342
Unbilled authorized consumption (m ³ /day)	5552
Meter error	610
Pressure head (m)	1.22
Supply system	Intermittent
Supply hour per day	6 hr
Zone-4 (Chan Mya Thar Si)	
System input volume (m ³ /day)	12641
Billed consumption (m ³ /day)	250
No. of service connection	245
Unbilled authorized consumption (m ³ /day)	392
Meter error	176
Pressure head (m)	1.12
Supply system	Intermittent
Supply hour per day	6 hr



Fig 5.Physical losses due to leakage at cap



Fig 6.Physical losses due to joint error



Fig 7. Physical losses due to pipe bursting

In the study area, the apparent losses are relatively low as compared to physical losses. These apparent losses are meter error and only 1141 meters are found to be error of the whole area. The meter error usually occurs in higher population area. The meter occurs due to aging and some unqualified meters and described in Fig 8.



Fig 8. Meter corruption

In the study area, the water utility distributes water into four different zones. The amount of NRW is derived from WB Easy Calc Software. The components of NRW, such as physical losses, commercial losses and unauthorized consumption are separately calculated for each zone. The NRW losses are calculated with water balance software. The NRW % is calculated by dividing the NRW losses values with system input volume.

For example zones (1),

$$NRW \% = (NRW \text{ losses} / \text{System input volume}) \times 100\%$$

$$NRW \% = (34157/42941) \times 100\% = 79.5\%$$

The results of NRW for each zone are described in Table 2.

Table 2. Result of Non-Revenue Water for each supply zone

Zone-1(Aung Myay Thar Zan)	
Physical losses (m ³ /day)	28593
Commercial losses (m ³ /day)	89
Unbilled authorized consumption (m ³ /day)	5475
Total NRW losses (m ³ /day)	34157
NRW %	79.5%
Zone-2 (Chan Aye Thar Zan)	
Physical losses (m ³ /day)	23251
Commercial losses (m ³ /day)	33
Unbilled authorized consumption (m ³ /day)	5622
Total NRW losses (m ³ /day)	28906
NRW %	67.5%
Zone-3 (Mahar Aung Myay)	
Physical losses (m ³ /day)	23249
Commercial losses (m ³ /day)	32
Unbilled authorized consumption (m ³ /day)	5634
Total NRW losses (m ³ /day)	28915
NRW %	67.8%
Zone-4 (Chan Mya Thar Si)	
Physical losses (m ³ /day)	487
Commercial losses (m ³ /day)	7
Unbilled authorized consumption (m ³ /day)	393
Total NRW losses (m ³ /day)	887
NRW %	10.3%

5. CONCLUSIONS

WB-Easy Calc software and Q-GIS software were used in the estimation of physical losses and commercial losses. And so maintenance of the pipe line should be done regularly. Lack of marking of the pipe line is the one of the components of pipe line leakage. Besides, the second highest amount at zone 4 was due to aging and lack of public’s appreciation to water value. The leakage report activation should be done for reduction of losses. For commercial losses, only 9 meters are found as error meters among 1987 meters. In conclusion, the amount of physical losses was found to be more than commercial losses were found to be more than commercial losses according to the calculation and research.

ACKNOWLEDGEMENT

The author is very grateful thanks to Dr. Yan Aung Oo, Pro rector, Technological University (Mandalay), for his permission. Special thanks are extended to Dr. Ni Lar Aye, Professor, Department of Civil Engineering, Mandalay Technological University, for her invaluable advices. Besides the author want to say special thanks to Daw Ei Ei Phyo, Assistant Director(Water and Sanitation Department , Mandalay Development Committee) and her colleagues at the department. Finally, the author sincerely wishes to think to thank her parents for their support and encouragements.

REFERENCES

- [1] Ison Simbeys; Lead Trainer in NRW, “*Water and Sanitation Consultant*”, Wave Pool member, Zamba, 2006.
- [2] Shiklomanov IA Word Fresh Water Resources, In Gluck PH.editor. *Water in Crisis: “A Guide to the world’s Fresh Water Resources”*, New York Oxford University
- [3] World Bank Discussion Paper No.8, December 2006.
- [4] Khin Thu Zar Htay, “*Evaluation Of Non-Revenue water And Proposed Management Plan For Reduction of Non-Revenue Water For Ottarathiri Downtown Area, Naypyitaw*”, Firat university Conference on Science Engineering and Research,2018
- [5] Global Water Partnersio (GWP), International Network of Basin Organizations (INBO). “*A Handbook for Integrated Water Resources Management in Basin*”, Sweden:Elanders,2009
- [6] Xin., K., Tao., Lu., Xiong., “*Apparent losses Analysis in District Metered Areas of Water Distribution Systems*”,2014.
- [7] Farely M, Wyeth G,Ghazali ZBM, Isalanddar A, Singh S. The Manger’s Non-Revenue Water Handbook: “*A Guide to Understanding Water Losses*”, IN Dijk NV, Rakakulthai V,Kirkwood E,editors. United States of America: United States Agency for International Development (USAID),2008.
- [8] Kingdom, B., Leimberger, R.,P. “*Water Supply and Sanitation Sector Board Discussion Paper Series*”, The Challenge of Reducing Non-Revenue Water (NRW) in Developing Countries, 2006
- [9] Farley M. “*Non-Revenue Water International Best Practice for Assessment, Monitoring and Control*”, Proceeding of the 12th Annual CWWA Water, Waste Water & Solid Waste Conference; 2003Sept 28-Oct 3; Atlantis, Paradise Island: Bahamas; 2003.
- [10] MYANMAR Census 2004, Department of Population, Ministry of Labour, Immigration and Population, October 2017
- [11] Water and Sanitation Department, Naypyitaw Development Committee.
- [12] Lewis A. Rossman, EPANET2 USERS MANUAL. “*Water Supply and Water Resources Division National Risk Management*”, Research Laboratory Cininnati, OH 45268,September 2000

- [13] SIDA, “*Water and Waste water Management in Large to Medium-sized Urban Centres-Experiences from the Developing World*” Colling Water Management AB. IUCN Water Demand Management Guideline Training Module, 2000.

Petrochemistry and Petrogenesis of Igneous Rocks in Yinmabin-Phayangazu Area, Thazi Township, Mandalay Region

Moe Moe Nwet⁽¹⁾, Yin Kay Thwe Tun⁽²⁾, Nyan Min Naing⁽³⁾

⁽¹⁾Technological University (Meiktila), Myanmar

⁽²⁾Loikaw University, Myanmar

⁽³⁾Magway University, Myanmar

Email: moemoenwet1983@gmail.com

yinkaygeol96@gmail.com

nyanminnaing@gmail.com

ABSTRACT: Yinmabin-Payangazu area is situated about 23 km southeast of Tharzi Township, Mandalay Region. The area occupies as the segment between the Shan Plateau and the central lowland. It is mainly composed of the igneous rocks. The metasedimentary rocks are exposed as only roof-pendant or scattered bodies. All rocks units of the Yinmabin-Phayangazu intrusions are calc-alkaline character. Granitoid rocks have been classified as both I-type and S-type. The igneous of the study area were originated by the product of calc-alkaline suite produced from the partial melting of the subducted oceanic crust of Indian Plate beneath the Burma Plate. The plutonic rocks of the study area were formed on the continent owing to the subduction of an oceanic plate beneath the continent.

KEYWORDS: *Yinmabin-Payangazu intrusions, Granitoids.*

1. INTRODUCTION

The present study area, Yinmabin-Payangazu area is situated about 23 km southeast of Tharzi Township, Mandalay Region (Figure 1). This area lies between latitudes 20°41'-20°48' N and longitudes 96°11'-96°20' E in one topographic map 93/D 1,2,5,6. The study area can be reached by car or by train and be accessible in all seasons.

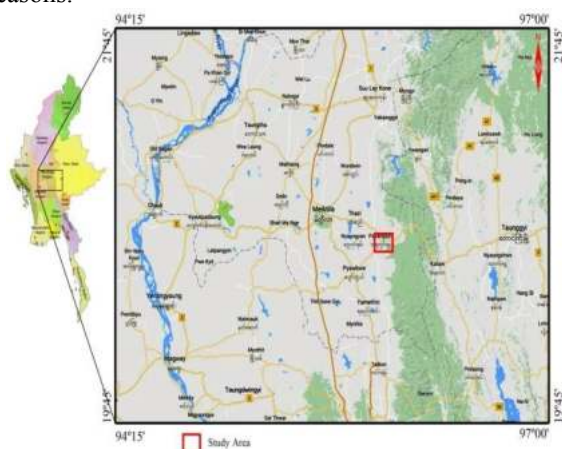


Fig1. Location map of the Phayangazu area.

eastern marginal zone of the central lowland. The study area is located in the eastern part of the Thazi-Pyawbywe plain which lies in the western marginal zone of Shan Plateau. The study area is an intensely deformed zone and so the rocks are subjected to the successive phases of deformation. Medium to high grade metamorphic rocks, exposed in the northern and central part of the area, are trending NNW-SSE. In general, the rock units dip moderately eastward. It also occupies the southern continuation of the western limb of the Kywedatson Syncline [1]. This area is structurally bounded by the two famous fractured zones, the Nwalabo fault [2] in the east and Sagaing fault in the west respectively.

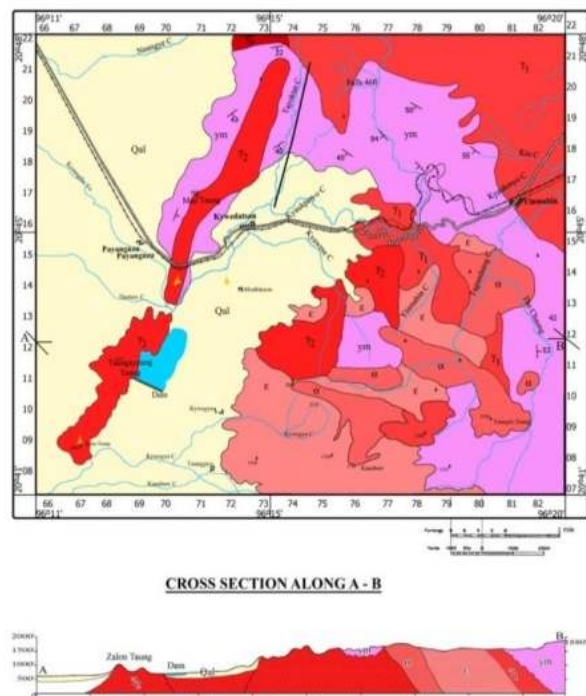


Fig2. Geological Map of the study area

The area occupies as the segment between the western marginal zone of the Shan Plateau and the

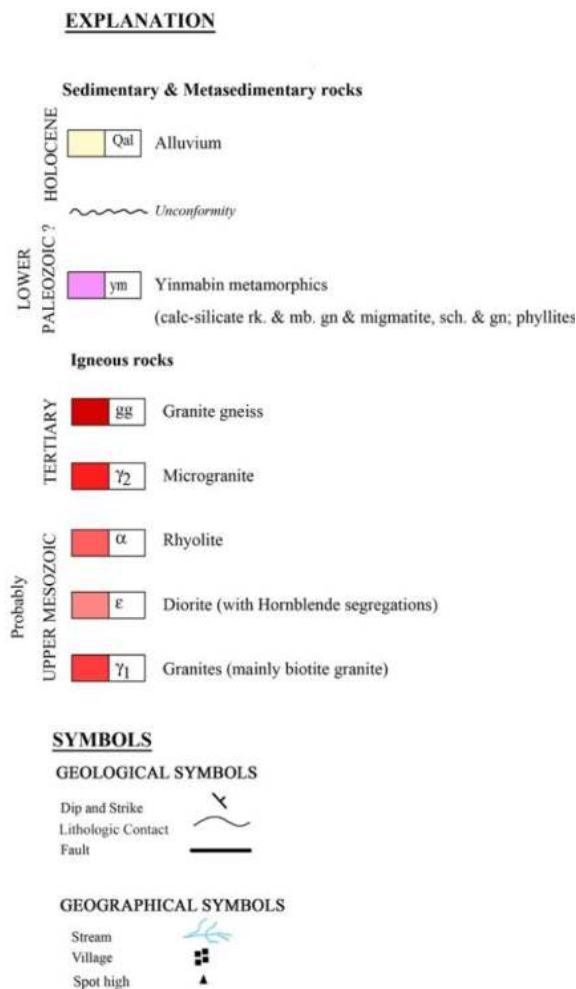


Table 1. Chemical composition of the granites (wt%) of the Yinmarbin-Phayangu area

Sample No	G 2	G 4	G 9	G 10	G 18
SiO ₂	70.98	74.12	75.12	72.41	73.40
Al ₂ O ₃	11.56	15.03	12.36	13.04	14.02
Fe ₂ O ₃	1.97	0.89	1.36	0.90	2.00
FeO	0	0	0	0	0
MnO	0.49	0.39	0.32	0.27	0.26
MgO	0.76	1.19	1.14	0.36	0.37
CaO	0.43	2.04	2.13	0.72	1.42
Na ₂ O	2.91	2.9	3.16	4.26	3.23
K ₂ O	3.86	0.66	2.30	3.43	2.11
TiO ₂	0.47	0.12	0.29	0.46	0.47
P ₂ O ₅	0.52	0	0.27	0	0
SO ₃	2.30	0.29	0.26	0.29	0.33
Cr ₂ O ₃	0.72	0.32	0.09	0.57	0.62
CoO	0.02	0.02	0.04	0	0.02
ZnO	0	0	0.35	0.78	0.03
Rb ₂ O	0.19	0.15	0.14	0.60	0.01
SrO	1.69	1.12	0.13	0.48	0.11
ZrO	0.21	0.16	0.11	0.29	0.91
BaO	0.59	0.49	0.43	0	0.39
Ni ₂ O ₃ [p;''	0	0.08	0	0	0
Nb ₂ O ₅	0	0	0	1.13	0
Total	99.67	99.97	100	99.98	100
ASI	1.46	1.72	1.47	1.52	1.54
FI	0.79	0.99	0.72	0.92	0.74
MI	29.64	57.89	26.19	35.81	23.82
LI	21.2	21.44	18.95	23.73	19.63

The study area is mainly composed of the igneous rocks. The metasedimentary rocks are exposed as only roof-pendant or scattered bodies. The major units of the area are granite, microgranite, leucogranite, hornblende, rhyolite, diorite, microdiorite, granodiorite, calc-silicate rock with the dykes of pegmatite and dacite as minor rock units (Figure 2).

2. MATERIALS AND METHODS

The GPS, Brunton compass, tape and geological hammers, sample bags, note book were used for the field works. The representative samples of the rock units were collected in the field and the photographs were taken as the field evidences. Good exposure and prominent panoramic view are taken as a photographic data.

For studying of geochemical characteristics of Yinmabin-Phayangu intrusion, ten samples from plutonic rocks and five samples from rhyolite dikes were analyzed at the DSSTRC and Ela laboratories for major, trace and rare earth elements by EDXRF and WDXRF analysis method.

3. PETROCHEMISTRY

The geochemical analyses of the igneous rocks are presented in Table (1, 2 & 3).

Table 2. Chemical composition of the Rhyolite (wt%) of the Yinmarbin-Phayangu area

Sample No	R 3	R 20	R 13	R 14
SiO ₂	66.39	68.52	74.75	74.59
Al ₂ O ₃	13.60	13.89	13.17	12.56
Fe ₂ O ₃	7.69	7.47	3.01	0
FeO	0	0	0	0
MnO	0.07	0.15	0.07	0.09
MgO	2.76	2.26	0.57	0.16
CaO	4.96	2.77	0.71	0.27
Na ₂ O	2.99	3.67	6.71	6.26
K ₂ O	0.07	0.08	0.17	0.15
TiO ₂	0.72	0.71	0.66	0.53
P ₂ O ₅	0.21	0.16	0	0.27
SO ₃	0.16	0	0.12	0.17
Rb ₂ O	0.003	0.004	0.002	0.003
ZnO	0.006	0.007	0.004	0.006
V ₂ O ₅	0.03	0.04	0.02	0.03
SrO	0.03	0.03	0.01	0.02
Y ₂ O ₃	0.004	0.009	0.006	0.005
Total	99.69	99.77	99.98	99.87
ASI	8.28	10.51	9.85	11.17
F.I	0.38	0.49	0.91	0.96
M.I	26.41	23.23	15.92	3.39
L.I	14.43	17.84	23.69	24.48

Table 3. Chemical composition of the diorites (wt%) of the Yinmarbin-Phayangu area

Sample No	D 9	D 28	D 15	D 1
SiO ₂	57.78	56.06	53.40	49.66
Al ₂ O ₃	17.91	16.81	16.72	16.93
Fe ₂ O ₃	10.67	10.83	8.23	7.91
FeO	0	0	0	0
MnO	0.21	0.17	0.12	0.71
MgO	4.81	25.62	9.41	5.76
CaO	4.12	5.89	7.29	8.93
Na ₂ O	2.56	3.40	2.29	3.57
K ₂ O	0.29	0.59	1.32	1.20
TiO ₂	0.43	0	0.31	4.43
P ₂ O ₅	0.18	0.11	0	0.16
SO ₃	0.34	0	0.33	0.42
Rb ₂ O	0.36	0.02	0.003	0.003
Cr ₂ O ₃	0.006	0.03	0.005	0.007
ZnO	0.004	0.003	0	0.002
ZrO ₂	0.015	0.006	0.03	0.03
V ₂ O ₅	0.019	0	0.002	0
SrO	0.09	0.002	0	0.001
Y ₂ O ₃	0.002	0.003	0.001	0.001
Total	99.79	99.54	99.96	99.72
ASI	2.57	1.70	1.47	1.24
F.I	0.41	0.41	0.36	0.35
M.I	31.07	34.16	53.34	42.14
L.I	10.43	3.37	1.54	2.26

The analyzed rocks show a restricted range in chemical composition. The concentration of SiO₂ in the hornblende granite are low SiO₂ (65.85-69.90) and high total iron (5.48-8.39) as compared to leucocratic granites: SiO₂ (73.89-77.74) and total iron (1.10-5.06). The average values of Al₂O₃, TiO₂, Na₂O, K₂O, CaO, MgO and P₂O₅ of the granites are 12.49, 0.79, 4.48, 4.96, 1.02, 0.27 and 0.20 which are comparatively same as Leucocratic granites: 12.19, 0.26, 3.60, 4.02, 0.71, 0.12 and 0.01 respectively.

In the total alkali versus silica (TAS) diagram, the mafic rock (SiO₂ content ranges from 56.6% to 68.90% Na₂O+K₂O ranges from 5.01% to 10.14%) fall within the field of diorite and granodiorite whereas the acidic rocks (SiO₂) content ranges from 51.8% to 75.5%, Na₂O+K₂O ranges from 8.02% to 11.28%) plot in the granite field and granodiorite field.

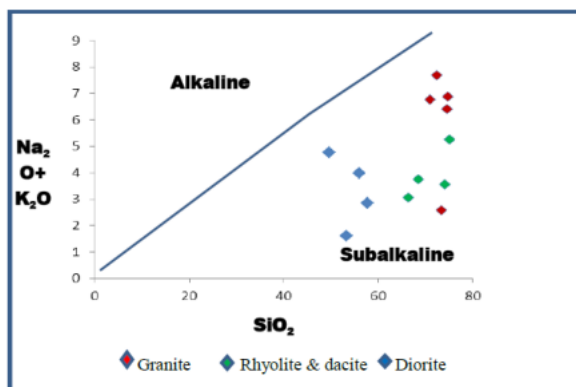


Fig3. SiO₂ versus Na₂O+K₂O diagram of igneous rocks of the study area with field after Rickwood (1989) in [7].

Based on K₂O + Na₂O versus SiO₂ diagram and the AFM triangular diagram, all rocks units of the Yinmabin-Phayangu intrusion are calc-alkaline character (Figure 3& 4).

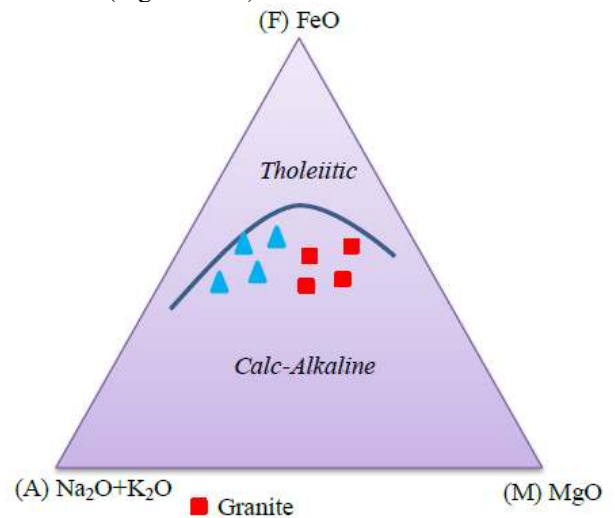


Fig4. AFM diagram of igneous rocks of the study area

At the SiO₂ against K₂O diagram, they are classified as high potassium calc-alkaline rocks (Figure 5). Their very low contents of CaO, MgO with Fe/Mg ratios and AI values signify alkali affinity of these granites. These magmatic rocks attained very high content of sodium and iron as well as strongly depleted in alumina along with calcium and magnesium in their final stages of magmatic and subsolidus processes. So, it can be considered that calc-alkaline nature of granitic rocks from the study area is genetically related to the subduction related plate tectonic process.

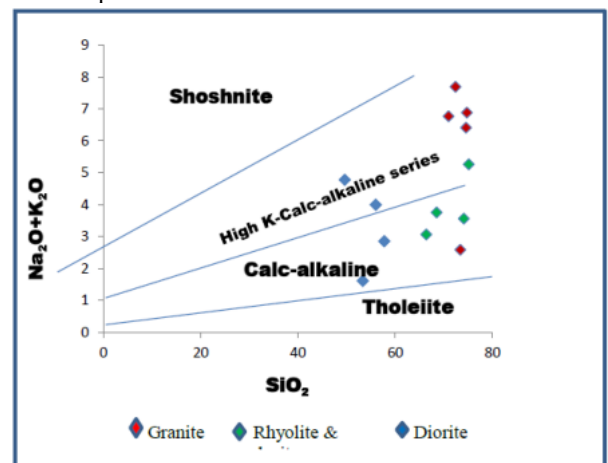


Fig5. SiO₂ versus Na₂O+K₂O diagram of igneous rocks of the study area with field after Rickwood (1989) in [7].

The alumina saturation index (ASI), defined as the molecular A/ CNK= Al₂O₃/ CaO+ K₂O+Na₂O, ranges from 1.83 to 1.97 for the granitic rocks. Shand (1927) grouped igneous rocks based on the total molecular alkali

versus alumina content as either peralkaline [$Al_2O_3 < (Na_2O + K_2O)$] peraluminous [$Al_2O_3 > (CaO + Na_2O + K_2O)$] or metaluminous [$Al_2O_3 < (CaO + Na_2O + K_2O)$] (in Winter, 2013). Chemically, the granitic rocks from the study area have alumina greater than the sum of lime, soda and potash [$Al_2O_3 > (CaO + Na_2O + K_2O)$]. In Al_2O_3 - CaO - $(Na_2O + K_2O)$ diagram too all the granitic rocks fall within the peraluminous field (Figure 6).

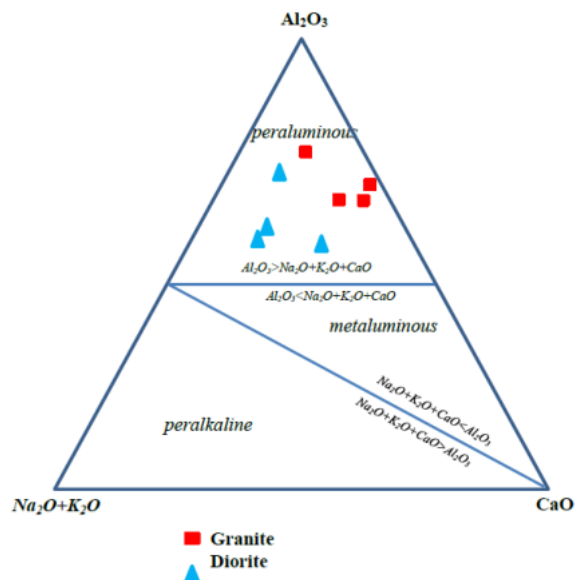


Fig6. Al_2O_3 – CaO – $(Na_2O + K_2O)$ diagram of plutonic rocks.

On the variation diagrams (Figure 7), with increasing SiO_2 , contents of Al_2O_3 , P_2O_5 , CaO , TiO_2 , MgO , MnO and Fe_2O_3 are decreased and K_2O and Na_2O demonstrate increasing trend. These trends may reflect the crystal fractionation process in the evolution of the Yinmabin-Phayangu intrusion.

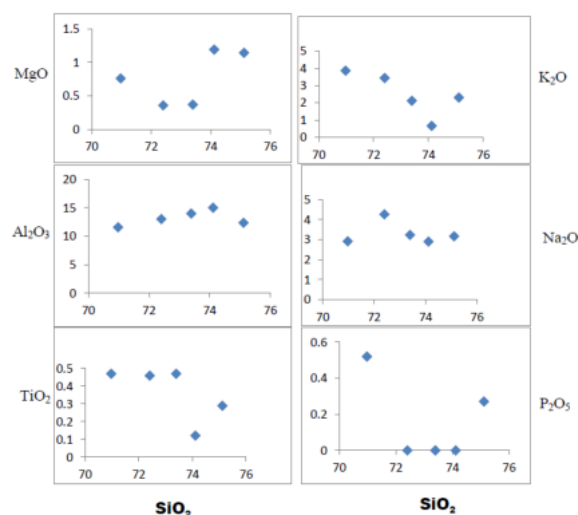


Fig7. SiO_2 versus major oxides (wt%) variation plots of the plutonic rocks.

4. PETROGENESIS

Granitoid rocks have been classified as both I-type and S-type [3]. Several evidences suggest that Yinmabin-Phayangu intrusion is I-type and S-type:

- Frequency of hornblende, magnetite, biotite and titanite in these rocks and absence of muscovite, garnet, cordierite, andalusite and sillimanite.

- SiO_2 content varies between 56.5% - 74.75% in these rocks.

- Presence of mafic dolerite enclaves in different parts of the intrusion and the absence of micaceous xenoliths.

- Some samples are metaluminous and some are peraluminous nature of them.

- Commonly present of pegmatites and aplite.

- Decreasing P_2O_5 versus SiO_2 .

- Based on SiO_2 vs. K_2O the Yinmabin-Phayangu intrusion classified as I-type and S-type granitoids.

Barbarin (1999) classified granitoids into 7 main groups. Based on this classification, Yinmabin-Phayangu intrusion is classified as amphibole-bearing calc-alkaline granitoids (ACG) [4].

Based on geochemical studies, Yinmabin-Phayangu granitoid can be classified as sodic granite ($Na_2O > K_2O$) and has low values of Ni, Cr, Co and V. Lower contents of these elements indicative for evolution of magma during ascending and before complete crystallization.

The granitic magma from the study area might have been generated at the liquidus temperature between $685^\circ C$ and $720^\circ C$ [5].

According to Khin Zaw (1990), the granitoid rocks in Myanmar can be subdivided into three main N-S trending belts viz. western belt, central belt and eastern belt extended from Putao, Kachin State in the north through Mogok, Mandalay to Tavoy and Mergui areas, Tenasserim in the south over a distance of 1450 km. The present study area, Yinmabin-Phayangu area is located in the central granitoid belt. The central belt granitoid plutons contain both I-type and S-type. The almost absence of cogenetic volcanic rocks and abundance of pegmatites, aplites and related quartzo-feldspathic vein materials suggest a relatively deeper environment of emplacement.

The potash-rich nature of the granitoids combined with high initial ratios of Sr^{86}/Sr^{87} ($0.717 + 0.002$) and Rb/Sr ratios of (0.40-33.07) with an average value of 6.70 suggest the derivation of the central belt granitoid magma from well-established continental, sialic materials perhaps by remelting of medium- to high-grade, regionally metamorphosed country rocks.

The granitoid rocks in the central belt were possibly emplaced during continent-arc collision at the early stage of westward migrating, east-dipping subduction zone Eocene. The W-Sn related, central belt granitoids and porphyry Cu (Au) related, western belt granitoids were considered to have been emplaced during the Upper Mesozoic and Lower Cenozoic interval but might not have been strictly contemporaneous.

The igneous complex, about 29 km long and 13 km wide, is the southern extension of the Pyetkaywe batholith in the north. Associated igneous rocks are diorites together with hornblendites; rhyolites occurring both as lava flows and dykes; hornblende granites, muscovite granites, felsic granites and pegmatites as younger

intrusive. The Yinmabin granitoids are medium- to coarse-grained, non-porphyritic to porphyritic biotite granites.

As the study area is located in back-arc of Myanmar, the igneous of the study area were originated by the product of calc-alkaline suite produced from the partial melting of the subducted oceanic crust of Indian Plate beneath the Burma Plate [6].

The occurrence of muscovite in the highly differentiated leucogranites in the central belt granitoids is also indicative of the emplacement at a depth greater than 2.5 km.



Fig8. Location of the studied samples on the AFM diagram after Bowden (1984) in [4].

diagrams also demonstrate a subduction setting relation for the Yinmabin-Phayangazu granitoids. With reference to [4], the tectonic setting of plutonic rocks from the study area has been treated. The studied rocks located in the continental arc granites (CAG) setting (Figure 8), indicating that these granitoids originated from the subduction of an oceanic crust under a continental crust at the active continental margins. The parental magma was medium to high K calc-alkaline. In Al_2O_3 vs SiO_2 diagram (Figure 9), the plutonic rocks can be subdivided into three groups (IAG+CAG+CCG, RRG+CEUG and POG) and the plutonic rocks of the study area plot within the fields of IAG+CAG+CCG.

Based on the above mentioned data, all plutonic rocks from the study area belong to the fields of CCG and CAG. It can be considered that the plutonic rocks of the study area were formed on the continent owing to the subduction of an oceanic plate beneath the continent.

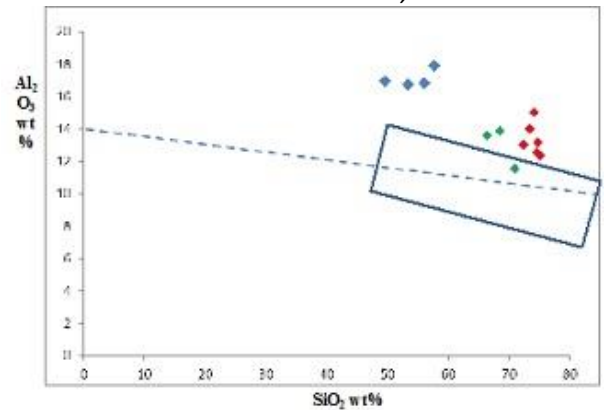


Fig9. Al_2O_3 vs SiO_2 diagram. Granites, rhyolites and diorite from the study area plot in the IAG+CAG+CCG field. IAG= Island arc granitoids, CAG= Continental arc granitoids, CCG= Continental collision granitoids, POG= Post orogenic granitoids, RRG= Rift related granitoids and CEUG= Continental Epeirogenic uplift granitoids) (The fields are based on [7]).

5. CONCLUSION

All the analyzed rocks show a restricted range in chemical composition. Based on $K_2O + Na_2O$ versus SiO_2 diagram and the AFM triangular diagram, all rocks units of the Yinmabin-Phayangazu intrusion are calc-alkaline character. In Al_2O_3 -CaO-(Na_2O+K_2O) diagram too all the granitic rocks fall within the peraluminous field. On the variation diagrams, with increasing SiO_2 , contents of Al_2O_3 , P_2O_5 , CaO, TiO_2 , MgO, MnO and Fe_2O_3 are decreased and K_2O and Na_2O demonstrate increasing trend. Yinmabin-Phayangazu intrusion is classified as amphibole-bearing calc-alkaline granitoids. Based on geochemical studies, Yinmabin-Phayangazu granitoid can be classified as sodic granite ($Na_2O > K_2O$) and has low values of Ni, Cr, Co and V. The granitic magma from the study area might have been generated at the liquidus temperature between 685°C and 720°C. The occurrence of muscovite in the highly differentiated leucogranites in the central belt granitoids is also indicative of the emplacement at a depth greater than 2.5 km. All plutonic rocks from the study area belong to the fields of CCG (Continental collision granitoids) and CAG (Continental arc granitoids). It can be considered that the plutonic rocks of the study area were formed on the continent owing to the subduction of an oceanic plate beneath the continent.

ACKNOWLEDGMENT

WE WOULD LIKE TO EXPRESS OUR HEARTFELT GRATITUDE TO RECTOR (ACTING), DR. AUNG MYO THU, OF TECHNOLOGY UNIVERSITY (MEIKTILA) AND DR. AUNG CHAN WIN, PROFESSOR AND HEAD OF DEPARTMENT OF CIVIL ENGINEERING, TECHNOLOGY UNIVERSITY (MEIKTILA) FOR THEIR INTEREST AND ENCOURAGEMENT ON OUR RESEARCH WORK.

REFERENCES

- [1] Maung Thein, 1972. Proposal for stratigraphic, Structural, Lithological symbols and Chronographic colour for use in the Burmese Geological Maps: paper read at 1972 Burma Research Congress on Dec, 31, 1972.
- [2] Ei Ei Myo, 2014. Geology and Petrology of Migmatites in Payangazu-Chauksu Taung and Kanabaw Areas, Thazi and Pyawbwe Townships, Mandalay Region. *Unpublished MRes (Thesis)*. Department of Geology, University of Yangon.
- [3] Khin Zaw, 1990. Geological, Petrology and Geochemical characteristics of granitoid rocks in Burma, with special reference to the associated of W-Sn mineralization and their tectonic setting. *Journal of Southeast Asia Each Science*. Vol-4.
- [4] R. Keshavarzi, D. Esmaili, M.R. Kahkhae, M.A. A. Mokhtari, R. Jabari, "Petrology, Geochemistry and Tectonomagmatic Setting of Neshveh Intrusion (NW Saveh)", *Open Journal of Geology*, 2014, 4, pp.177-189
- [5] Hein Min Htike, 2016. Petrology of Plutonic Rocks exposed in Kywedatson Area, Tharzi Township, Mandalay Region. Unpublished M.Sc (Thesis), Department of Geology, Pakokkou University.
- [6] Khin Zaw, 1998. Geological evolution of selected granitic pegmatites in Myanmar (Burma); constraints from Regional Setting, Lithology and fluid-inclusion studies. *International Geology review*, 40:7, p647-662.
- [7] A.K. SINGH & R.K.B SINGH, "PETROGENETIC EVOLUTION OF THE FELSIC AND MAFIC VOLCANIC SUITE IN THE SIANG WINDOW OF EASTERN HIMALAYA, NORTHEAST INDIA", *GEOSCIENCE FRONITERS* 3(5), 2012, PP 613-634.

GEOCHEMICAL CLASSIFICATION OF SANDSTONES OF CHAUK OIL FIELD IN CHAUK TOWNSHIP, MAGWAY REGION

May Thu Aye⁽¹⁾, Dr.Pike Htwe⁽²⁾, Kyi Myo Khaing⁽³⁾

⁽¹⁾ Department of Civil Engineering Technological University, Magway, Myanmar

⁽²⁾ Associate Professor, Geology Department, Pakokku University, Myanmar

⁽³⁾ Department of Civil Engineering Technological University, Monywa, Myanmar

Email: ms.maythuaye86@gmail.com

ABSTRACT: The research area is situated on the eastern bank of Ayeyarwaddy River, in Chauk Township, Magway Region. It is bounded by latitudes N 20° 50' 00" and N 20° 55' 00", longitude E 94° 48' 00" and E 94° 52' 00" in 2094-13 UTM Map. It is covered by the Oligocene to Pliocene clastic sedimentary rocks. Among them, Pyawbwe and Kyaukkok formations were studied to predict the geochemical characteristics of the study area. To conduct XRF analysis, six sandstone samples were taken from the selected layer of sandstone in the Pyawbwe Formation and six sandstones were taken from the selected sandstone layers in the Kyaukkok Formation. According to the chemical classification of sandstone diagram, the sandstones of Pyawbwe and Kyaukkok formations fall within the ‘Litharenite’.

KEYWORDS: River, rocks, Pyawbwe, Kyaukkok, sandstones, Litharenite.

1. INTRODUCTION

The study area, Chauk Oil Field, is situated on the eastern bank of Ayeyarwaddy River, in Chauk Township, Magway Region. Basin. It is bounded by latitudes 20° 50' 00" and N 20° 55' 00", longitude E 94° 48' 00" and E 94° 52' 00" in 2094-13 UTM Map (Fig 1).

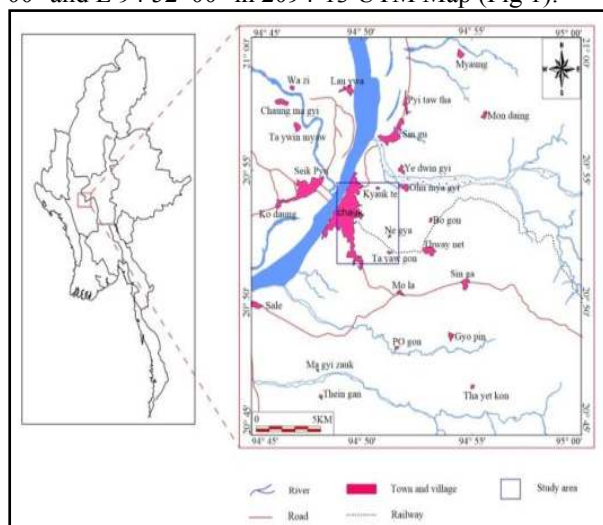


Fig 1. Location map of Chauk Area

The present area is approximately 63 square kilometer (24.1 square mile), 9 km (5.6 mile) long in

north-south direction, and 7 km (4.3 mile) wide in east-west direction.

The present area is approximately 63 square kilometer (24.1 and 7 km (4.3 mile) wide in east-west direction.

2. TOPOGRAPHY

Topographically, the study area can roughly be said as the rolling terrain topography and a range of small hills is running NNW-SSE direction in the eastern part. The highest point of the study area located at the northeastern margin is about 180m above sea level. The western part of the area is bounded by the Ayeyarwaddy River flowing from NNE to SSW. Low land topography is present in the western and central parts of the area (Fig 2).

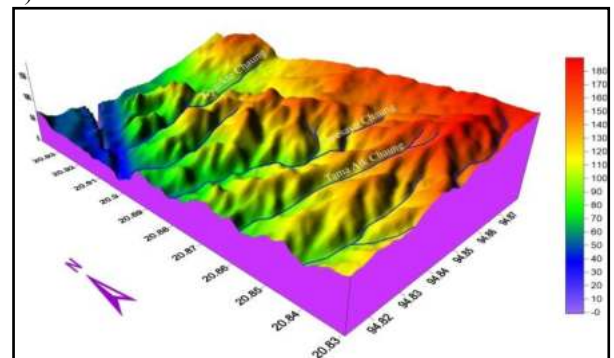


Fig 2. Physiographic map of Chauk Area

3. METHODOLOGY

There are four types of laboratory work; Microscopic analysis, XRF analysis, sieving analysis and porosity analysis. The laboratory works include sample preparation before analysis. All laboratory analysis will be undertaken at chemical Laboratory of Material Science Research Centre, Ela and Laboratory of Geology Department in Magway University.

Microscopic analysis will be conducted to determine the petrology of siliciclastic rocks. The sample preparation for microscopic analysis generally will follow the procedures described in high quality section-making process of Miller (1988). Microscopic identification can be done to characterize the composition and sedimentary texture.

The X-ray Fluorescence (XRF) analysis conducted to know the chemical composition of sandstone and to classify the sandstone. The samples collected in the field were performed chemical analysis as X-Ray Fluorescence. This method is most widely used analysis techniques in the application of quantitative major element analysis, minor and trace element analysis (Hutchison, 1974). Selected samples from the mineralization of the research area were analyzed using X-Ray fluorescence (XRF) for major oxides and some trace elements. In this research-ray fluorescence (XRF) analyses were be done to interpret the chemical classification and weathering of the clastic sediments.

4. STRATIGRAPHY

The research area can be classified into four major stratigraphic units such as (1) Okhmintaung Formation of lower Pegu Group (2) Pyawbwe Formation, and (3) Kyaukkok Formation of Upper Pegu Group and (4) Irrawaddy Formation (Fig 3).

The late Oligocene strata are constituted mainly of yellowish-brown colored, medium-grained sandstones interbedded with the laminated shale. The Miocene of Upper Pegu Group is yellowish-brown colored sandstones and light-gray colored shale and fossiliferous conglomerate band. Late Miocene-Pliocene Irrawaddy Formation is characterized by buff color to yellowish grey, thick-bedded to massive, unfossiliferous friable sandstones which are widely exposed in the flank of the major anticline. The stratigraphic succession and lithology of the Chauk area are shown in Table (1).

Table 1. Stratigraphic succession of Chauk Area

Age	Formation	Lithology	Thickness
Late Mio-Pliocene	Irrawaddy Formation	Yellowish brown to buff colored , medium to coarse -grained, massive sandstone with large scale cross-bedding and fossil wood	629m (Than Htiike Oo, 2012)
Middle Miocene	Kyaukkok Formation	Yellowish brown colored, medium to thick - bedded sandstone with concretion intercalated with shale	266m
Early Miocene	Pyawbwe Formation	Light grey colored mudstone and sandstone with interformational conglomerate containing mud clasts	290m
Late Oligocene	Okhmintaung Formation	Yellowish grey colored , thick -bedded to massive sandstone with subordinate shale and fossiliferous conglomerate band	164m

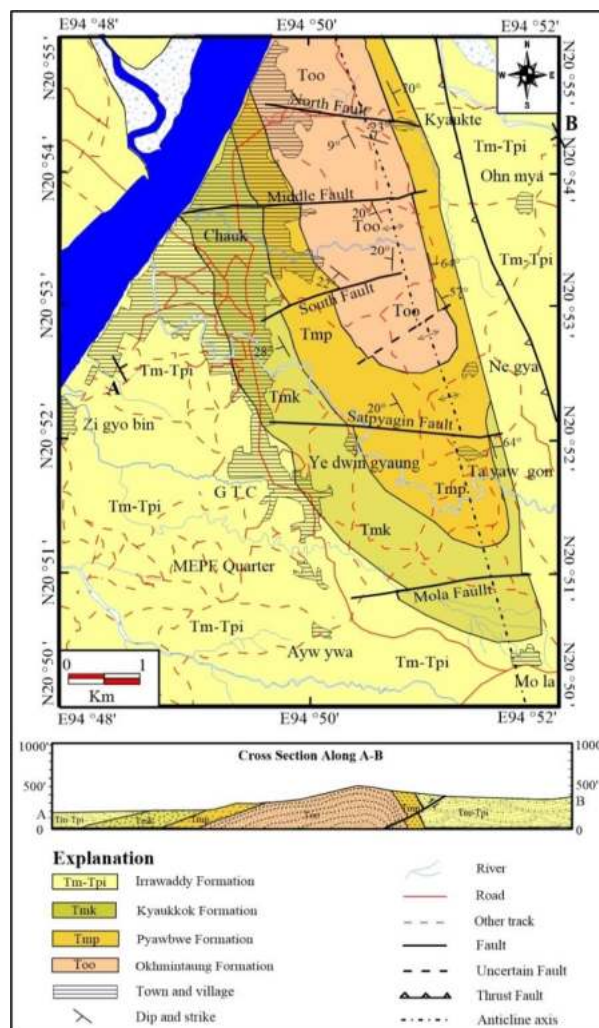


Fig 3. Geological Map of Chauk Area (Modified after M.O.G.E, 1980)

4.1 Okhmintaung Formation

This unit is composed of sandstone with minor amount of conglomerate and thinly grey shale exposing at Okhmintaung Ridge (N 19° 30', E 94° 54') NNW of Thayet, Magway Region. The stratigraphic thickness in type section is 3000 feet.

4.1.1 Distribution and Thickness

The Okhmintaung Formation generally occupies in the core of Chauk Anticline, in the SE of Patamyataung and near the Kyaukte village. The best exposure of this formation is exposed along Kyaukte - Ohnmya road section and east of Chauk. The thickness of Okhmintaung Formation exposed in the present area is 164 m in the present study (Fig 4).

4.1.2 Lithology

The Okhmintaung Formation is composed of medium to thick bedded sandstone intercalated with shale beds and minor thin conglomerate beds. In the study area, yellowish brown colored, fine to medium - grained, medium to thick - bedded sandstone with mud lamination and indurated sand (Fig 5). In the lower part

of this formation. In the upper part, the shale becomes more frequent.

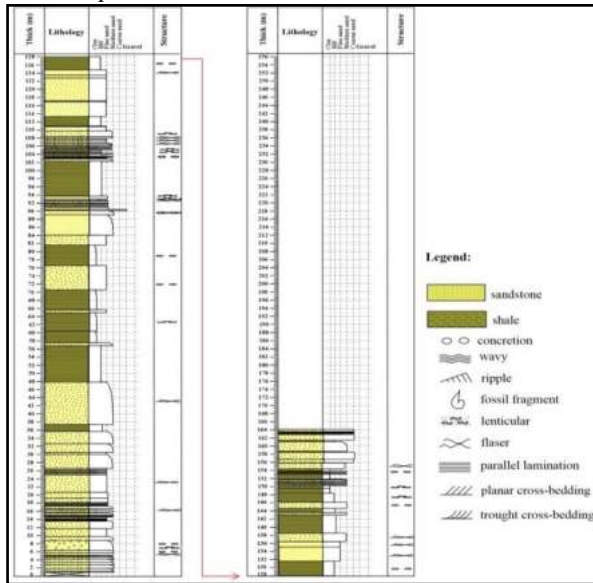


Fig 4. Stratigraphic column of Okhmintaung Formation at Kyaukte Chaung section.



Fig 5. The alternation of light brown, medium bedded sandstone and grey to bluish grey shale with gypsum near the west gate of Kyaukte Village (N20° 54' 38", E 94° 50' 33")

4.2 Pyawbwe Formation

The name of this formation was first introduced by Lepper (1933) as “Pyawbwe Formation” which crops out near the Pyawbwe village (N 20° 01', E 94° 38') in Minbu Township, Magway Region. It is typically about 600 meters thick. The Pyawbwe Formation was previously called the Pyawbwe Clays.

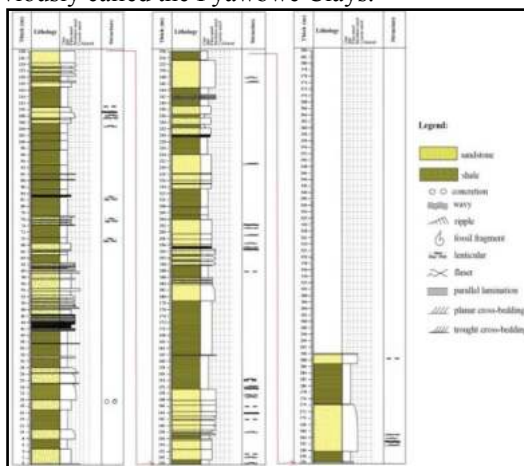


Fig 6. Stratigraphic column of Pyawbwe Formation at Kyaukte Chaung section.

4.2.1 Distribution and Thickness

In the study area, the Pyawbwe Formation exposed both eastern and western flank of Chauk Anticline. According to the asymmetrical nature of the anticline, the exposure of the Pyawbwe Formation in the western flank of major anticline may be wider than that of the eastern flank. In the study area, the best exposure of this formation is exposed near Kyaukte village and along the railway section from Chauk to Tayawgon station. In present study, the thickness of Pyawbwe Formation is about 290 m in Kyaukte section (Fig 6).

4.2.2 Lithology

The Pyawbwe Formation consists mainly of pale brown to bluish grey shale (Fig 7), grey sandy concretionary shale with thin fossiliferous sandstone, occasionally intercalated with indurated sandstone bands and thin conglomerate band. In the upper part of this formation, light brown to dark brown, fine to medium - grained, medium to thickly - bedded, planar and through cross bedding .



Fig 7. Pale brown to bluish grey shale lenticular sand at the stream section near the east entrance of Kyaukte Village (20° 54' 23 "E 94° 49' 40 ")

4.3 Kyaukkok Formation

The name of this formation was given by Lepper (1933) as “Kyaukkok Formation” and exposed near the Kyaukkok village (N19° 54", E94° 43") in the Minbu District, Magway Region.

4.3.1 Distribution and Thickness

The Kyaukkok Formation is well exposed in both flanks of the Major Anticline in the study area. This formation is well cropped out around the Ayesayti Pagoda Hill, Yankintaung (Aungmyay monastery) and west of Chauk railway station. The exposed thickness of this formation is different in places. Generally it was 266 m thick in the western flank of anticline (Fig 8).

4.3.2 Lithology

This formation is dominantly made up of brown to buff colored, fine to medium - grained, medium to thick-bedded sandstone with thin shale partings and sandstones with calcareous concretions rich in fossils. Thinly to medium - bedded, yellowish brown sandstone interbedded with light grey shale are also found within the Kyaukkok Formation (Fig 9). In the lower part of the formation, medium - grained sandstones are more

common, and gradually coarser towards the upper part of this unit.



Fig 8. Yellowish brown sandstone interbedded with light grey shale (N 20° 53' 01", E 94° 49' 57")

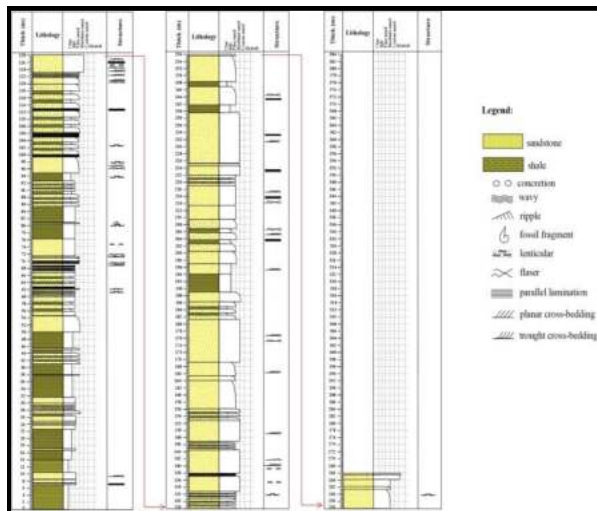


Fig 9. Stratigraphic column of Kyaukkok Formation at railway section in the western flank of anticline

4.4 Irrawaddy Formation

The term “Fossil Wood Group” was firstly used by Theobald (1873) to a sandy, gritty to pebbly sandstone containing abundant silicified wood fossils which overlies the Upper Pegu Group. Later, Noething (1900) described the term “Irrawaddy Series” for the same lithostratigraphic unit.

4.4.1 Distribution and Thickness

The Irrawaddy Formation is well exposed in the Pinmagon, near the Ayeyarwaddy Bridge in the western flank of Chauk Anticline and near the Ohnmya village, NE of Chauk in the eastern flank. This formation is composed of brown to whitish color, coarse to gritty sandstones, mottle clays and occasional pebbly sandstones with silicified wood fossil.

4.4.2 Lithology

The sandstones of yellowish brown to buff colored, massive to thick - bedded with large scale cross bedding are mainly composed in Irrawaddy Formation of Chauk area. Gritty sandstones with pebbly layers are dominant in the lower part. The pebbles are ranging from ½ to 2 inches in diameter and they are well rounded and fairly

sorted. Silicified wood fossils are locally developed in the lower part of this formation.

5. RESULT AND DISCUSSION

The Pyawbwe Formation and Kyaukkok Formation are generally exposed along North - South trending in the study area. A number of good outcrops are situated at both eastern and western flank of Chauk Anticline. Kyaukte stream section and the road section from Taywagon to Chauk are measured in the study area.

To conduct XRF analysis, six sandstone samples were taken from the selected layer of sandstone in the Pyawbwe Formation and six sandstones were taken from the selected sandstone layers in the Kyaukkok Formation.

The three samples (KP.36, KP.84, and KP.128) are selected from the Pyawbwe Formation in Kyaukte stream section and three samples (KP.11, KP.21, KP.34) are selected from the Pyawbwe Formation in Tayawgon railway station.

The three samples (NK 29, NK.60, and NK.95) are taken in the Kyaukkok Formation cropped out in the western flank of Anticline and (NK.19, NK 36, Nk.51) are taken in the Kyaukkok Formation exposed in the eastern flank of Anticline.

The geochemical composition (Wt%) of Pyawbwe Sandstone is shown in Table 2 and Table 3 shows the log ratios of Log ratios of SiO₂/Al₂O₃ and Na₂O/K₂O and Fe₂O₃/K₂O concentration (%) for Sandstone of Pyawbwe Formation.

The weight of geochemical composition (Wt%) of Kyaukkok Sandstone is shown in Table 4 and Table 5 shows Log ratios for SiO₂/ Al₂O₃ and Na₂O/K₂O and Fe₂O₃/K₂O concentration (%) for Sandstone in Kyaukkok Formation.

The classification schemes used are the geochemical classification diagrams of Pettijohn *et al*, (1972). Pettijohn *et al*, (1972) examined the importance of these major oxide variables. The geochemical classification diagram by Herron (1988) classifies them mainly as Fe-sands with little portions on the wacke zone.

The result of log ratio are plotted on chemical classification of sandstone of Pettijohn *et al*, (1972) and Herron (1988). According to the chemical classification of sandstone diagrams (Fig 10), the sandstone of Pyawbwe Formation fall within the Litharenite.

The chemical classification of sandstone diagrams (Fig 11), interpreted that the sandstone of Kyaukkok Formation also fall within the litharenite zone. The litharenite are in fluvial, deltatic environments associated with active continental margins. The source area of these lithic fragments are volcanism, thin-skinned faulting and continental collisions.

Table 2. Oxide composition of sandstone in Pyawbwe Formation

	KP. 128	KP. 36	KP. 84	NP(W). 21	NP(W). 11	NP(W). 34
SiO ₂	70.09	72.4	73.44	68.11	69.82	74.36
Al ₂ O ₃	10.26	9.1	6.84	8.19	10.24	9.48
Na ₂ O	4.65	3.85	3.5	4.85	4.75	3.9
Fe ₂ O ₃	5.98	4.98	5.35	6.57	5.99	4.95
CaO	3.01	3.93	-	3.34	2.93	2.97
K ₂ O	2.92	2.97	2.58	2.97	2.95	2.88
TiO ₂	0.51	0.6	0.39	1.07	0.69	0.54
SO ₃	0.46	0.7	1.04	-	0.55	0.48
Cr ₂ O ₃	0.07	0.17	0.16	0.47	0.13	0.02
MnO	0.21	0.31	3.39	0.53	0.27	0.07
V ₂ O ₅	0.27	-	0.16	0.47	0.13	0.03
ZrO ₂	0.07	0.17	0.16	0.47	0.13	0.02
SrO	0.14	0.18	0.24	0.48	0.13	0.03
CuO	0.07	0.17	0.17	0.46	0.11	0.02
NiO	0.07	0.16	0.16	0.47	0.01	0.04
ZnO	0.064	0.18	0.153	0.48	0.14	0.02
Ag ₂ O	-	-	-	-	0.11	-
Rb ₂ O	-	0.18	0.16	0.48	-	0.04
Y ₂ O ₃	0.064	0.19	0.16	0.46	-	-

Table 3. Log ratios of SiO₂/Al₂O₃ and Na₂O/K₂O and Fe₂O₃/K₂O concentration (%) for sandstone in Pyawbwe Formation

	SiO ₂	Al ₂ O ₃	Na ₂ O	K ₂ O	Fe ₂ O ₃	Log (SiO ₂ /Al ₂ O ₃)	Log (Na ₂ O/K ₂ O)	Log (Fe ₂ O ₃ /K ₂ O)
KP.128	70.09	10.26	4.65	2.92	5.98	0.83	0.2	0.31
KP.36	72.4	9.1	3.85	2.97	4.98	0.9	0.11	0.22
KP.84	73.44	6.84	3.5	2.58	5.35	1.05	0.31	0.31
NP(W)21	68.11	8.19	4.85	2.97	6.57	0.91	0.13	0.34
NP(W)11	69.82	10.24	4.75	2.95	5.99	0.83	0.2	0.3
NP(W)34	74.36	9.48	3.9	2.88	4.95	0.94	0.13	0.23

Table 4. Oxide composition of sandstones in Kyaukkok Formation

	NK.29	NK.60	NK.95	NKe19	NKe36	NKe51
SiO ₂	72.68	70.68	72.03	72.83	69.35	73.29
Al ₂ O ₃	9.04	9.52	8.34	7.63	10.69	7.6
Na ₂ O	2.5	2.65	4.85	4.63	4.5	6.65
Fe ₂ O ₃	4.5	4.08	4.24	4.47	6.49	5.97
CaO	2.98	3.34	3.47	2.89	3.03	2.97
K ₂ O	1.69	1.83	2.11	2.83	2.83	2.91
TiO ₂	0.94	0.94	0.72	0.58	0.6	0.53
SO ₃	0.43	-	0.76	0.63	-	-
Cr ₂ O ₃	0.27	0.47	0.33	0.23	0.16	0.02
MnO	0.24	3.5	0.43	0.4	0.37	0.12
V ₂ O ₅	0.19	0.46	0.33	0.24	0.16	0.02
ZrO ₂	0.18	0.47	0.32	0.23	0.16	0.03
SrO	0.18	0.46	0.34	0.26	0.17	0.03
CuO	0.16	0.45	0.32	0.22	0.143	0.02
NiO	0.16	-	-	-	0.15	0.01
ZnO	0.16	0.45	0.32	0.22	0.134	0.02
Ag ₂ O	-	-	0.32	0.23	-	-
Rb ₂ O	-	-	-	0.23	-	-
Y ₂ O ₃	-	-	-	-	0.134	0.04

Table 5. Log ratios for SiO₂/Al₂O₃ and Na₂O/K₂O and Fe₂O₃/K₂O concentration (%) for Sandstone in Kyaukkok Formation

	SiO ₂	Al ₂ O ₃	Na ₂ O	K ₂ O	Fe ₂ O ₃	Log (SiO ₂ /Al ₂ O ₃)	Log (Na ₂ O/K ₂ O)	Log (Fe ₂ O ₃ /K ₂ O)
NK.29	72.68	9.04	2.5	1.69	4.5	0.905	0.17	0.42
NK.60	70.68	9.52	2.65	1.83	4.08	0.87	0.16	0.34
NK.95	72.03	8.34	4.85	2.11	4.24	0.93	0.36	0.3
Nke.19	72.83	7.63	4.63	2.83	4.47	0.97	0.21	0.19
Nke.36	69.35	10.69	4.5	2.83	6.49	0.81	0.2	0.36
Nke.51	73.29	7.6	6.65	2.91	5.97	0.98	0.35	0.31

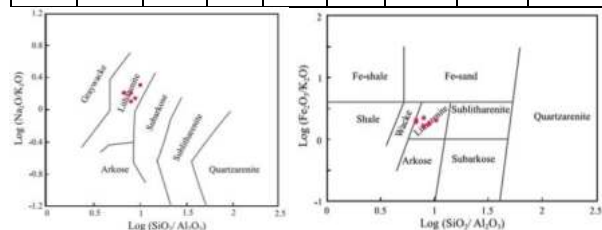


Fig 10. Chemical classification of sandstone samples from Pyawbwe Formation based on (a) log (SiO₂/Al₂O₃) vs.log (Na₂O/K₂O) diagram of Pettijohn *et al.* (1972), and (b) log (SiO₂/Al₂O₃) vs.log (Fe₂O₃/K₂O) diagram of Herron (1988).

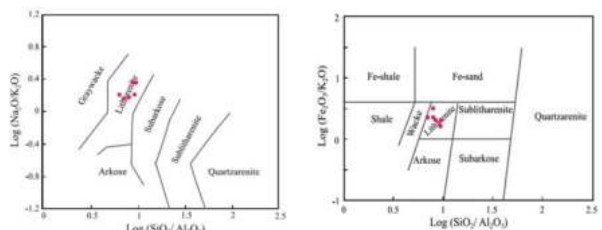


Fig 11. Chemical classification of sandstone samples from Kyaukkok Formation based on (a) log (SiO₂/Al₂O₃) vs.log (Na₂O/K₂O) diagram of Pettijohn *et al.* (1972), and (b) log (SiO₂/Al₂O₃) vs.log (Fe₂O₃/K₂O) diagram of Herron (1988).

6. CONCLUSIONS AND RECOMMENDATIONS

The composition of sandstone can be got from XRF analysis. Sandstone is classified and named based on their major oxides elements. The concentration of three major oxide groups have been used to classify sandstones; silica and alumina, alkali oxides, and iron oxides plus magnesia.

Based on the chemical classification of sandstone diagrams of Pettijohn *et al.*, (1972), and of Herron (1988) the sandstones of Pyawbwe and Kyaukkok formations are litharenite sandstone. These sandstones are derived from volcanism, thin-skinned faulting and continental collisions. The depositional environments of litharenite sandstones are fluvial and deltatic environments.

The feldspar composition of litharenite sandstone is less than 25 percent. The Early to Middle Miocene litharenite sandstones in Chauk Oil Field are mainly composed of 65-75% quartz. Quartz is one of hard and the most stable mineral. It is also high resistant to weathering process. Therefore, the reservoir quality of

litharenite sandstones of Pyawbwe and Kyaukkok formations may be fair to good.

ACKNOWLEDGEMENTS

I am greatly thankful to my supervisor, Dr. Khin San, Professor (Head of Geology Department), Magway University, her permission, supervision and for her departmental facilities.

The author would like to express Dr. Paik Htwe, Associate Professor, Geology Department, Pakokku University, for his reading and repairing and suggesting of the manuscript and for his supervision throughout the course of this study. Finally, I wish to thank to all teachers in Geology Department, Magway University, and my colleagues of the same department for their help and encouragement throughout the course of this research work.

REFERENCES

- [1] Eames, F.E., 1951, 'The Peguian System of Central Burma': *Rec.Geol.Surv. India.V-91*, pp . 2.
- [2] Lepper, G .W., 1933, 'Geology of the oil bearing regions of the Chindwin- Irrawaddy valley of Burma and of Assam-Arakan, Proc. World Petroleum Congress', vol.1, p.15-25.
- [3] MGS, 2014, Myanmar Geosciences Society, 'Geological Map of Myanmar (2014)', Scale 1:2,250,000.
- [4] M.O.G.E, 1980, 'Geological Map of Central Myanmar Basin', Scale 1inch to 4 miles.
- [5] Pettijohn, F. J, Potter, P. E., Siever, R., 1972, 'Sand and Sandstones'; New York, Springer- Verlag.
- [6] Herron, M. M, 1988, 'Geochemical classification of terrigenous sands and shale from core or log data': *Journal of Sedimentary Petrology*, 58, 820-829.
- [7] Noethling. F., 1990, 'The Miocene of Burma', *Verhandelingen der Koninklijke Akademie van Wetenschappenerhandelingen*, (2)7(2), 1-131,1 map.3 figs. Amsterdam
- [8] Theoblad, 1873, 'The Geology of Pegu', *Memoirs of the geological survey of India*, 10 (2), p.189-359.
- [9] Than Htike Oo, 2012, 'Mechanical analysis of Kyaukkok Formation in Chauk Area Magway Region', Unpublished MSc thesis, Magway University
- [10] Miller, J., 1988, 'Microscopic techniques: 1, Slices, slides, strains and peels: in *Techniques in Sedimentary:*' Tucker, M, Eds, Blackwell Scientific Publications, Oxford, p.86-107.
- [11] Hutchison C.S., 1974, 'Laboratory Hand Book of Petrographic Techniques'

Stratigraphy and Geochemical Characteristic of Volcanic and Pyroclastic rocks in Yedwet-Wetkyikan area, Kyaukpadaung Township, Mandalay Region

Kyi Myo Khaing⁽¹⁾, Hline Wint Wint Hmue⁽²⁾, May Thu Aye⁽³⁾

⁽¹⁾Technological University (Monywa), Myanmar

⁽²⁾Technological University (Lashio), Myanmar

⁽³⁾Technological University (Magway), Myanmar

Email: kyimykhaingcivil@tumonywa.edu.mm

hlaingwintwinthmue@tulashio.edu.mm

maythuaye@tumg.edu.mm

ABSTRACT: The investigated area is situated in the Kyaukpadaung Township, Mandalay Region. Physiographically, the study area is a low-land area with high denudation hills, Kyaukpadaung Taung (Gaungni Taung), Yedwet Taung, Wetkyikan Taung trending NNW-SSE. The rocks exposed in this area are volcanic rocks (silicified rhyolite and hornblende-biotite dacite), pyroclastic rocks (rhyolitic tuff and dacitic tuff), ferruginous conglomerates, mud pebbly gritty sandstones, sandstones and mudstones of Irrawaddy Formation. The age of these rocks probably range from Late Miocene to Pliocene. Geochemical data has been used to characterize the volcanic rocks in the present area. These lava and pyroclastic, rhyolites and dacites are plotted within the field of low, medium, high K series. In classified diagram $\text{Na}_2\text{O}+\text{K}_2\text{O}$ vs SiO_2 made between alkaline and sub alkaline series, all samples fall in the field of tholeiitic series.

KEYWORDS: volcanic rocks, irrawaddy formation, K series, sub alkaline series, tholeiitic series

1. INTRODUCTION

In the present area, clastic sediments of considerable thickness and volcanic and volcanoclastic rocks are exposed. These rocks range in age from late Miocene to Recent. In the study area, the Irrawaddy Formation is a unit of sedimentary rocks composed of (coarse to gritty sandstones, mud pebbly sandstones, intraformational conglomerates and tuffaceous sandstones with silicified wood-fossils), about 2 furlongs NW of the Kyaukpadaung area. The sandstones are reddish brown to dark colored, very coarse-grained, highly jointed and very thick bedded. Gritty sandstones with mud pebbles are dominant and ferruginous in the lower part. The mud pebbles are 6 inches to 1 foot in diameter and they are greenish gray, subrounded and poorly sorted. Intraformational quartz pebbly conglomerates are locally present in this lower part. They overlie the mud pebbly gritty sandstones. The tuffaceous sandstones are medium to

coarse grained and very thick bedded. They are white to ash-gray in color. Silicified wood-fossils are locally developed in this formation of the study area.

1.1 Location of the Study

The study area is located in the Kyaukpadaung Township, bounded by north latitudes $20^{\circ}45'00''$ - $20^{\circ}49'32''$ and east longitudes $95^{\circ}04'40''$ - $95^{\circ}13'35''$. It occupies parts of one inch topographic maps 84P/1 and 84P/5. The location of the study area is shown in Fig.1.

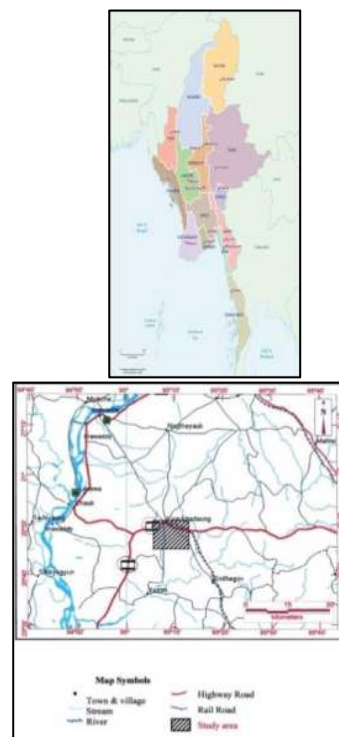


Fig 1. Location map of the Kyaukpadaung area

The present area is about 11 miles long and 7.5 miles wide in east-west and north-south directions, respectively, covering 70 square miles of fairly rugged terrain because of high denudational hills. It is situated

at about ½ miles S of Kyaukpadaung and readily accessible through the year.

1.2 Topography

Physiographically, the study area is a low-land area with high denudational hills trending NNW-SSE. The highest point is Kyaukpadaung Taung (Gaungni Taung) of 1888 feet in height in the northern part of the area. The other conspicuous features are the isolated hills which are trending from NNW-SSE, Yedwet Taung (1250 feet), Wetkyikan Taung (1505 feet) in the vicinity of the Wetkyikan village.

The present area lies in the dry zone of the Central Myanmar. The monsoon normally starts from the near end of May and ends in October, and the annual rainfall is approximately about 46 inches. The average temperatures are 102.4°F in summer and 58.3°F in winter. Digital elevation map (DEM) of dome-shape hills are seen to slope up in the form of the volcanic dome (looking north-east) as shown in fig.2.

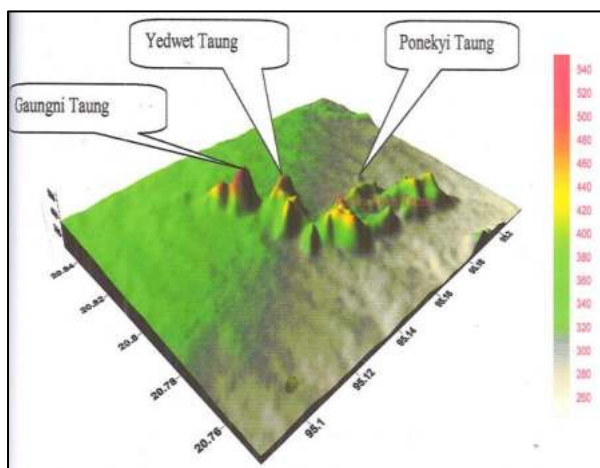


Fig 2 Digital elevation map of the Kyaukpadaung area

1.3 Regional Geologic Setting

The area occupies a part of the eastern through and is situated near the Central Volcanic Line that runs north-south. About 8 miles north-east of the area, there lies the best known distinct Mount Popa volcano which rises magnificently and majestically above the arid plains. It is considered to be a dormant volcano. The study area is falling in the Central Igneous Belt among the four igneous belts in Myanmar (Maung Thein, 2010). The Central Volcanic Line is a 1500 km-long volcanic arc, consisting of igneous rocks ranging in age from Early Triassic to Pleistocene (Chhibber, 1934). The Eastern and Western Troughs (separated by the Central Volcanic Line) contain sequence of deformed shallow marine and fluvial sediments up to 800m thick. The sediments reflect a gradual filling of the basin during Tertiary Period (Aung Khin and Kyaw Win, 1969).

The present area is situated at the northern tip of Bago Yoma which has been considered as an

anticlinorium. In the SW part of the area, the Mio-Pliocene clastic sediments are overlain by the Quaternary deposits.

The intermittent volcanism in the mapped area during the Pliocene time resulted in the interfingering of the Irrawaddy sediments and pyroclastic rocks.

2. METHOD OF STUDY

2.1 Field Method

Field method of the study area was carried out during the winter of 2010, using a field map on a scale of 1 inch to 1 mile. Photo geological structures plotted on the base map were thoroughly checked in the field and corrections were made where necessary. While traversing along stream and road cutting and the visible outcrops exposed at the slope-sides and on the tops of the hills the geological structures such as dip, strike, and joints were measured and recorded in the field note book. Formation boundaries, marker beds and lithology were plotted on the base map. While measuring the stratigraphic sections, detailed lithological features were recorded, thickness of individual beds was measured, and representative samples were collected and randomly selected for detailed laboratory study. Both hard and loose sandstone and volcanic rock samples were collected, carefully packed, and labelled. The outcrop data are usually located by using the G.P.S and the necessary photographs of the outcrops are taken by the digital camera.

2.2 Analytical Method

A total of fresh 20 rock samples from the several location were selected for geochemical analysis. These samples were crushed and pulverized into powder from by using tungsten carbide crushes and milling respectively for geochemical analysis. The geochemical analysis was conducted by using X-ray Fluorescence (XRF). Geochemical X.R.F analysis of major oxides was obtained from the URC (University Research Centre) in Yangon University.

3. STRATIGRAPHY

In the present area, clastic sediments of considerable thickness and volcanic and volcanoclastic rocks are exposed. These rocks range in age from late Miocene to Holocene. The rock sequence and stratigraphic column of the study area are shown in Fig.3.

Being situated on the middle part of the Central Volcanic Line of Myanmar, the present area chiefly includes various volcanic rocks which form all dome-shaped hills associated with the sedimentary rocks of Irrawaddy Formation. The volcanic and volcanoclastic rocks are well exposed in the Kyaukpadaung area. The

sedimentary units cover the remaining three-fourth of the study area.

The sedimentary rocks are generally sandstones, mudstones, gritty sandstones and conglomerates of Irrawaddy and Quaternary deposits. The Quaternary deposits (Plateau Gravel and Red Earth) are well exposed in the south western part of the study area, and overlie unconformably the sedimentary rocks of the Irrawaddy Formation which are intruded by the volcanic rocks in some places. The alluvium deposit covers the western part of the study area.

3.1 Sedimentary of Rock Units

Irrawaddy Formation: A unit of sedimentary rocks composed of (coarse to gritty sandstones, mud pebbly sandstones, intraformational conglomerates and tuffaceous sandstones with silicified wood-fossils), about 2 furlongs NW of the Kyaukpadaung area, is referred to as the Irrawaddy Formation. Stratigraphically, they form the topmost part of the Tertiary succession. These sedimentary strata are previously named as "Fossil Wood Group" by Theobald in 1873, on account of the abundance of silicified woods. Later on this unit was treated as a time stratigraphic unit by Noetling (1900) and he introduced the name "Irrawaddy Series" for those groups of rocks formed in the late Tertiary Period. The Irrawaddy Formation, in the study area, is best exposed near the Kyaukpadaung where it is mainly composed of less-indurated coarse to gritty, mud pebbly sandstones and conglomerates.

When weathered, the sandstones are reddish brown to dark color, when fresh, they are whitish gray to reddish brown colored, very coarse-grained, jointed sandstone and very thick bedded (Fig 3). In some places, these sandstones are medium to coarse-grained, yellowish brown to reddish brown colored with the large scale trough type cross bedding (Fig. 4)



Fig 3. Very coarse-grained, jointed sandstone and very thick bedded sandstone in Irrawaddy Formation (N 20°49'36" and E 95°07'30")



Fig 4. Medium to coarse-grained, yellowish-brown to reddish brown colored sandstone with large-scale trough type cross-bedding in Irrawaddy Formation (N 20° 49'30" and E 95°07'34")

Plateau Gravel and Red Earth: The Plateau Gravel and Red Earth is nearly horizontal and it unconformably overlies the Irrawaddy Formation. The angular relationships between the gravels and older units are visible in deeply dissected stream sections.

The Plateau Gravel is well exposed in the western part of the study area where characteristic badland topography is developed. The Plateau Gravel is composed dominantly of quartz pebbles with deep red ferruginous sand. The sizes of clasts range from 1/2 to 5 inches in diameter.

The structures of the Plateau Gravel are sub parallel wedge-shaped deposits and cross-bedded bodies. The maximum thickness of the gravels is estimated to be 150 feet at some places. These bodies are thinning towards south-west. Sometimes, the Plateau Gravel is difficult to differentiate from those of the lower part of the Irrawaddy Formation.

Recent alluvium covers the Plateau Gravel conformably in westerly part of the Yedwet-Wetkyikan area.

3.2 Igneous Rock Unit

General Statement: Chhibber (1934) classified the volcanic rocks of the study area into "older volcanics" and "younger volcanics". The former are interbedded and filled with sediments, while the latter are represented by the rocks of Mt. Popa (4981 feet). In this respect, the rhyolites associated with other volcanoclastic rocks of the present area are much older than the rocks of Mt. Popa.

The igneous rocks of the older group mainly crop out in the study area. These older volcanics are subdivided into the two units:

1. Hornblende-biotite dacite and its pyroclastics (Volcanic breccias and tuffs) and
2. Rhyolite and its pyroclastics (Volcanic breccias and tuffs)

These units are distinct petrologically from one to another. Rock sequences for the study area are shown in Table 1.

TABLE 1. EXPOSED ROCK SEQUENCE OF THE YEDWET-WETKYIKAN AREA

Rock Unit	Age
Sedimentary Rocks	
- Alluvium	Holocene
- Plateu Gravels and Red Earth	Pleistocene

- Irrawady Formation	Late Miocene – Pliocene
Igneous Rocks	
-Hornblende-biotite dacite and its pyroclastics (Volcanic breccia & tuffs)	Late Miocene - Pliocene
- Rhyolite and its pyroclastics (Volcanic breccia & tuffs)	

Rhyolite and its pyroclastics (Volcanic breccias and tuffs): These volcanic rocks occur as the blocky lavas and occasional silicified lava domes. They are white, grey or light yellow in color and usually form small hillocks. All of the hills, such as Kyaukpadaung Taung or Gaungni, Yedwet Taung, and Wetkyikan Taung are built up of rhyolite and its pyroclastics (volcanic breccias & tuffs).

The units form fine-grained, reddish brown, holocrystalline rock with the phenocrysts of quartz and feldspar. The rhyolites of the hills commonly occupy the western slopes of the hills and the pyroclastic rocks, the eastern slopes of the hills.

At the east side of the Wetkyikkan Taung, the rhyolitic tuffs may be intruded by the quartz vein. In some places, the joint planes of the tuffs are oxidized and caused by the alteration of the mafic minerals in these tuffs (Fig.5).

At the west of the Wetkyikan Taung, the tuffs are found associated with the volcanic breccias, constituted of the pebbles of the tuffs and silicified rhyolites (Fig.6).



Fig 5. The joint planes of the tuffs of the mafic minerals in the rhyolitic tuffs (N 20°47'19" and E 95°10'52")



Fig 6. The tuffs associated with the volcanic breccia, constituted of the pebble of the tuff and silicified rhyolites at the west of Wetkyikan Taung (N 20°47' 32" and E 95°10'27")

The Gaungni Taung is a dome-shaped hill made up of silica-rich lava. At the base of Gaungni Taung the silicified rhyolites are found as the scattered blocks and irregular bodies. Some rhyolites may be altered to ironstones due to the oxidation along their joint planes (Fig.7).

At the middle part of the Gaungdi Taung, the volcanic breccias about 15 feet in thickness are associated with the silicified rhyolites and tuffs (Fig.8).



Fig 7. Rhyolite altered to ironstones due to the oxidation along their joint planes (N 20°49'10" and E 95°08'11")



Fig 8. Volcanic breccias about 15 feet in thickness associated with silicified rhyolite and tuff at Gaungni hill (N 20°40'06"and E 95° 08' 13")

Biotite dacite and its pyroclastics: North of the Wetkyikan village, about 2 forlongs occur as the scattered blocks and dykes of the shallow type with trending N-E. They may be considered to have intruded after complete sedimentation of Irrawaddy Formation and intrusion of rhyolite and its pyroclastics. In this place, the layer deposits of tuffs may probably be intruded by the later-formed dacite dykes, because of the presence of tuff xenoliths are formed within the dacites (Fig.9 & 10).



Fig 9. Layer deposits of tuffs probably intruded by the later-formed dacite dykes (N 20°47'52" and E 95°11'05")



Fig 10. Xenolith of tuff occurred within later-formed hornblende-biotite dacite (N 20°47'52" and E 95° 11' 05")

4. GEOCHEMICAL CHARACTERISTICS OF VOLCANIC AND PYROCLASTIC ROCKS

Twenty six samples are collected from the several locations in the Kyaukpadaung area for geochemical analysis. These data has been used to specify and characterize the volcanic rock in the present area. Geochemical X.R.F analysis of major oxides was obtained from the U.R.C (Universities Research Center) in Yangon University. Representative major elements analysis of the volcanic and pyroclastic rocks of the area is shown in Table 2 and 3.

The total alkali-silica diagram (TAS) is one of the most useful classification schemes available for volcanic and pyroclastic rocks. Major element data suggest that the lava of the study area predominantly rhyolites according to their position in the (Na₂O + K₂O) vs SiO₂ diagram. They are plotted within the field of silicified rhyolite, rhyolitic tuff, dacite, and dacitic tuff. They are better classified using the K₂O-SiO₂ diagram (Peccherillo and Taylor, 1976) shown in fig. 12. These lavas and pyroclastics are plotted within the field of high- K series.

Volcanic rocks may be subdivided into major magma series-alkaline and sub alkaline (original termed tholeiitic) series. The classified diagram Na₂O+K₂O vs SiO₂ of Cox *et.al.*, (1979), fig 13, gives the boundary line on the diagram which allows a distinction to be made between alkaline series and sub alkaline series. In this diagram the rocks of the study area plotted fall in the alkalic part of the diagram. They are plotted within the field of rhyolites and dacites. It is known that rhyolites are dominant rock type in this area. In fig. 14, the alkali content that separate the sub alkaline from the alkaline varies with the silica content of the rock. According to the figures, the samples show the sub alkaline nature.

TABLE 2.MAJOR OXIDE COMPOSITION (W %) OF THE RHYOLITES IN THE STUDY AREA (X.R.F ANALYSIS OBTAINED FROM U.R.C)

Sample No.	YR1	WR1	GR1	Yt1	Wt1	Gt1
SiO ₂	69.15	70.24	70.44	70.12	70.32	69.76
TiO ₂	0.36	0.37	0.33	0.38	0.38	0.40
Al ₂ O ₃	9.27	11.25	10.90	10.42	9.13	10.37
Fe ₂ O ₃ ⁺	2.53	2.67	2.94	2.97	1.21	-
FeO	-	-	1.23	-	1.18	-
MnO	0.09	-	-	-	0.08	-
MgO	1.22	1.30	1.31	1.32	1.13	1.09
CaO	3.42	3.360	3.38	3.38	3.42	3.40
Na ₂ O	2.51	2.64	2.60	2.48	2.70	2.80
K ₂ O	5.59	5.80	5.13	5.26	5.30	5.36
H ₂ O	1.73	1.12	0.34	2.16	2.08	1.87
H ₂ O ⁻	0.87	0.73	0.75	0.74	0.85	0.76
P ₂ O ₅	0.21	0.27	0.26	0.23	0.27	0.29
Total	97.71	99.68	99.61	100.05	98.05	97.43

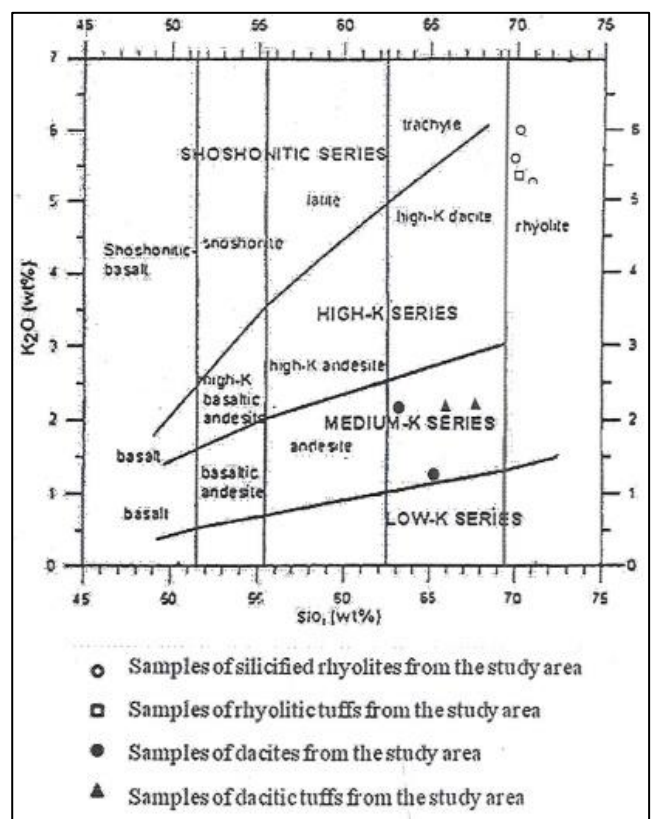


Fig 11. Plot of the studied lava and pyroclastics in the classification diagram K₂O-SiO₂ (Peccherillo and Taylor, 1976)

TABLE 3.MAJOR OXIDE COMPOSITION (W %) OF THE TUFFS IN THE STUDY AREA (X.R.F ANALYSIS OBTAINED FROM U.R.C)

Sample No.	Pd1	Td1	Pdt1	Tdt1
SiO ₂	57.75	64.17	68.53	66.97
TiO ₂	0.04	0.42	0.39	0.59

Al ₂ O ₃	13.61	14.26	10.94	10.40
Fe ₂ O ₃ ⁺	1.67	2.29	3.30	3.41
FeO	3.74	1.04	-	1.68
MnO	0.09	-	-	0.09
MgO	1.51	1.32	1.35	1.81
CaO	5.43	5.39	5.38	6.95
Na ₂ O	3.36	3.67	3.39	3.63
K ₂ O	2.34	1.47	2.94	2.85
H ₂ O	2.70	1.18	2.98	1.20
H ₂ O-	1.05	0.81	1.09	0.79
P ₂ O ₅	0.30	0.25	0.32	0.15
Total	99.55	97.27	100.61	99.82

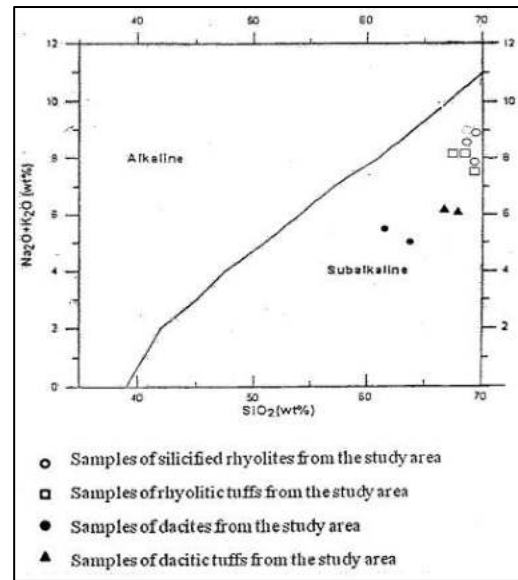


Fig 13. Plot of the studied lavas and pyroclastics in the classification diagram Na₂O+K₂O vs SiO₂ diagram separating the tholeiitic series (After Kuno, 1966)

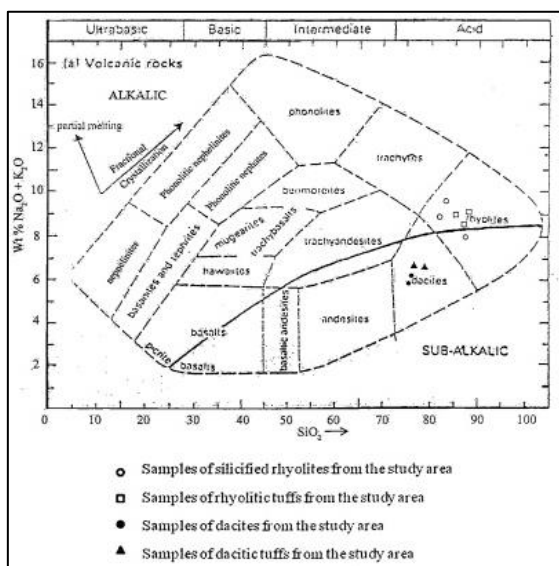


Fig 12. Plot of the studied lavas and pyroclastics in the classification diagram Na₂O+K₂O vs SiO₂(Cox et. al., 1979)

4. CONCLUSIONS

In the present area, clastic sediments of considerable thickness, volcanic and volcanoclastic rocks are exposed. These rocks range in age from Late Miocene to Pliocene. In the study area, the Irrawaddy Formation is a unit of sedimentary rocks composed of (coarse to gritty sandstones, mud pebble sandstones, conglomerates and tuffaceous sandstones with silicified wood fossils) about 2 furlongs NW of the Kyaukpadaung area.

The igneous rocks of the older group mainly crop out in the study area. These older volcanics are subdivided into two units: (2) Hornblende-biotite dacite and its pyroclastics (Volcanic breccias and tuffs), (1) Rhyolite and its pyroclastics (Volcanic breccias and tuffs).

Geochemical data has been used to characterize the volcanic rock in the present area. Geochemical X.R.F analysis of major oxide was obtained from the U.R.C in Yangon University. They are better classified using K₂O+SiO₂ diagram (Peccherillo and Taylor, 1976). These lava and pyroclastic rocks are plotted within the field low, medium, high K series. In classified diagram Na₂O +K₂O vs SiO₂ of Cox et.al.(1979) made between alkaline series and sub alkaline series, the rock of the study area plotted fall in the sub alkaline part of the diagram. They are plotted within the field of rhyolites and dacites. In the Na₂O + K₂O vs SiO₂ diagram. All samples fall in the field of tholeiitic series. In Na₂O + K₂O vs SiO₂ diagram (Irvine & Baragar, 1971) the sample show the sub alkaline nature.

ACKNOWLEDGEMENT

I would like to express deep gratitude to U Myint Zaw Han (Head of Department of Geology, University of Magway, Retired) for valuable suggestions, systematic guidance of the research work.

REFERENCES

- [1] Aung Khin and Kyaw Win, "Preliminary studies of the paleogeography of Burma during the Cenozoic". Union of Burma Journal. *Sci. & Tech.* Vol.1.no.2. pp. 241-251.1969.
- [2] Chhibber, H. L. "The Geology of Burma. Macmillan London".1934.
- [3] Cox, K.G., Bell J.D. and Pankhurst, R.J, "The interpretation of igneous rocks". London: Alen un win.1979.
- [4] Irvin, T.N., Baragar, W.R.A., "A guide to chemical classification of common volcanic rocks". *Canadian Journal of Earth Sciences.* 8. pp.211- 218.1971.
- [5] Maung Thein, "A preliminary syntaxis of the geological evolution of Burma with reference to the tectonic development of Southeast Asia". *Geological Society of Malaysia Bulletin.* 6, pp. 87-116.2010.
- [6] Neotling, F. "The Miocene of Burma: Mem". *Geol. Surv. India, Vii*, pp. 2.1900.
- [7] Peccerillo, A. and Tayer, S.R, "Geochemistry of Eocene cal-alkaline volcanic rocks from the Kustamanu Area, northern Turkey, Contrib". *Mineral Petro.* 58, p. 63-81.1976.
- [8] Theobald, W. "The Geology of Pegu, Memoirs of the geological survey of India". 10(2). pp. 224- 302. 1873.

Provenance study of The Zigyaing Formation of Thegyaung-Mawdin Area, Ngapudaw Township, Ayeyarwady Region

Chaw Su Hlaing ⁽¹⁾, Su Hnin Lwin ⁽²⁾

⁽¹⁾ Lecturer, Department of Geology, West Yangon University

⁽²⁾ Assistance Lecturer, Department of Geology, West Yangon University
chawsuhlainggeol09@gmail.com, suhninlwin26@gmail.com

ABSTRACT

The petrography of sandstone of Zigyaing Formation exposed at the coastal area near Zigyaing Village, have been investigated to determine their provenance by petrographic analysis. The sandstones of the Paleocene-Eocene unit have been analyzed for their provenance, and diagenetic history. These sandstones are fine to very coarse grained and poorly- to moderate sorted. The constituent mineral grains are subangular to subrounded. Detail petrographic studies of sandstone samples from the Zigyaing sandstone contain abundant quartz and lithic grains with subordinate feldspars, accessory amount of mica. These sandstones comprise (62% to 78%) of the detrital grains and about 32% of the argillaceous matrix. According to the Folk (1974) sandstone classification, the Zigyaing sandstone falls within the field of Feldspathic - lithic graywacke, and Lithic graywacke. The petrofacies analysis reveals that these sandstones belong to the Recycled orogen provenance.

Key words: Zigyaing Formation, Petrofacies, Provenance, Recycled orogen Tectonic settings

1. INTRODUCTION

Thegyaung-Mawdin area is situated in Ayeyarwaddy Region, south-western part of the Myanmar. It is bounded between North Latitudes 15° 57' 00" to 16° 17' 30" and East Longitudes 94° 9' 30" to 94° 16' 30" covering about 50 square miles (Fig.1). The study area can be divided into two regions, physically, the western upland and the adjoining coastal shoreline in the west. The upland region constitutes the rugged hilly terrain with north-south trending ridges of Rakhine Yoma. Along the shoreline, the wave-cut platforms reveal water polished exposures. Geological mapping prepare by using tape and compass traverse method (Fig.2).The study area comprises the three sedimentary rock units of flysch type sediments.

1.1. Purpose of Study

The present study mainly emphasized on the petrographic characteristics of the sandstone of the Zigyaing Formation.

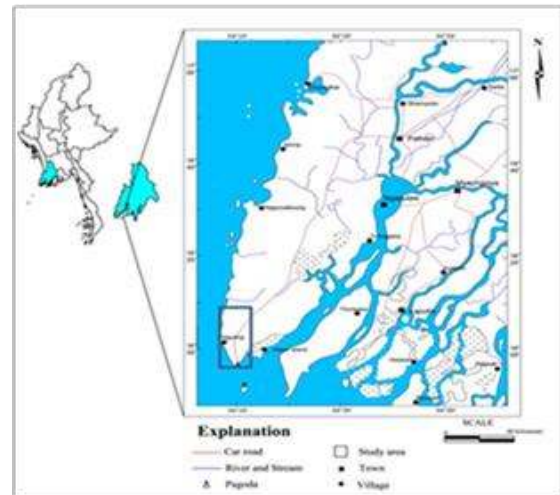


(Fig .1) Location Map of the study Area

1.2. Methodology of Research

The researcher collected the detail data of area in order to construct the geological map of research area. The sample has to collect within the research area to do the analysis about petrography. Then, the researcher tries to identify the provenance of the research area.

1.3. Tectonic Settings

Myanmar has been divided geomorphologically and tectonically into four main belts (Stamp 1922, Chibber 1934, Tuinsh 1950, Win Swe 1981, Maung Thein 1973, 1983, 2000). The study area constitutes the southwestern coast of Rakhine Yome Ranges, the southern segment of Western Ranges or Indo Burma Ranges.

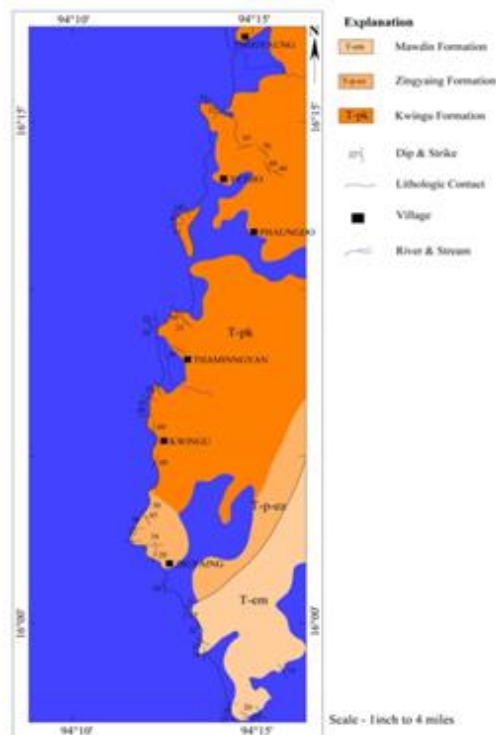


(Fig. 2) Geological map of the study area (Modified from Paw Tun 1974)

2. RESULT AND DISCUSSION

Petrographic Study

Representative sandstones samples were collected from the Kwings Formation, Zigyaing Formation, and Mawdin Formation exposing along coastal of Thegyaung-Mawdin area. Among them selected thin sections were prepared and examined under polarizing microscope for petrology and provenance analysis of Zigyaing sandstones. Fairly detailed point counts of Lithic grains as well as standard QFL % plotted on triangular classification scheme of Folk (1974) is utilizing for classification purpose. A total of 400 framework grains were identified per thin section for QFL mode and lithic population at spacing of 0.33mm.

2.1 Petrography of the Sandstones of Zigyaing Formation

Microscopically, Zigyaing sandstones constitute 62% to 78% of detrital grains and about 32% of matrix to the total rock volume. These sandstones are generally medium to coarse grained, light grey to grey colored and are mainly comprised of quartz, feldspar, mica and rock fragments, and minor accessories minerals. Various types of grain to grain contacts such as point, long, tangential and concavo-convex contact are observed in sandstones of Zigyaing Formation. The detrital elements are embedded in the argillaceous matrix. The maximum grains size varies from 0.3mm to 0.8 mm in diameter and the minimum grain size varies from 0.05mm to 0.45mm in diameter.

Quartz

In the Zigyaing sandstones, quartz is abundant detrital mineral. Detrital quartz grains, both monocrystalline and polycrystalline, which comprise about 25% to 40% of total detrital fractions (Fig.5, 6). Most of monocrystalline quartz grains are sub-angular to sub-round and sub-sequent to sub-elongate in shape. Nearly 4% to 10% of the monocrystalline quartz grains show undulatory extinction and some grains show wavy extinction. A few polycrystalline quartz grains of igneous derivation and metamorphic derivations are present. The maximum grains size varies from 0.2mm to 0.4 mm in diameter and the minimum grain size varies from 0.05mm to 0.15mm in diameter.

Feldspar

Plagioclase and orthoclase feldspar grains consist about 15% to 25% of the total detrital fractions. Plagioclase feldspars are more common than orthoclase feldspar. Plagioclase feldspar is more than 80% of the total feldspar and some are slightly altered and found as dusty, cloudy or brown colored appearances in PPL. The size of feldspar ranges from 0.5 to 0.85 mm in diameter. Most of plagioclase twin bands are distinct (Fig.7, 8). The maximum grains size varies from 0.05mm to 0.2 mm in diameter and the minimum grain size varies from 0.03mm to 0.07mm in diameter.

Mica

In the Zigyaing sandstones, biotite and muscovite are fairly common detrital fraction ranging from about 1% to 3 % of total detrital fractions are micas, in which biotite is much more dominate. Both biotite and muscovite are distorted by grain to grain compaction (Fig.8). Trace amounts of muscovite occur as flakes in the studied samples. They show bending due to deformation. In addition to muscovite, biotite also occurs. However, it mostly appears to be irregularly bifurcated due to the effect of compaction processes. Biotites are identified by its brown color under plane polarized light and strong pleochroism.

Rock Fragments

The rock fragments comprise about 20% to 30% of the total detrital fractions. Igneous rock fragments consists 10% to 18% of the total rock fragments. Sedimentary rock fragments including fine-grained sandstone, shale and chert are present (Fig.9), which is more than metamorphic rock fragments but less than igneous rock fragments (Fig.10, 11, 12, 13, and 14). Metamorphic rock fragments comprise, averaging above 1% to 3% of the total rock fragment content including schist. The maximum grains size varies from 0.2mm to 0.6mm in diameter and the minimum grain size varies from 0.03mm to 0.15mm in diameter.

Cement and Matrix

In Zigyaing sandstones, the matrix is more than cement. Calcite cement and iron oxide cement are present in the sandstones of Zigyaing Formation. The detrital grains are well cemented by calcite. Hematite is

mostly common iron oxide cement which may show typical blood red color strong transmitted light. This is a characteristic of primary cementation before calcite precipitation. In argillaceous matrix, white mica or micaceous clays and chlorite, some carbonates, fine chips of quartz, feldspar from silty sizes to rock flour are essentially composed as the matrix materials.

Nomenclature of Zigiaying Sandstone

According to the sandstone classification of Folk (1974), most of the Zigiaying sandstones fall in the field of “Feldspathic Lithic graywacke” and “Lithic graywacke” (Fig. 4).

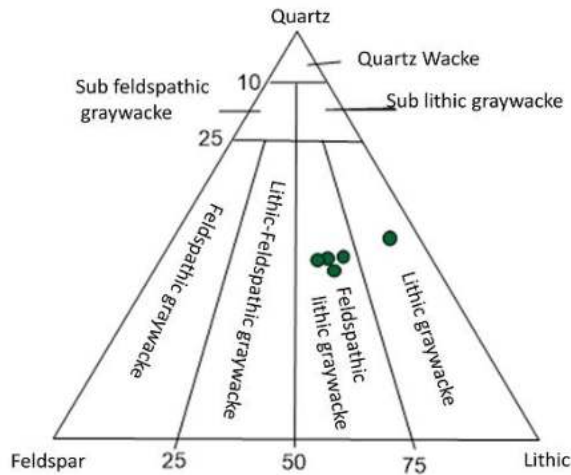


(Fig. 4) Ternary compositional Diagram (Q-F-L% plot) of sandstones from Zigiaying Formation, Southwestern part of Rakhine Yoma, (After Folk’s (1974).

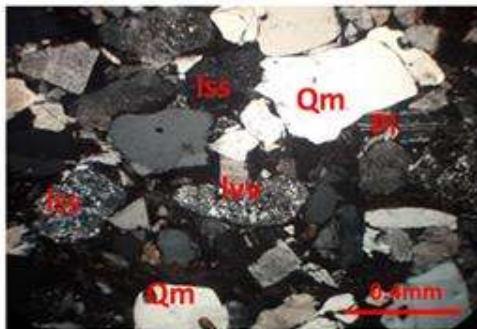


(Fig.5) Photomicrograph showing the monocrysstalline quartz, sedimentary rock fragment, igneous rock fragment and plagioclase feldspar (Under XN)

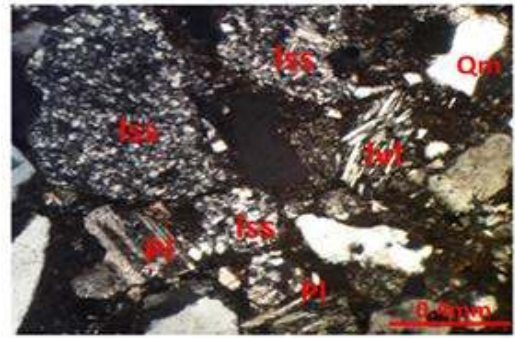


(Fig.6) Polycrystalline quartz, igneous rock fragment, plagioclase feldspar of Zigiaying Formation(Under XN)

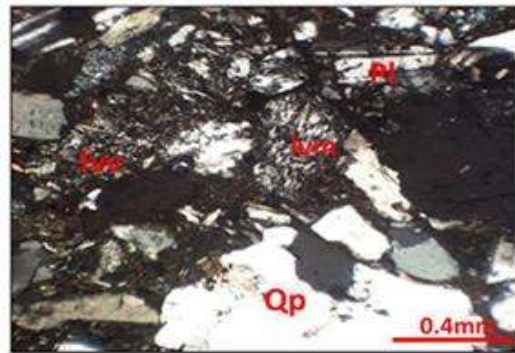


(Fig.7) Photomicrograph showing the albite (multiple twinning) of plagioclase, sedimentary rock fragment, monocrystalline quartz and igneous fragment (Under XN)



(Fig.8) Photomicrograph showing the monocrysstalline quartz (Qm), orthoclase feldspar (or), plagioclase feldspar (pl), and biotite mica (bm) of the Zigiaying Formation (Under X.N).

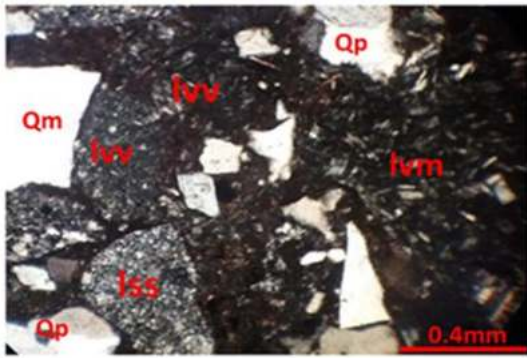


(Fig.9) Photomicrographs showing the Monocrystalline quartz (Qm), polycrystalline quartz (Qp), igneous rock fragment and sedimentary rock fragment (Under X.N)



(Fig.12) Photomicrograph showing monocrystalline quartz (Qm), volcanic lithic grain with lathwork texture (Lvl), and sedimentary rock fragment (Lss) (Under XN)

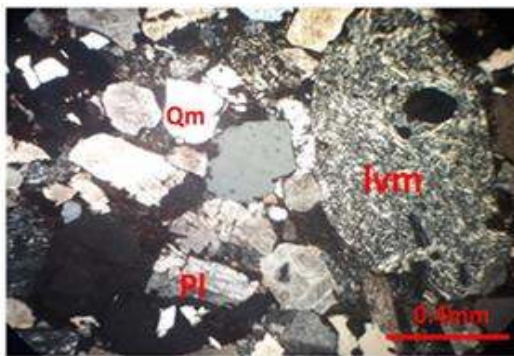


(Fig.10) Photomicrograph showing the monocrystalline quartz, plagioclase feldspar and igneous rock fragment of Zigyaing Formation (Under XN)



(Fig.13) Photomicrographs showing the volcanic lithic grain with microlithic texture (Ivm) of the Zigyaing Formation (Under X.N)

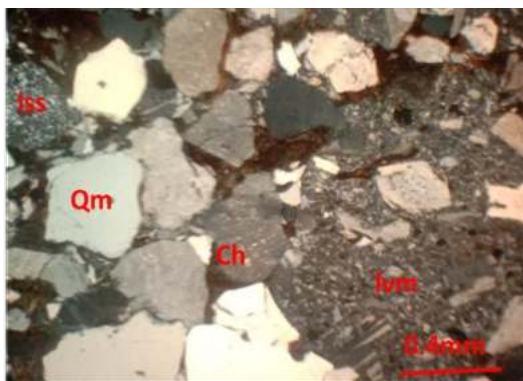


(Fig.11) Photomicrograph showing monocrystalline quartz (Qm), volcanic lithic grain with microlithic texture (Lvm), chert (ch), and sedimentary rock fragment (Lss) (Under XN)



(Fig.14) Photomicrographs showing the volcanic lithic grain with lathwork texture (Ivl) of the Zigyaing Formation (Under X.N)

3. ROVENANCE OF THE SANDSTONES

“Provenance” refers to the terrain or parent rocks from which any association of sediments was derived. Petrographic and petrological criteria were used to determine the provenance. Grain parameters proposed by Graham et al., (1976) is used in the provenance study. Dickinson (1979) classified all provenances and

derivative sandstones suites into three general group: (1) continental blocks, for which sediment sources are on shields and platforms or in faulted basement blocks,(2) magmatic arc, for which sediment sources are within active arc orogen of island arcs or active continental margins and (3) recycled orogen, for which sources are deformed and uplifted strata sequences in subduction zones, along collision orogen, or within foreland fold-thrust belts. Point counting data were recalculated to produce the grain parameters proposed by Dickinson 1979; Graham et al. 1976; Ingersoll and Suczek 1979; and Ingersoll et al. 1984.

Moreover, petrographic and petrological criteria were used to determine the provenance. Triangular plots of QtFL, QmFLt and QmPk were drawn from the point counting data. When QtFL diagram of Dickinson (1985) is applied, most of the data plot falls in the field of recycled orogenic belt (Fig. 15). Typical sands composed largely of recycled sedimentary materials, have intermediate quartz contents, a high ratio of quartz to feldspar, and an abundance of sedimentary-metasedimentary lithic fragments (Dickinson and Suczek, 1979). On the QmFLt diagram, the emphasis is shifted toward the grain-size of the source rocks. Vecarse finer grained rocks yield more lithic fragments in the sand-sized range. By using the QmFLt diagram, the sediments fall in the Transitional recycled (Fig.16).

On the QmPK diagram (Fig.17), the samples belong to the end of Qm. The more feldspathic end of the trend reflects an increase in the ratio of plutonic to volcanic detritus in sands derived mainly from magmatics (William, turner and Gilvert, 1954). The more quartzose end of trend reflects increasing maturity or stability for detritus derived from continental blocks or recycled through derivative orogenic terranes. On the QpLvLs diagram (Fig. 18), the samples of the studied Formation fall in Arc Orogen Sources, Collision Orogen Sources and a few fall Subduction Complex Sources.

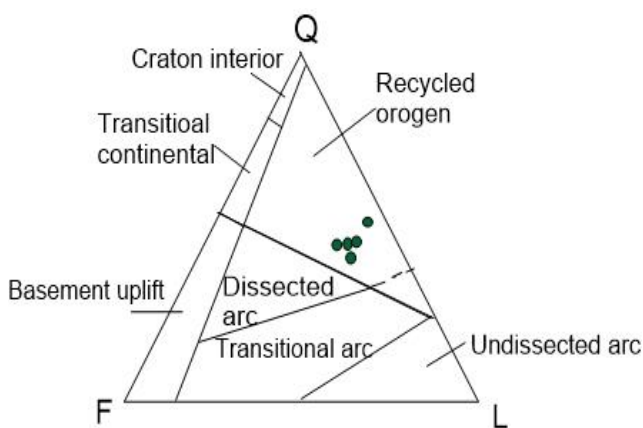


(Fig. 15)Ziyaing sandstone samples plot as recycled orogen on a QFL diagram (Dickinson, 1985).

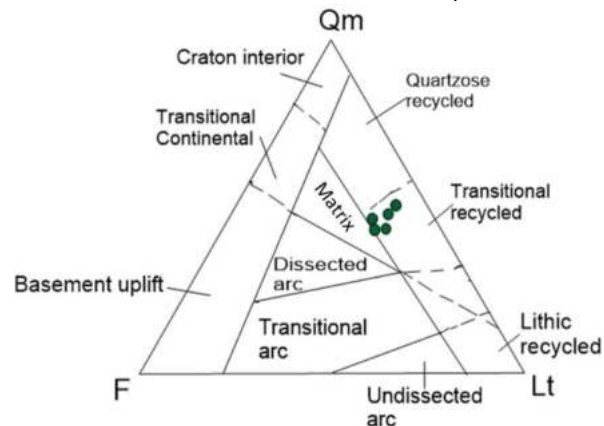


(Fig. 16)Triangular plots of QmFLt showing the selected sandstone Transitional recycled provenances after Dickinson (1985)

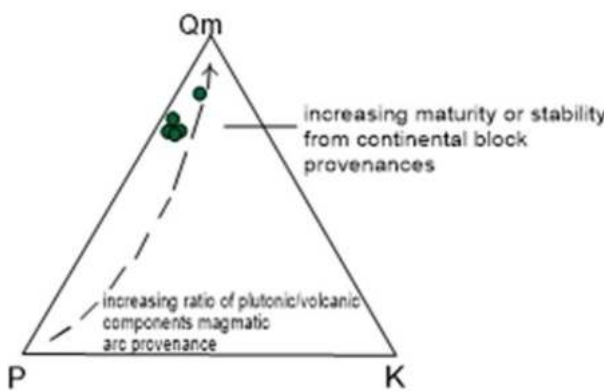


(Fig. 17)Triangular plot of monocrystalline component QmPK, Dickinson (1975) showing source rock composition becoming more quartzose, decreasing K-feldspar content during Paleocene- Eocene time, and increasing maturity reflecting detritus derived from continental blocks or recycled

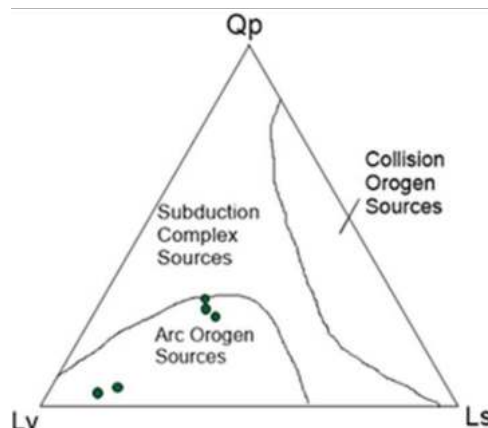


(Fig. 18)Triangular Qp-Lv-Ls plot showing mean proportions of polycrystalline lithic fragments for selected sandstone suites derived from the Arc Orogen sources after Dickinson (1975)

CONCLUSIONS

The Research Area is situated in the Ayeyarwady Region, south-western part of the Myanmar

and covering part of the UTM Map No. 1694-04, 1694-06, 1694-07, 1694-08, 1594-01 and 1594-05 of Myanmar Survey Department. There are three types of formations, (1) Kwingu Formation, (2) Zigyaing Formation and (3) Mawdin Formation of the Paleocene to Eocene Units. In this research, the researcher only focuses on the analysis of Zigyaing Formation. For the petrography of research area, the Zigyaing sandstone is mainly comprised of quartz, feldspar, mica and rock fragments and minor accessories minerals respectively. According to the analysis by using Folk (1974) classification, most of the samples from Zigyaing Formation fall in the region of Feldspathic Lithic Graywacke and other a few samples are fall in the Lithic Graywacke. In order to identify the Provenance, the researcher used the QFL diagram, QmFLt diagram by Dickinson (1985) diagram and QmPk diagram, Qp-Lv-Ls diagram by Dickinson (1975). In the data analysis by using QFL diagram, the provenance can be assumed recycled orogen and transitional recycled provenances in QmFLt diagram. According to triangular plot of monocrystalline component in QmPK, the rock can be assumed the quartzose component has been increased and decreased in K-feldspar during Paleocene-Eocene time and derived from continental blocks or recycled. Qp-Lv-Ls diagram plot shows the proportions of polycrystalline lithic fragments for selected sandstone has been derived from the Arc Orogen respectively.

ACKNOWLEDGEMENTS

I am inscribed my prim thank to supervision, Prof. Dr. Day Wa Aung, Head of Department of geology, for his kind supervision, valuable suggestions and fruitful discussion, critically reading and guidance through this studying in various ways. I am mostly obliged to co-supervisor, Dr. Me Me Thein, Professor and Head, Department of Geology, West Yangon Technology University, for valuable suggestions. Cordial thanks are due to personnel of Zegyain and Kanchaing village for their various helps and hospitality.

REFERENCES

- [1] Ahmad, A.H.M., Bhat., G.M, (2006), Petrofacies, provenance and diagenesis of the dhosa sandstone member (Chari Formation) at Ler, Kachchh sub-basin, Western India Journal of Asian Earth Sciences 27, 857–872.
- [2] Arribas, J.M., Ochoa, R., Mas, Arribas., M E., González-Acebrón, L., (2007), Sandstone petrofacies in the northwestern sector of the Iberian Basin Journal of Iberian Geology 33 (2): 191-206.
- [3] Dickinson, W.R., (1970) Interpreting detrital modes of graywacke and arkose. J. sedim. Petrol., 40.695-707.
- [4] Dickinson, W. R., and Suczek, C. A. (1979) Plate Tectonics and Sandstone Composition, AAPG Bulletin, v.63. No. 12, p.2164-2182.
- [5] Dickinson, W. R. (1985) Interpreting provenance relations from detrital modes of sandstones. in:

- Provenance of Arenites (Ed. By G. G. Zuffa), pp. 333-362. NATO ASI Series. Reidel, Dordrecht, Holland.
- [6] Kyaw Linn Oo (2002) Regional Geology and Sedimentary Facies Study of the sinma- Ngwesaung Area, Southwest Coast of Rakhine Yoma, Patheingyi Township. M. Sc Thesis, University of Patheingyi, Department of Geology. (unpublished).
 - [7] Masroor Alam., M., and Ahmad, A.H.M., (2000), Lithofacies and petrofacies Analysis of Alluvial Fan Deposits of the bayana Formation, Bharatpur District, Indian Minerals. Volume 54, No.3 & 4 , pp. 233-244.
 - [8] MPRL Report, (2009), Geology Field Report of Gwa-Mawdin Pagoda Point Area (Rakhine Coastal Region of Offshore Block A-6 Area).
 - [9] Sam Boggs, JR, (2009), Petrology of Sedimentary Rocks (second edition). Shanmugam, G, (2016), Submarine fans, A critical retrospective (1950be, 2015) journal of paleogeography, , 5 (2).
 - [10] Shaista Khan, M. Adnan Quasim *1 , Ahmad, A. H. M., Alam, M. M, (2017), Petrofacies and Tectono Provenance of the Sandstones of Jara Dome, Kachchh, Gujarat Jour. Indian Association of Sedimentologists, Vol. 34, Nos. 1 & 2. pp. 17-28.

Study on Behavior of Raft Foundation Using Bearing Capacity Mapping in Lanmadaw Township, Yangon

Khin Myo Thant⁽¹⁾, Zar Lee Tint⁽²⁾

⁽¹⁾Technological University (Mandalay), Myanmar

Email: khinmyothant.kmt777@gmail.com
zarleetint@gmail.com

ABSTRACT: Soft soil is situated in important areas all over the world along rivers and seas. Construction built on natural soft soil is a risk because of its low shear strength and high compressibility. The study aims to study the behavior of raft foundation by using PLAXIS 3D Foundation Engineering Software. Firstly, it is collected representative borehole data in Lanmadaw and the bearing capacity of soil is investigated by Meyerhof's Bearing Capacity Equation to generate the bearing capacity maps. The bearing capacity map is developed by using ArcGIS 10.8 Software. Besides, the bearing capacity of raft foundation is calculated by using Meyerhof's, Hansen's, and Standard Penetration Test (SPT) Bearing Capacity Equation. The study is to investigate the settlement of raft foundation to apply each uniformly distributed load until the allowable limit. Moreover, the study is to prove the bearing capacity maps which are useful tools for site planners and decision-makers in Lanmadaw Township and how to control less bearing capacity value.

KEYWORDS: *Meyerhof's bearing capacity, Hansen's bearing capacity, SPT bearing capacity, geographical information system, settlement of raft foundation.*

1. INTRODUCTION

Urban geology involves a key place for planning and mapping the geological environment of cities all over the world. Studying land resources and geologic hazards are related to the development of urban areas. Many constructions (building, bridge, road, tunnel, dam, box culvert, and so on) need soil investigation because most of building failure deals with the geotechnical problem [Barja (2011), Kolat (2006), Moufida (2010)]. The soil investigation is caused by time-consuming. To reduce costs and shorten the time, it is essential to need the geotechnical map. Geotechnical maps are useful tools for soil description in particular areas. These maps are developed in several ways and several programs.

A geographic information system (GIS) is a system designed to analyze and present spatial or geographical data. GIS applications are tools to analyze spatial information and create the map and edit the data in the maps [Kolat (2006), Moufida (2010), Xie (2006)]. GIS

is a commonly used application for maps concerning geotechnical fields. Many geotechnical maps have been developed and upgraded by many researchers in recent years.

In addition to data acquisition, geological knowledge concerning geological analysis and the development of maps provides planners and politicians for the development of urban planning [Joseph]. Many urban geological studies in some cities have been provided good examples corresponding to the development of geological maps.

Raft foundation is one of the shallow foundations. The performance of raft foundation is affected by several factors such as soil condition, raft dimensions, and arrangements. Raft foundation is an economical option for circumstances where the performance of the single footing does not satisfy the design requirements. The raft foundation system is to use when the level of applied loads is heavy and the bearing capacity of the soil is weakness.

Lanmadaw Township is selected as a study area because it is located in the downtown parts of Yangon city and a lot of public buildings have been built in it. Therefore the geological maps are needed as helpful tools for site planners. The purpose of this paper is to develop the bearing capacity maps for shallow foundations in Lanmadaw Township and to investigate the behavior of raft foundation at a site location (Latitude = 16.77° and Longitude = 96.14°).

2. STUDY AREA

Lanmadaw Township is situated in the western part of downtown Yangon, bordering with Ahlone Township and Latha Township. Lanmadaw and Latha Township are denoted as China Town for Yangon. The Yangon City Map composed of twenty-nine townships is shown in Fig 1. There are seven boring data collected from Lanmadaw Township. The location map of borehole points is described in Fig 2.

3. DATA ACQUISITION AND METHODOLOGY

There are seven representative borehole data in Lanmadaw Township for this paper. In this analysis, the ultimate bearing capacity is investigated by using

Meyerhof's Equation (1963). The Meyerhof (1963) suggested the following form of bearing capacity equation:

$$q_{ult} = c'N_c F_{cs} F_{cd} F_{ci} + qN_q F_{qs} F_{qd} F_{qi} + \frac{1}{2} \gamma B F_{rs} F_{rd} F_{ri} \quad (1)$$

- Where, c' = cohesion
- q = effective stress at the level of the bottom of the foundation
- γ = unit weight of soil
- B = the smallest dimension of foundation
- F_{cs}, F_{qs}, F_{rs} = shape factors
- F_{cd}, F_{qd}, F_{rd} = depth factors
- F_{ci}, F_{qi}, F_{ri} = load inclination factors
- N_c, N_q, N_r = bearing capacity factors

The equations for determining the various factors given in Equation (1) are described as the following equations.

The shape, depth and inclination factors for Meyerhof (1963) are described as the following equations:

$$N_c = (N_q - 1) \cot \phi' \quad (1)$$

$$N_q = \tan^2 \left(45 + \frac{\phi'}{2} \right) e^{\pi \tan \phi'} \quad (2)$$

$$N_r = (N_q - 1) \tan(1.4\phi') \quad (3)$$

For Shape factor,

$$F_{cs} = 1 + \left(\frac{B}{L} \right) \left(\frac{N_q}{N_c} \right) \quad (4)$$

$$F_{qs} = 1 + \left(\frac{B}{L} \right) \tan \phi' \quad (5)$$

$$F_{rs} = 1 - 0.4 \left(\frac{B}{L} \right) \quad (6)$$

For Depth Factor, $\frac{D_f}{B} \leq 1$:

For $\phi' > 0$:

$$F_{cd} = F_{qd} - \left(\frac{1 - F_{qd}}{N_c \tan \phi'} \right) \quad (7)$$

$$F_{qd} = 1 + 2 \tan \phi' (1 - \sin \phi')^2 \tan^{-1} \left(\frac{D_f}{B} \right) \quad (8)$$

$$F_{rd} = 1 \quad (9)$$

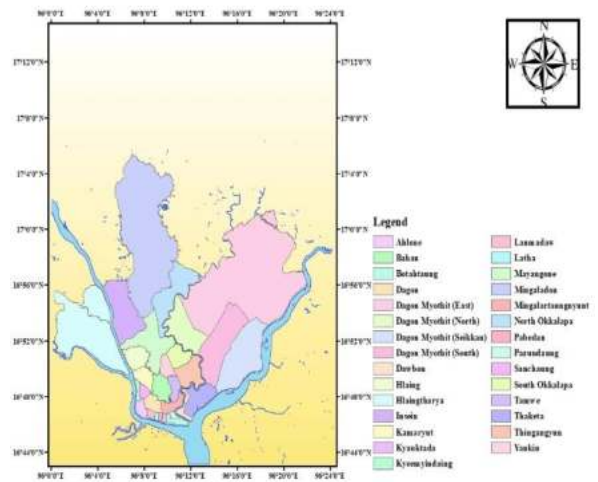


Fig 1. Twenty-nine Townships in Yangon City Map

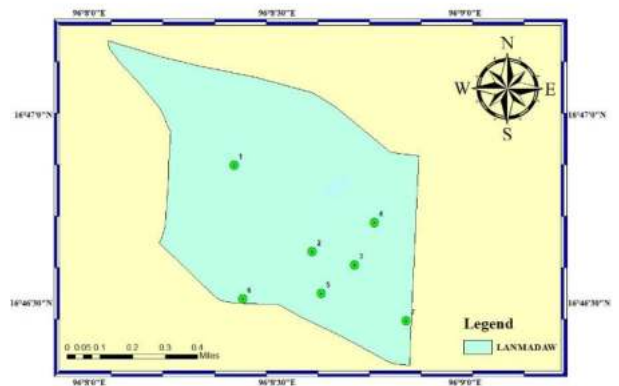


Fig 2. Location Map of Borehole Points

Above all equations are used to investigate the bearing capacity of soil for this particular area. Moreover, the bearing capacity maps are developed by using ArcGIS 10.8 software. In this analysis, The Inverse Distance Weighted Method (IDW) is determined to calculate the interpolation of bearing capacity value. The IDW is used to determine a linear-weighted combination of the points which is a function of the distance between an input point and output cell location.

The bearing capacity of raft foundation is evaluated by using Meyerhof's, Hansen and SPT Bearing Capacity Equation. In Hansen Bearing Capacity Equation, The bearing capacity factors N_q and N_c given by Equation (1) and (2) are calculated by bearing capacity equation.

$$N_r = 1.5(N_q - 1) \tan \phi' \quad (10)$$

The equations of the shape factor are the same above the Meyerhof's shape factor.

Depth factors,

$$F_{cd} = 1 + 0.4 \frac{D_f}{B} \quad (11)$$

$$F_{qd} = 1 + 2 \tan \phi' (1 - \sin \phi')^2 \frac{D_f}{B} \quad (12)$$

$$F_{rd} = 1 \quad (13)$$

The SPT is popularly used to obtain the bearing capacity of soils directly. Considering the accumulation of field observations and the stated opinions of the authors and others, this author adjusted the Meyerhof equations for an approximate 50 percent increase in allowable bearing capacity to obtain the following:

$$q_a = \frac{N}{F_1} k_d \quad B \leq F_4 \quad (14)$$

$$q_a = \frac{N}{F_2} \left(\frac{B + F_3}{B} \right)^2 k_d \quad B > F_4 \quad (15)$$

Where, q_a = allowable bearing pressure for $\Delta H_0 = 25$ mm or 1 in settlement, kPa or ksf

$$k_d = 1 + 0.33 \frac{D}{B} \leq 1.33 \quad (16)$$

The ultimate bearing capacity is evaluated by using Meyerhof, Hansen's, and SPT bearing capacity equations. The allowable bearing capacity is obtained that the ultimate bearing capacity is divided by the factor of safety. The factor of safety is 3. In these three methods, the lowest value controls. Moreover, the settlement of raft foundation is obtained from the analyzing PLAXIS 3D Foundation Engineering Software.

4. RESULT OF BEARING CAPACITY MAPPING AND SETTLEMENT OF RAFT FOUNDATION AND DISCUSSION

The ultimate bearing capacity is evaluated by using Meyerhof's equation. In this analysis, there are seven representative borehole data in Lanmadaw Township. The result of the bearing capacity of soil is described in Table 1. The allowable bearing capacity of soil is 1500 psf (0.67 tsf) according to Myanmar National Building Code 2016. The minimum safety factor is 3 for the study. In this result, the bearing capacity of soil at depth 10 ft is greater than the minimum bearing capacity. Nevertheless, the bearing capacity values of points 2 and 5 are less than the allowable bearing capacity value.

The ultimate bearing capacity map at 5 ft depth is described in Fig 3. In this figure, the value of bearing capacity of soil are arranged between minimum value to maximum value. The bearing capacity of soil near the rivers is lower than the other areas in Lanmadaw Township according to the results. To be performed in these results, the bearing capacity of soil varies from 1.5 to 12.2 ton per square foot at 5 ft depth from the natural ground level. The bearing capacity value in this map is not suitable to use the shallow foundation because the values of some areas are not greater than the limitation. The southern part of the Lanmadaw Township is the

value of bearing capacity arranged from 1.5 to 3.3 ton per square foot. The northern part of Lanmadaw Township is the highest bearing capacity value varied from 9.4 to 12.2 ton per square foot in this map.

Table 1. Results for Ultimate Bearing Capacity

Borehole Point	q_{ult} (tsf) (psf) (depth = 5 ft)	q_{ult} (tsf) (psf) (depth = 10 ft)
1	12.22 (27372.8)	26.3 (58912)
2	1.86 (4166.4)	4.11 (9206.4)
3	2.31 (5174.4)	4.75 (10640)
4	2.39 (5353.6)	5.26 (11782.4)
5	1.65 (3696)	3.09 (6921.6)
6	4.71 (10550.4)	3.75 (8400)
7	3.23 (7235.2)	5.98 (13395.2)

Moreover, the bearing capacity of soil is analyzed using ArcGIS software. In this software, the spatial analysis is determined by Inverse Distance Weighted Method which is a simple interpolation based on Tobler's First Law of Geography. In this analysis, there are two maps for bearing capacity of soil at depth 5 ft and 10 ft from the ground level.

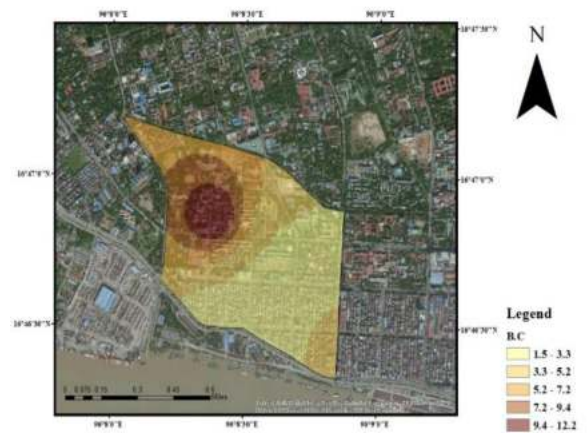


Fig 3. Ultimate Bearing Capacity Map at 5 ft depth

Fig 4 shows the ultimate bearing capacity map at depth 10 ft from the natural ground level in Lanmadaw Township. The bearing capacity value are ranged between minimum to maximum value shown in Fig 4. The value is varied from 3.3 to 26.3 ton per square foot. In this map, most of the areas are good soil conditions and the bearing capacity is greater than the minimum

Table 2. Soil Properties for Study Area (16.77° Lat and 96.14° Long)

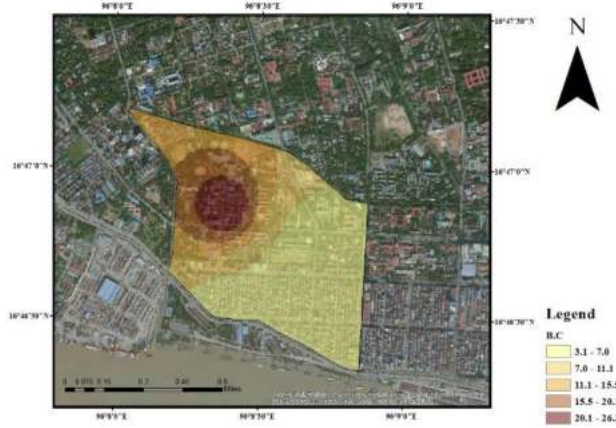


Fig 4. Ultimate Bearing Capacity Map at 10 ft depth

Besides, the dimension of raft foundation is 40 ft length, 30 ft breadth, and 1 ft thickness. The required soil profile is shown in Table 2 obtained from the soil report at a site. The bearing capacity of raft foundation is calculated by using Meyerhof's, Hansen's, and SPT Bearing Capacity Equation at a site located 16.77° Latitude and 96.14° Longitude. The bearing capacity value of raft foundation is shown in Table 3. The minimum allowable bearing capacity value is 56.98 kN/m² obtained from SPT bearing capacity equation. In three methods, the lowest value controls.

Table 3. Results for Allowable Bearing Capacity by Three Methods

Method	q _{ult} (kN/m ²) (psf)	q _{all} (kN/m ²) (psf)
Meyerhof	534.33 (1160)	178.11 (3720)
Hansen	191.04 (3990)	63.68 (1330)
SPT	170.43 (3570)	56.78 (1190)

Therefore, it is easy to determine bearing capacity value by using the bearing capacity map. The location site of soil report is demonstrated in Fig 5. The site is located the range from 1.5 and 3.3 tsf of ultimate bearing capacity value. For example, it is assumed as 1.5 tsf (3360 psf) and 3.3 tsf (7390 psf) of ultimate bearing capacity value. The raft foundation size is designed as the length (40 ft), the width (30 ft) and the thickness (1 ft). The procedures are expressed as:

Raft foundation size = 40 ft x 30 ft x 1 ft

For 1.5 tsf (3360 psf)

Ultimate bearing capacity = 3360 psf

Allowable bearing capacity = 3360/3 = 1120 ksf

For 3.3 tsf (7390 psf)

Ultimate bearing capacity = 7390 psf

Allowable bearing capacity = 7390/3 = 2460 psf

Depth (m)	w (%)	G _s	γ (kN/m ²)	c (kN/m ²)	Ø	Blow (N)
0-2.7	24.72	2.67	18.20	14.84	7°	4
2.7-3.7	25.87	2.74	19.63	32.07	6°	8
3.7-5.5	20.31	2.67	18.52	27.05	7°	6
5.5-7.3	22.01	2.68	18.35	16.76	15°	9
7.3-9.1	22.71	2.68	19.78	7.1	16°	14
9.1-12.2	23.55	2.64	19.49	-	36°	12
12.2-15.2	22.45	2.63	17.02	-	30°	16
15.2-18.3	25.12	2.62	17.39	-	31°	20
18.3-21.3	24.27	2.61	17.38	-	30.5°	28
21.3-24.2	23.56	2.64	17.165	-	29°	41
24.2-27.4	20.22	2.62	16.87	-	30°	42
27.4-30.5	19.67	2.61	17.3	-	31°	46

All of the above reasons, the allowable bearing of raft foundation has situated the range between 1120 and 2460 psf. According to the reasons, the bearing capacity map is easy to know the allowable bearing value at particular area.

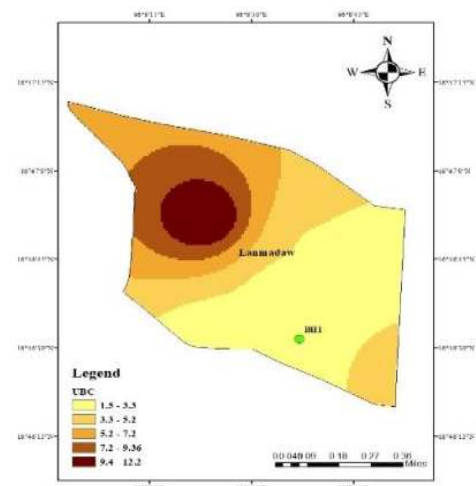


Fig 5. Location Map of Soil Report

Moreover, the settlement of raft foundation is generated to apply each uniformly distributed load using PLAXIS 3D Foundation Engineering Software. The maximum allowable settlement is 25 mm (1 in) for the shallow foundation. The settlement of raft foundation is shown in Table 4. Each settlement of raft foundation are investigated by analyzing PLAXIS 3 D Foundation Software demonstrated in Fig 6, 7, 8, and 9.

Table 4. Results for Settlement of Raft Foundation

Uniformly Distributed Load (kN/m ²)	Settlement (mm)
50	10.4
60	13.5
80	19.97
100	27.09

For 100 kN/m² (2088.54 psf), the value of the settlement is greater than the allowable limit. Therefore, the raft foundation is resisted to apply 80 kN/m² (1670.83 psf) uniformly distributed load. Therefore, SPT bearing capacity is safe to decide the resisting bearing capacity of the foundation. So, SPT bearing capacity value is controlled to use for shallow foundation.

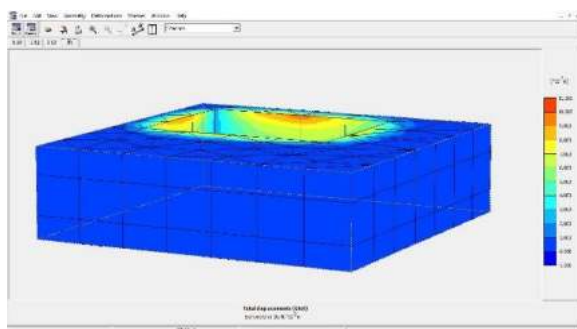


Fig 6. Settlement of Raft Foundation (50 kN/m²) in PLAXIS 3D

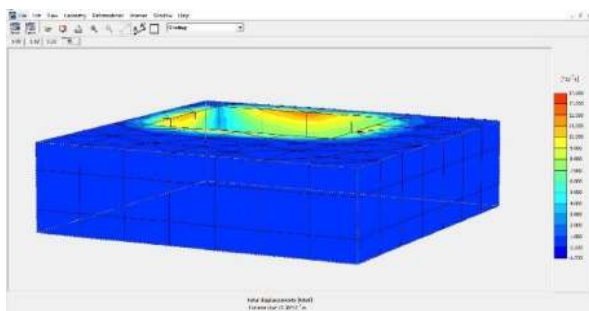


Fig 7. Settlement of Raft Foundation (60 kN/m²) in PLAXIS 3D

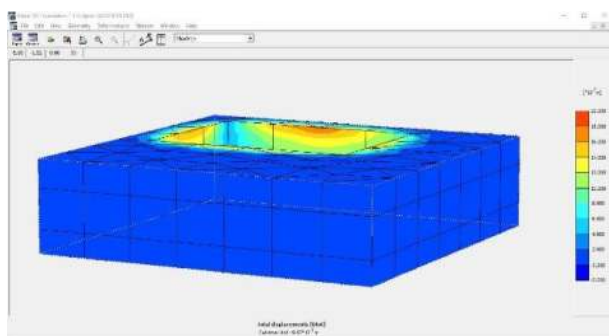


Fig 8. Settlement of Raft Foundation (80 kN/m²) in PLAXIS 3D

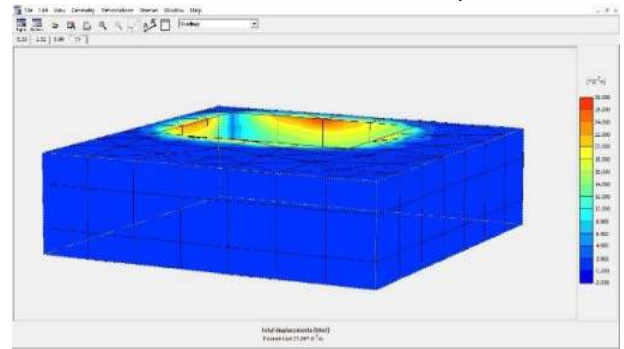


Fig 9. Settlement of Raft Foundation (100 kN/m²) in PLAXIS 3D

Above the figures, the bearing capacity maps are determined whether the soil condition is good or not. And, these maps reduce to loss of time and cost for decision marker and site planner. Therefore, these maps are useful tools for geotechnical engineers and site engineers. Moreover, the settlement of raft foundation is investigated to apply each uniformly distributed load and is proved to control SPT bearing capacity value.

5. CONCLUSIONS

This study demonstrated the usefulness of the bearing capacity maps for shallow foundations in Lanmadaw Township. The advantages of using these maps are easy to know the soil condition in particular areas. In this paper, there are two layers of the soil profile in Lanmadaw Township. The bearing capacity maps are beneficial tools for site planners and decision-makers in particular areas.

Besides, the allowable bearing capacity is investigated by using Meyerhof's, Hasen's, and SPT bearing capacity equation. The settlement of raft foundation is evaluated by using PLAXIS 3D Foundation Engineering Software to apply each uniformly distributed load. These analyses were shown that the less bearing capacity values in the three methods were proved to consider foundation design. Therefore, the raft foundation is suitable for the study area. Besides, the allowable bearing capacity is investigated by using Meyerhof's, Hasen's, and SPT bearing capacity equation. The settlement of raft foundation is evaluated by using PLAXIS 3D Foundation Engineering Software to apply each uniformly distributed load. These analyses were shown that the less bearing capacity values in the three methods were proved to consider foundation design. Therefore, the raft foundation is suitable for the study area.

The author wishes to thank Geotechnical engineering company for providing soil reports.

REFERENCES

- [1] Barja M. Das., “*Principles of foundation engineering*”, SI. 7th ed. USA. *Global Engineering*:Christopher M. Shortt. 2011.
- [2] Kolat, Ç., Doyuran, V., Ayday, C., Süzen, M.L., “Preparation of a geotechnical microzonation model using Geographical Information Systems based on multicriteria decision analysis”, *Engineering Geology*, 2006, vol. 87, pp 241–255
- [3] Moufida El May, Mahmoud Dlala and Ismail Chenini., “Urban geological mapping: geotechnical data analysis for rational development planning”, *Engineering Geology*, 2010, 116, pp 129 – 138.
- [4] Xie, M., Esaki, T., Qiu, C., Wang, C., “Geographical information system-based computational implementation and application of spatial three-dimensional slope stability analysis”, *Computers and Geotechnics*, 2006, 33, pp 260–274.
- [5] Joseph E. Bowles, RE., S.E, "Foundation Analysis and Design", Fifth Edition.

Hydraulics Simulation of Rural Water Distribution System for Painhnaegone Village

Kyi Lin Wai⁽¹⁾, Ba Nyar Oo⁽²⁾

⁽¹⁾Technological University (Thanlyin), Myanmar

⁽²⁾ Technological University (Thanlyin), Myanmar

kyilinwai@gmail.com

banyaroo.90@gmail.com

ABSTRACT: This study represents the handling of EPANET software in water distribution network system. EPANET software helps to design and simulate the water distribution network for any required area such as commercial, industrial, domestic and local areas. EPANET is a computer program that performs extended period simulation of hydraulic and water quality behavior with a pressurized pipe networks. A pipe networks consists of pipes, pumps, valves, nodes (pipe junctions) and reservoirs or tanks. In this paper, it was used to carry out water distribution system for Painhnaegone village. The study examined water demand analysis of public water supply in rural area using EPANET 2.0 software. Design period is taken as 20 years and arithmetical progression method is used to estimate the future population of study area. Daily water consumption is taken as 100 Lpcd in this study area. The layout of distribution system is dead-end system or tree system and is supplied by gravity system. Continuous system is used and the network model consists of 28 junctions, 38 pipe lines, and one reservoir. The aim of the study is to supply safe water for the people who live in Painhnaegone that has no existing water supply system. Therefore, a design for taking decision such as the new water supply network is given.

KEYWORDS: *water supply; continuous system; pipes; junctions; EPANET 2.0*

1. INTRODUCTION

Water is the major resource for every human being and also for living organisms. Not only for the domestic purposes, but also for industrial and irrigation purposes the water distribution can be utilized. Water served human beings and living organisms in past centuries by rivers valleys and small streams. Water supply had taken an initiative role to give the convenience for every domestic user by giving water to respective house hold nodes through water distribution network from past few decades. Mainly, the city or any place of village growth development will depend on many constraints. Water distribution is also one of the major aspects in it. Many cities which are in the development stage depend on the population growth. The water distribution network should meet the demand of increased growth of

population. To increase the living standards water distribution.[2]

Water distribution is required in a major role. Water supply deficiency is the major drawback in urban area since the water distribution system is intermittent system. Under this scheme water is distributed to the residents intermittently for few hours in a week. Due to the intermittent water supply most of the time the pipelines in the distribution network are either empty or partially filled. These conditions make the water in pipelines vulnerable to cross contamination via sewage and contaminated groundwater.[1]

In order that we are providing continuous water distribution system to give 24hours, day and night and 365days to every house hold who are in end of the network also without falling into any negative pressure. Intermittent system will not supply water continuously through network pipes, by this contamination of pipes dues to empty space and also bacteria formation takes place. That contaminations and bacteria formation results harmful effects in the consumer health. To avoid this continuous water system has been designed in this study to avoid negative pressures and full length supply for every node in all the time.[2]

2. STUDY AREA

Painhnaegone village is in the boundary of Hmawbi Township. It is located between East longitude 96° 6' 9.58" and 96° 5' 47.58" and North latitude 17° 4' 0.98" and 17° 3' 55.84". It has an area of about 0.09 square miles. To the North West of the village, there are Phan Ga Gone village and Yay Pyar Chaung village and to the South West of the village, Nyaung Ta Khar village and Thae Phyu village are existed. The location of the study area is shown in Fig.1.



Fig. 1. Location of Study Area

3. MATERIALS AND METHODS

In this study, the required topological data such as elevation and length for proposed design are measured with Google Earth Pro software. The total population of Painhnaegone village changes during past decade according to the births, deaths, migration in and migration out. The calculation of population estimation is computed by arithmetical increase method. The design period is taken as 20 years for the future. Table.1 shows increase of population per decade of Painhnaegone village. Table 1 shows increase of population per decade of Painhnaegone village. Other daily water demand is considered as 10% times of daily water demand. Daily water consumption of per capita demand is 100 liters per capita per day. Design water demand is the sum of the daily water demand and other daily water demand. Maximum daily water demand is taken into account 180% times of design water demand. Table 2 shows the calculation of maximum daily water consumption.

Table 1 Increase of Population Per Decade of Painhnaegone Village

Year	Population(P) (No.)	Increment for a decade (I) (No.)
2018	851	386
2008	465	
Average I		386

Table 2 Calculation of Maximum Daily Water Consumption

Design Population	Daily Water Demand (GPD)	Other Daily Water Demand (GPD)	Design Water Demand (GPD)	Maximum Daily Water Demand
1623	162300	16230	178530	321354

After drawing the distribution network system, there are 28 numbers of junctions, 38 numbers of pipe links and one reservoir. The design detail of study area is shown in Table 3.

Table 3 Design Detail for Study Area

No	Number of Reservoir (Nos)	Number of Junction (Nos)	Number of Pipe (Nos)	Number of Household (Nos)
1	1	28	38	204

Base Demand for each junction = 321354/28

= 11476.93 GPD

= 11476.93/(24*60)

= 7.97 GPM

There are two types of distribution system. These are: (1) continuous system and (2) intermittent system. In the presented study, continuous system is considered. There are three basic fundamental equations in EPANET software. These are: Hazen-William, Chezy-Manning and Darcy-Weisback formula. Hazen-William’s formula is applied in this study because water is distributed by pipes. Therefore, this formula is especially based on pipes flow. The material of distribution pipes is considered as P.V.C pipes. Pipe roughness is considered as 120.

To obtain the total head or hydraulics head, Bernoulli’s equation is applied to estimate the total head. Total head is equal to the sum of the pressure head, velocity head, datum head and losses. Moreover, the sum of velocity and pressure head is assumed approximately 50 ft and thus should be added in total head of reservoir. Losses of system appurtenances are considered when running the network analysis program but quantity and locations are not considered in detail.

4. RESULT AND DISCUSSION

By using the required data like base map, road network, elevation details, pipe lengths, and reservoir generated a distribution network in EPANET by using road network map and assigned the hydraulic properties like pipe length, pipe diameter, roughness values, node elevation and nodal demand to the network. The water distribution network of Painhnaegone village consists of 38 pipe links of uniform material, 28 junctions, and 1 reservoir from which water is distributed to the entire network.

The pipes used in the network system are of different diameter ranges 12 in, 8 in and 4 in. The

PVC pipes having roughness coefficient of 120 are used throughout the network system. Simulation of this network had done using EPANET, during the network simulation, changes in selected parameters such as head, flow, velocity, unit head loss and water pressure at various nodes and links were observed and found that the output values are in the range of standard output values. Tables 4 and 5 show the results of water distribution system.

Table 4 Junction of Simulated Pressure

Node ID	Elevation (ft)	Base Demand (GPM)	Pressure (psi)
2	107	7.97	18.19
3	108	7.97	17.75
4	97	7.97	22.52
5	96	7.97	22.94
6	109	7.97	17.31
7	112	7.97	16
8	112	7.97	16.01
9	111	7.97	16.44
10	99	7.97	21.6
11	99	7.97	21.6
12	96	7.97	22.9
13	95	7.97	23.34
14	109	7.97	17.3
15	106	7.97	18.6
16	92	7.97	24.64
17	80	7.97	29.87
18	103	7.97	19.91
19	101	7.97	20.77
20	95	7.97	23.38
21	86	7.97	27.28
22	108	7.97	17.74
23	97	7.97	22.51
24	83	7.97	28.58
25	118	7.97	13.43
26	119	7.97	12.99
27	119	7.97	12.99
28	115	7.97	14.73
29	125	7.97	10.39
Resvr 1	149	#N/A	0

Table 5 Pipe Links of Simulated Diameters and Velocities

Link ID	Length (ft)	Diameter (in)	Velocity (fps)	Unit Headloss (ft/Kft)
Pipe 1	804	12	0.26	0.04
Pipe 2	333	12	0.17	0.02
Pipe 3	819	12	0.04	0
Pipe 4	275	4	0.19	0.07
Pipe 5	793	4	0.01	0
Pipe 6	432	8	0.24	0.05
Pipe 7	331	8	0.19	0.03
Pipe 8	184	4	0.1	0.02
Pipe 9	675	4	0.25	0.11
Pipe 10	198	4	0.04	0
Pipe 11	502	4	0.07	0.01
Pipe 12	222	4	0.13	0.04
Pipe 13	225	8	0.1	0.01
Pipe 14	735	4	0.23	0.1
Pipe 15	185	4	0.17	0.06
Pipe 16	240	8	0.01	0
Pipe 17	1323	4	0.17	0.06
Pipe 18	131	8	0.1	0.01
Pipe 19	1326	4	0.16	0.05
Pipe 20	207	8	0.19	0.03
Pipe 21	938	12	0.05	0
Pipe 22	799	4	0.21	0.09
Pipe 23	207	12	0.15	0.01
Pipe 24	220	12	0.21	0.02
Pipe 25	284	12	0.19	0.02
Pipe 26	467	12	0.24	0.03
Pipe 27	745	8	0.08	0.01
Pipe 28	1014	8	0.14	0.02
Pipe 29	477	8	0.1	0.01
Pipe 30	377	4	0.01	0
Pipe 31	458	8	0.05	0
Pipe 32	922	12	0.26	0.04
Pipe 33	823	12	0.11	0.01
Pipe 34	954	12	0.09	0
Pipe 35	188	12	0.04	0
Pipe 36	751	8	0.05	0
Pipe 37	686	8	0.05	0
Pipe 38	170	4	0.01	0

The summary results of pipe links and junctions for study area by using EPANET are as following Table 6 and 7.

Table 6 Summary Result of Pipe Links

Item	Size of Pipe	Total (feet)
1	12 inches diameter	6959
2	8 inches diameter	5697
3	4 inches diameter	7594
Total Length (ft)		20250

Table 7 Summary Result of Junctions

No	System	Maximum Pressure (psi)	Minimum Pressure (psi)
1	Continuous System	29.87	10.34

Junction and links ID of pipe network for study area are shown in Fig 2 and 3.

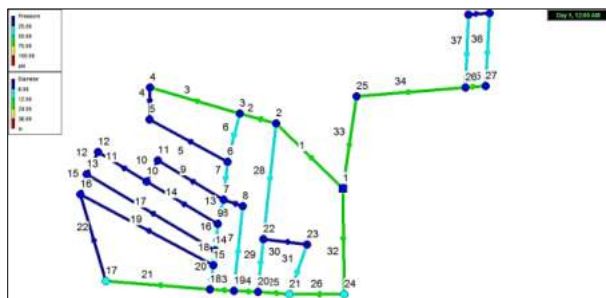


Fig.2 Junction Pressure and Pipe Links Diameter Plan for Study Area

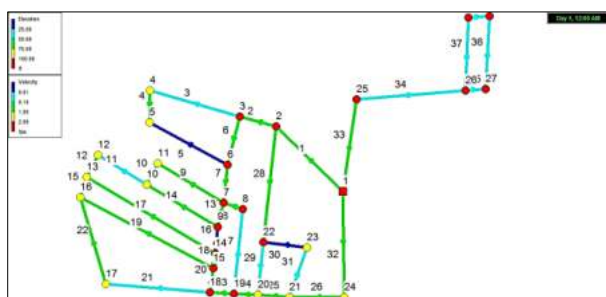


Fig.3 Junction Elevation and Pipe Links Velocity Plan for Study Area

5. CONCLUSIONS

The source of water supply for the Painhnaegone village is the ground water, it is sufficient to meet the future demand for more than the next ten years. It is a dependable water source which can supply sufficiently to the study area. Since the village is located in a foot hills area, with respect to topography of the study area, gravity

system is used in the distribution network to provide the required demand and pressure at all nodes.

Water pressure range is considered between 20 psi and 45 psi in this study, in order to provide for adequate operation. Water is supplied by intermittent system to meet the optimal design for operation and maintenance. The intermittent system is more suitable for the Myanmar rural areas rather than the continuous system. The total length of distribution pipe lines is 6397.45 feet with sizes from 4 inches to 12 inches are used in this new distribution system. Moreover, water from this resource is usually satisfactory with the water quality. Although it is likely to need to do more tests, only disinfection is enough for the treatment process.

ACKNOWLEDGEMENT

The author would like to acknowledge Dr. Tin San, Pro Rector of Technological University (Lashio), for his kind permission to carry out this research work. The author would like to express U Ba Nyar Oo, Assistant Lecturer, Department of Civil Engineering, TU (Thanlyin) thanks to all preparation period of this paper.

REFERENCES

[1] Saminu, A., Abubakar, Nasiru and Sagir, L. (2013), "Design of NDA Water Distribution Network Using EPANET" International Journal of Emerging Science and Engineering, Vol. 1, Issue 9, pp. 1-2.

[2] Arjun Kumar, Kankesh Kumar, BharanidharanB, "Design of Water Distribution System using EPANET", International Journal of Advanced Research (2015), Volume 3, Issue 9, Sep 2015, pp. 789 – 801

[3] US Environmental Protection Agency. (2008), Distribution System Research, <http://www.epa.gov/NRMRL/wswrd/dw/dsr.Tml>

[4] Rossman, LA. (2000), EPANET 2 User's Manual, <http://www.epa.gov/nrmrl/wswrd/dw/epanet/EN2manual.PDF>

[5] IS:1172 (1993), Code of Basic Requirements for Water Supply, Drainage and Sanitation, pp.2.

[6] Richard Ainsworth (2004), Safe Piped Water: Managing Microbial Water Quality in Piped Distribution Systems, pp.39-40.

[7] Adeniran, AE. andOye-lowo, MA. (2013), "An EPANET Analysis of Water Distribution Network of the University of Lagos, Nigeria", Journal of Engineering Research, 18(2), pp.69-84

EXPERIMENTAL STUDY ON PRODUCTION OF BAMBOO FIBRE REINFORCED CEMENT CEILING SHEET

Ei Mon Phyu⁽¹⁾, Win Mar Htet⁽²⁾

⁽¹⁾Pyay Technological University, Myanmar

⁽²⁾Pyay Technological University, Myanmar

Email: eimonphu82@gmail.com

ABSTRACT: The ceiling sheet can be adapted particularly for hot climates due to its high insulation properties and therefore suitable to provide shelter for livestock by using the locally available natural fibre materials for its production. In this study, natural fibre namely bamboo fibre as reinforcement in cement and three different percentages of fly ash as cement replacement material are used for producing ceiling sheets. The ceiling sheet samples (300mm x 300mm x 5mm) were manufactured by using three different contents of fly ash (20%, 30%, 40%), water cement ratios of 0.4 and 0.5, 0.8% of waste paper and 8% of bamboo fibre respectively. For all samples, bending strength was carried out for ages of 7 days and 28 days. From the test results, it has been observed that the ceiling sheet at 30% fly ash with water cement ratio 0.4 gives highest bending strength and the lowest bending strength is at 40% fly ash with water cement ratio 0.5. It can be studied that the optimum percentage of fly ash is 30% for replacement of cement and the bamboo fibre reinforced cement ceiling sheet at 30% fly ash with water cement ratio 0.4 is suitable for local use.

KEYWORDS: *bamboo fibre, fly ash, bamboo fibre reinforced cement ceiling sheet, bending strength.*

1. INTRODUCTION

Myanmar is a developing and tropical country. Therefore, most of the people in rural area will affect the thermal effect in hot season. Science and technology make rapid advances and unforeseen changes about construction in short period of time. The techniques to produce low cost ceiling sheet are needed for rural areas in our country. Among the many part of a house, ceiling sheets are essential part of a house in the two major climatic regions (warm humid and hot dry climates) in order to insulate thermal effect. So, good quality and low cost ceiling sheets should be manufactured by using locally available materials. Natural fibres carry a major portion of the tensile stress in the composite materials. Plant fibres have a high strength and good insulation properties (sound, electrical, and thermal). Bamboo fibres can be got easily in our country and its strength is enough to utilize in making ceiling sheets. To be lightweight ceiling sheet, fly ash can be used in some percentage of cement mix. Pozzolans may often be cheaper than the cement and it can be used as a cement

replacement material. So, manufacturing cost can be reduced by using fly ash (artificial pozzolan) as a cement replacement material. Since fly ash is waste material from the coal industries, it makes advantages on environment.

2. METHODOLOGY

Bamboo fibre reinforced cement ceiling sheet had been produced by using materials of cement, class C fly ash, Bamboo fibre, waste paper and water. In this study, the mixing of materials is done by weighting. Three ratios of fly ash contents of 20%, 30%, 40% were used as a cement replacement material. The percentage of fibre and waste paper were 8% and 0.8%. Two water-cement ratios of 0.4 and 0.5 were used. The size of specimen is 300 mm x 300mm x 5 mm. Physical properties (Fineness, Soundness, Consistency, Setting time and specific gravity) of cement and fly ash were tested according to ASTM standard. Bending stress of ceiling sheet sample was carried out to find the stress in a material just before it yields in a flexure test.

3. MATERIALS USED

3.1 Cement

Ordinary Portland cement (Type I) was used in the present experimental study. Double-Rhinoceros Cement brand was used. Standard consistency is 30.1% according to ASTM C187 [9]. The value of its specific gravity was 2.9. The initial and final setting times were found as 79.5 minutes and 165 minutes respectively which were within ASTM Standard limits. Soundness of this cement is good because its increase expansion of this result test is 3 mm.

3.2. Fly Ash

Fly ash, also known as pulverized fuel ash in the United Kingdom, is a coal combustion product. It is composed of the particulates that are driven out of coal-fired boilers together with the flue gases. In this study Class C fly ash is used as cement replacement material. According to ASTM 618, this fly ash is suitable as a replacement material of cement. Test results of Class-C fly ash are described in Table 1.

3.3 Bamboo fibres

Bamboo fibres are all cellulose fibres extracted from natural bamboo. As natural cellulose fibre, it can be 100% biodegradable in soil by micro-organism and

sunlight. Its decomposition process doesn't cause any pollution to environment. Bamboo used for fibre preparation is usually 3-4 years old. The bamboo fibre used in this study is shown in figure 1. The value of water absorption for bamboo fibre is 46%. According to ACI, this value must be between 40 and 50. So, the fibre is suitable to use.

Table 1. Test Results of Class-C Fly Ash

Physical Properties	Test Results	Standard ASTM limits
Fineness	21.68%	<34
Standard Consistency	29.25%	26 to 33
Initial Setting Time (hr:min)	1:35	>45 min
Final Setting Time (hr:min)	4:15	>10 hr
Specific Gravity	2.26	2.1 to 3.0



Fig 1 Bamboo fibre

3.4 Waste paper

This world also had facing the high amount of waste product which including waste paper. Waste materials can be reused directly or recycled to produce the same or other products. This has benefits of not only reducing the amount of waste material requiring disposal, but also can produce usable production materials with significant saving over the old ones. The waste paper can be reused or used as recycled paper in the construction field. Paper has been considered one of the most highly insulated material and has regular pores and fibrous nature. So, the paper pulp holds the moisture in these pores. Fibrous nature gives very high energy absorbing ability and the high compressive strength. In this manufacturing process, paper bag of cement which is discarded after using cement is used as waste paper. The average water absorption of waste paper is 157%. Waste paper is shown in figure 2.



Fig 2 Waste paper

4. MANUFACTURING PROCESS OF BAMBOO FIBRE REINFORCED CEMENT CEILING SHEET SPECIMEN

First of all, formwork (300 mm x 300 mm) which is shown in figure 3 was prepared for ceiling sheet fabrication. For quick and easy removal of ceiling sheets, formworks were painted by red oxide and engine oil.

In the production of ceiling sheet, it is necessary to make bamboo fibre before mixing. The bamboo is collected from local sources and then it is properly cleaned and cut into appropriate size of one inch. The fibre should be clean and free from silt and dust.

In this study, the mixing of materials is done by weighting. The mixing ingredients are cement, class C fly ash, Bamboo fibre, waste paper and water. When dry mix is completed, the right amount of water is added into the mix on the impervious plate form. Water-cement ratio of 0.4 and 0.5 is used to produce ceiling sheet. The freshly mixed fibre reinforced cement mortar paste is poured into formwork. The mortar paste is rammed manually by using wooden rod for good compaction. After about 24hr, the ceiling sheets can be removed from the formwork. Finally, these ceiling sheets are emerged into the water tank for curing. Ceiling sheet samples is shown in figure 4. After curing, ceiling sheets reinforced with bamboo fiber were tested by bending tester machine and the ceiling sheets gained acceptable strength are ready to use.



Fig 3 Formwork

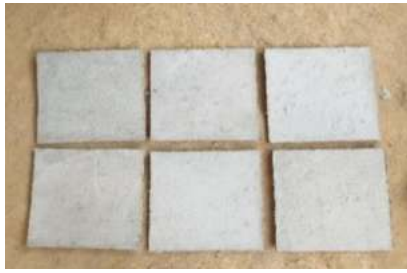


Fig 4 Ceiling Sheet Samples

5. BENDING STRENGTH TEST AND RESULTS

5.1 Bending Strength Test

The purpose of this research is to study the bending strength of bamboo fibre reinforced cement ceiling sheet with different fly ash. Bending strength is a material property. It is defined as the stress in a material just before it yields in a flexure test. The bending strength of ceiling sheet is calculated by the following equation. Bending strength test machine is shown in figure 5.

$$f = \frac{3PL}{2be^2} \tag{1}$$

Where, f = Bending strength, psi

P = Breaking load, kg

L = Clear span between the supports, mm

b = Width of test specimen, mm

e = Actual average thickness of test specimen, mm



Fig 5 Bending strength test machine

5.2. Results

The size of ceiling sheet sample is 300 mm x 300 mm x 5mm. The bending strength of ceiling sheet is carried out for 7 day and 28 day under testing machine. By studying the test results, it can be found that bending strength decreases as water cement ratio increases for each percentage of fly ash at ages of 7 days and 28 days. From the test results of 28 day, the specimen of 30 % fly

ash with water cement ratio 0.4 gives largest bending strength of 886.3 psi in all ratios of fly ash and that of 40% fly ash with water cement ratio 0.5 produces smallest bending strength of 777.7 psi. Bending strength test results for 7 day and 28 day are shown in Table 2, 3, 4 and 5. Average bending strengths of ceiling sheet samples for different content of fly ash after 7 and 28 days curing are also described in figure 6 and 7 respectively.

Table 2. Test Results of Bending Strength of Sample for Water Cement Ratio 0.4 (7 day)

w/c	Fly ash (%)	Sample No	Bending Strength (psi)
0.40	20%	1	556.2
		2	560.8
		3	548.3
	Average		555.1
	30%	1	660.8
		2	652.6
		3	655.2
	Average		656.2
	40%	1	515.4
		2	528.6
3		523.7	
Average		522.6	

Table 3. Test Results of Bending Strength of Sample for Water Cement Ratio 0.5 (7 day)

w/c	Fly ash (%)	Sample No	Bending Strength (psi)
0.50	20%	1	518.46
		2	511.2
		3	516.8
	Average		515.5
	30%	1	572.9
		2	575.6
		3	580.3
	Average		576.3
	40%	1	463.1
		2	469.9
3		476.8	
Average		469.9	

Table 4. Test Results of Bending Strength of Sample for Water Cement Ratio 0.4 (28 day)

w/c	Fly ash (%)	Sample No	Bending Strength (psi)	
0.40	20%	1	840.9	
		2	846.9	
		3	848.5	
	Average			845.4
	30%	1	886.9	
		2	885.2	
		3	886.9	
	Average			886.3
	40%	1	810.9	
		2	808.6	
		3	809.6	
	Average			809.7

Table 5. Test Results of Bending Strength of Sample for Water Cement Ratio 0.5 (28 day)

w/c	Fly ash (%)	Sample No	Bending Strength (psi)	
0.50	20%	1	833.6	
		2	830.2	
		3	829.9	
	Average			831.2
	30%	1	866.8	
		2	867.2	
		3	868.9	
	Average			867.6
	40%	1	778.4	
		2	774.9	
		3	779.8	
	Average			777.7

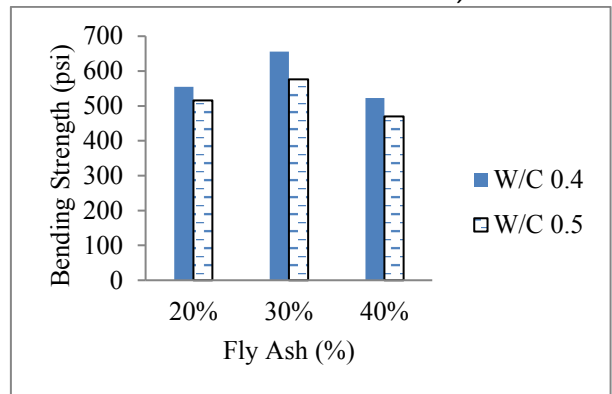


Fig 6 Average bending strengths of ceiling sheet samples for different content of fly ash after 7 days

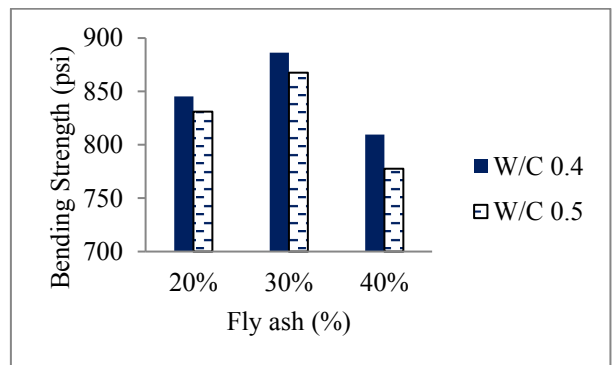


Fig 7 Average bending strengths of ceiling sheet samples for different content of fly ash after 28 days

6. CONCLUSIONS

The bamboo fibre is available significant quantities as a natural fibre and also fly ash is easily available and economical among so many kinds of cementitious materials in Myanmar. That is why it should be considered to use bamboo fibre and fly ash for reinforcement and replacement of cement in producing ceiling sheet. Moreover, according to experimental result of 28 days curing, the highest bending strength of bamboo fibre reinforced cement ceiling sheet is at water cement ratio 0.4 and 30 % replacement of fly ash with the value of 886.3 psi and the lowest bending strength is at water cement ratio 0.5 and 40% replacement of fly ash with the value of 777.7 psi. It can be concluded that the optimum percentage of fly ash is 30% for replacement of cement and so the bamboo fibre reinforced cement ceiling sheet has enough strength for local use.

ACKNOWLEDGEMENT

First and foremost, the author thanks to Professor Dr. Nyunt Soe, Rector of Pyay Technological University, for his invaluable permission. The author would like to express heart-felt gratitude to Dr. Mya San Wai, Professor and Head of Civil Engineering Department of PTU, for her encouragement and enthusiastic instruction. Special Thank to Dr. Yin Min Han, Professor and Head of Civil Engineering Department of Technological

University (Toungoo) for her support, guidance and suggestions. The author would like to express her gratefulness to Daw Win Mar Htet, Lecturer, Civil Engineering Department of Pyay Technological University, for her sharing ideas and knowledge.

REFERENCES

- [1] Ataguba, Clement Oguche, "Properties of Ceiling Board produced from A composite of Waste Paper and Rice Husk", International Journal of Advances in Science Engineering and Technology, (Feb 2016)
- [2] Ma War War Aung, "Study on Natural Fibre Reinforced Roofing Sheet Using Locally Available Materials", 2009
- [3] Khairul Nizar Ismail, Kamarudin Hussin, Mohod Sobri Idris, "Physical, Chemical and Mineralogical Properties of Fly Ash", Journal of Nuclear and Related Technology Vol-4, (2007)
- [4] Meyers-Levy, Joan, Zhu, Rui (Juliet), "The Influence of Ceiling Height: The Effect of Priming on the Type of Processing That People Use", Journal of Consumer Research, (August 2007)
- [5] Naw Myat Su Mon Htun, "A Study on the Application of Fly Ash as a Cement Replacement Material with Super Plactizer for High Strength Concrete", May 2005
- [6] James I. Daniel Chairman, Vellore S. Gopalaratnam Secretary, Melvyn A. Galinat Membership Secretary, "Report on Fibre Reinforced Concrete", ACI 544.1R-96, 2002
- [7] [90 Fai] Faisal Fouad Wafa, " Properties and Application of Fibre Reinforced Concrete", January 1990. King, B. Zhu, and S. Tang, "Optimal path planning," *Mobile Robots*, vol. 8, no. 2, pp. 520-531, March 2001.
- [8] H. Simpson, *Dumb Robots*, 3rd ed., Springfield: UOS Press, 2004, pp.6-9.
- [9] American Standard Test Method for Normal Consistency of Hydraulic ASTM C187-98
- [10] American Standard Test Method for Time of Setting of Hydraulic Cement by Vicat Needle ASTM C191-04

Structural Behaviors Comparisons of RC Buildings with Two Different Flat Slab Types

Khine Zar Aung^{#1}, Aung Min Tun^{#2}

[#] Department of Civil Engineering, West Yangon Technological University
Yangon, Republic of the Union of Myanmar

¹khinezar229@gmail.com

²aungaungtamuvillager@gmail.com

ABSTRACT: There are many different systems constructing reinforced concrete structure. Among them, the flat slab system is the most popular in reinforcement concrete structure for reduction the height of building. Therefore, it is necessary to know the structural behaviours of it. There are two types of flat slab systems: one without drop panels and one with drop panels. The objective of this journal is to compare between the analysis results of the two buildings with above two systems. This study deals with structural behaviours of six-storeyed reinforced concrete building which is 45 feet wide, 60 feet long and 76 feet high. The proposed buildings are situated in seismic zone 2B. Structural Engineering Software (ETABS 2016, Version 16.2.0) is used for analysis and design of the buildings. The behaviours of the buildings have been investigated using static analysis. According to MNBC 2016, all gravity loads and lateral loads have to be applied. Soil profile type is considered as (SD) stiff soil profile. Wind force is exposure type B and basic wind velocity is 100 mph. Finally, the results obtained are compared to investigate the effects on structural behaviours of the building when there is a difference in the type of flat slab used for the building.

KEYWORDS: flat slab systems, structural behaviors.

1. INTRODUCTION

Nowadays, the high-rise reinforced concrete buildings are widely used in Myanmar according to political, social and economic demands and the potential of its popularity will be greater in future. However, there are encounter the height restriction laws in the location of the proposed building. In this situation, flat slab structures become a solution to the problem between the height restriction law and the demand building height.

The use of flat slab provides many advantages over conventional slab. The benefits of using flat slab construction are becoming increasingly recognized. Flat slabs without drops (thickened areas of slab around the columns to resist punching shear) can be built faster because formwork is simplified and minimized. Flat slab construction places no restrictions on the positioning of horizontal services and partitions, and can minimize floor-to-floor heights when there is no requirement for a deep false ceiling. This can have knock-on benefits in terms of lower building height, reduced cladding costs and prefabricated service. Flat slab construction offers considerable flexibility to the occupier who can easily

alter internal layouts to accommodate changes in the use of the structure. Lower storey height will reduce building weight due to lower partitions and cladding to facade.

2. MODELLING OF REINFORCED CONCRETE STRUCTURE WITH AND WITHOUT DROP PANELS

The preparations for analysis and design requirements and presentations of the analysis and design results of the proposed buildings are considered. The proposed reinforced concrete structure is 60 feet in length, 45 feet in width and 76 feet in height.

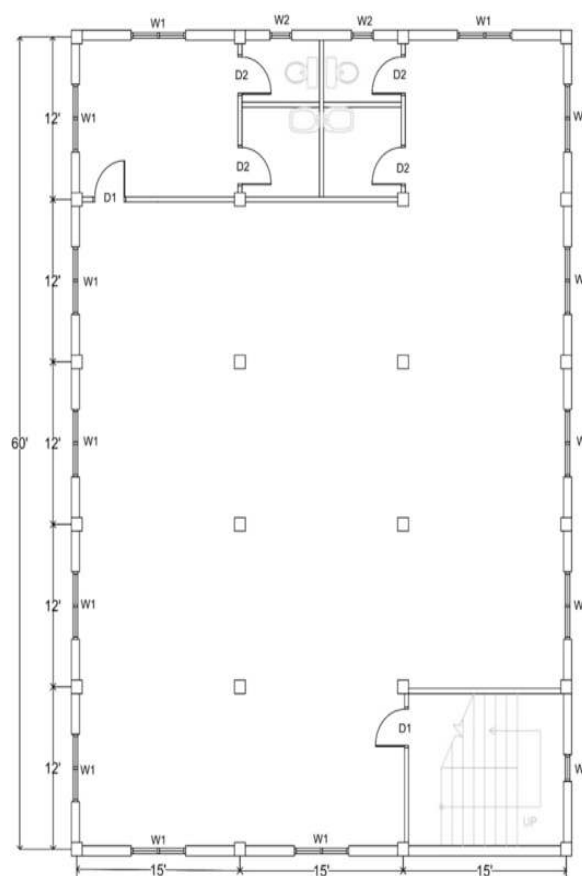


Fig 1. Typical Floor Plan of Proposed Buildings

The site location and structural system are chosen before modeling for the design of proposed buildings. Then, there are considered material properties of the structures, determination of load combinations, and selection of codes according to MNBC 2016 and ACI 318-14 for the analysis and design of proposed buildings. ETABS 2016 (Version 16.2.0) is used to analysis and

design the structures in this study. In the analysis and design of structures, the purpose of analysis is to determine the stress and displacements in the various member of a structure. Structural stability check is made whether it is satisfactory or not. Then, the reinforcements of structural members are calculated.

2.1 Material properties

- Analysis property data,
- Weight per unit volume of concrete : 150 pcf
- Modulus of elasticity : 4.0305×10^6 psi
- Poisson’s ratio : 0.2
- Coefficient of thermal expansion : 5.5×10^{-6} in/in per °F
- Reinforcing yield strength (f_y) : 60000 psi
- Concrete cylinder strength (f_c) : 5000 psi
- Shear reinforcing yield strength (f_{ys}) : 60000 psi

2.2 Loading Data for gravity load

- Data for gravity load which are used in structural analysis are as follows:
- Superimposed dead load = 20 psf
(Ceiling is considered as superimposed dead loads)
- Design data for live loads which are used in the analysis are as follows.
- Live load on stair = 100 psf
- Live load on roof = 20 psf
- Live load all other areas = 40 psf

2.3 Data for wind load

- Data for wind load which are used in structural analysis are as follow:
- Site Location - Yangon
- Exposure type - B
- Effective height for wind load - 76 feet
- Method - Analytical Procedure
- Basic wind Speed - 100 mph
- Gust factor - 0.85
- Directionality factor - 0.85
- Topographical factor - 1.0
- Wind important factor - 1.0

2.4 Data for earthquake load

- Data for earthquake load which are used in structural analysis are as follow:
- Seismic zone = 2B (Yangon)
- 0.2 sec spectral acceleration = 0.77
- 1 sec spectral acceleration = 0.31
- Soil profile type = SD
- Design moment frame type = IMRF
- Response modification factor (R) = 5

- System over-strength factor (Ω) = 3
- Deflection amplification factor (C_d) = 4.5
- Long-period transition (TL) = 6 sec
- Seismic importance factor (I) = 1.00

Approximate period parameters for concrete moment resisting frames are:

$C_t = 0.016$
 $\alpha = 0.9$

2.5 Load Combinations

Design codes applied are ACI 318-14 and MNBC-2016. There are 23 numbers of load combinations in MNBC-2016.

3. DESIGN CONSIDERATIONS

In this study, the structural members are analyzed and design according to ACI 318-14. The design sections of structural member are C24x24, C22x22 and C20x20 in columns and B 14x18 is used as perimeter beam. Both building have the same layout plans of beams and columns, but with different reinforcement, especially in beams. In slab thickness, 10 inches is used as flat slab in RC building without drop panel and 8 inches is used the one with drop panel. The size of drop panel is 5 feet.x 4 inches.

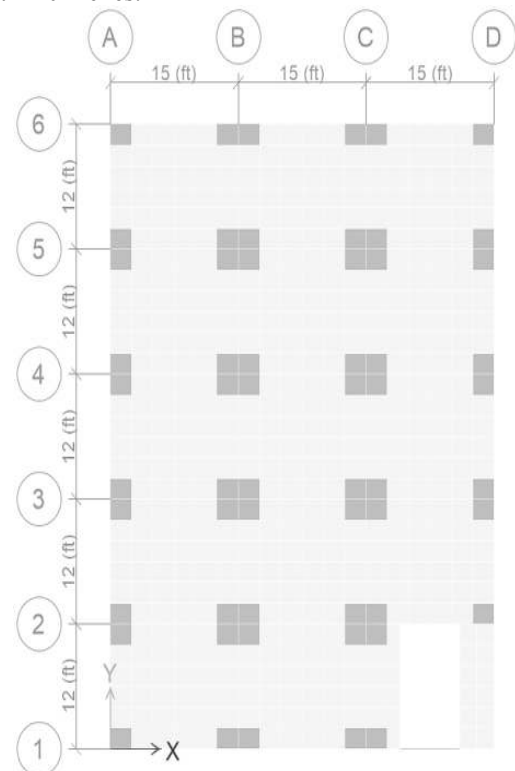


Fig 2. Layout Plan of Drop Panels

After the sizes of members are satisfied under MNBC-2016 load combinations, the buildings with and without drop panels are also checked in stability such as base shear, overturning moment, sliding, drift ratio, P-Del effect, torsional irregularity and soft storey effects.

Punching shear check is required in flat slab in both systems.

Table1. Slab Schedule for Building With Drop Panels

Storey	Thickness		Layer	Reinforcement		Distribution
	Slab	Drop Panel		Shorter	Longer	
RF and SR	8 in	10 in	Top	14mm@12 in c/c	14mm@12 in c/c	-
			Bottom	14mm@12 in c/c	14mm@12 in c/c	-
1F to 5F	8 in	10 in	Top	14mm @ 8 in c/c	14mm@ 8 in c/c	-
			Bottom	14mm @ 8 in c/c	14mm@ 8 in c/c	-
Stair	6 in		Top	-	12mm@6 in c/c	10mm @10in c/c
			Bottom	-	12mm@6 in c/c	10mm @10in c/c

Table 2.Slab Schedule for Building Without Drop panel

Storey	Thick ness	Layer	Reinforcement		Distribution
			Shorter	Longer	
RF and SR	10 in	Top	14mm@ 10 in c/c	14mm@ 10in c/c	-
		Bottom	14mm@ 10in c/c	14mm@ 10in c/c	-
1F to 5F	10 in	Top	14mm @ 8 in c/c	14mm @ 8 in c/c	-
		Bottom	14mm@ 8 in c/c	14mm@ 8 in c/c	-
Stair	6 in	Top	-	12mm @6 in c/c	10mm @10in c/c
		Bottom	-	12mm @6 in c/c	10mm @10in c/c

4. ANALYSIS RESULTS AND DISCUSSIONS

The gravity loading due to dead load and live load and lateral loading due to wind or earthquake are the major factors that cause different displacements and forces in reinforced concrete structure with and without drop panels. There are seven critical behaviours on this structure. In this section, comparisons between two buildings based on storey drifts, P-Δ, torsional irregularity, overturning, sliding, punching shear and soft storey are presented.

4.1 Comparison on Storey Drift

According to the fig. 3 and fig.4 for the two buildings, the drifts of the building without drop panels are larger in both directions than the building with drop panels. The drift of the former is 15% greater than that of the latter at stair roof in X-direction .

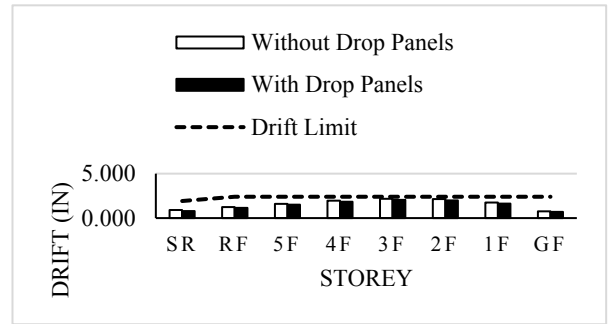


Fig 3. Comparison on Storey Drift in X-direction

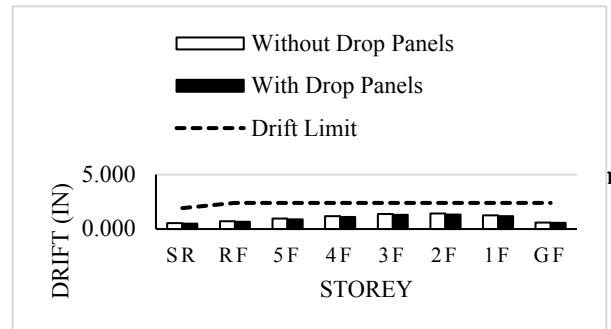


Fig 4. Comparison on Storey Drift in Y-direction

4.2 Comparison on P-Δ Effect

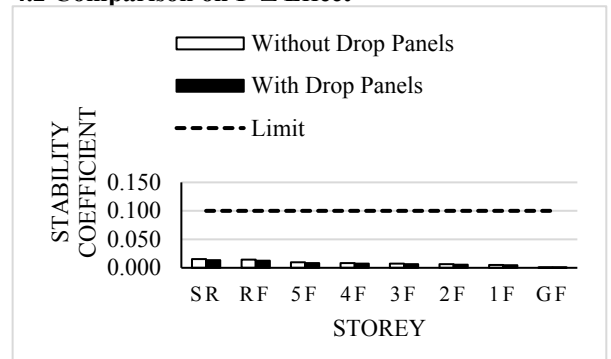


Fig 5. Comparison of P-Δ in X-direction

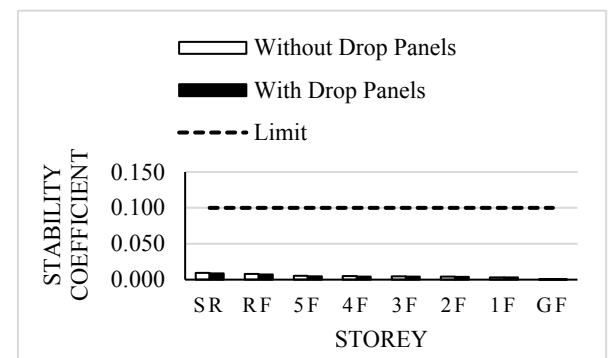


Fig 6. Comparison of P-Δ in Y-direction

According to the fig. 5 and fig. 6 for the two buildings, the stability coefficient values of the building without drop panels are larger in both directions than the building with drop panels since the former has higher secondary moment (larger weight and higher drift) than the latter. The coefficient value of the former is 17% greater than that of the latter at roof in X-direction.

4.3 Comparison on Torsional Irregularity

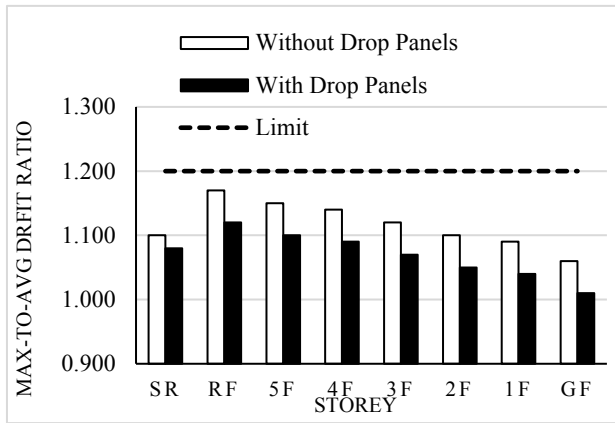


Fig 7. Comparison of Torsional Irregularity in X-direction

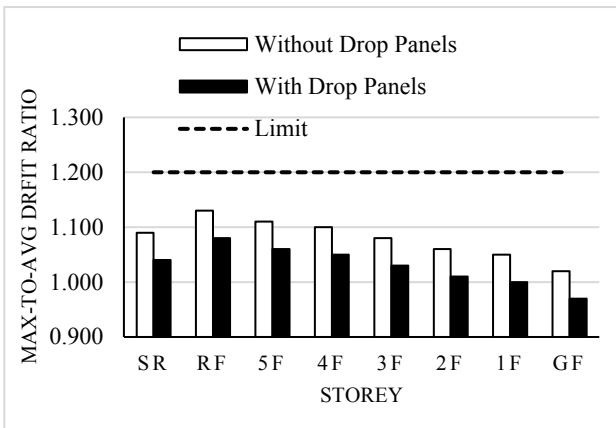


Fig 8. Comparison of Torsional Irregularity in Y-direction

As for the two buildings, the building with drop panels is reasonably stronger in resistance to torsional irregularity for both directions than the building without drop panels, relating with variation in cross-section and weight of slab according to fig. 7 and 8.

4.4 Comparison on Overturning and Sliding

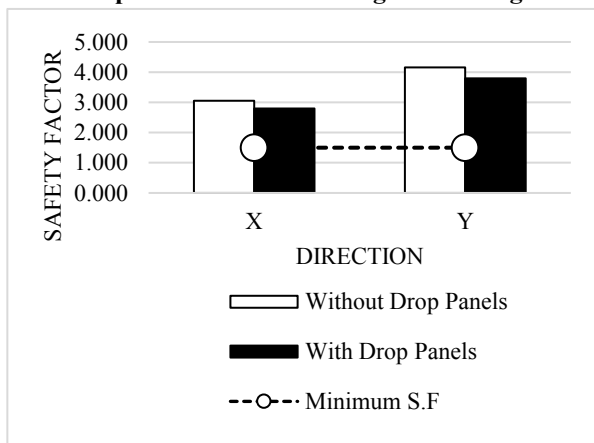


Fig. 9. Comparison on Overturning

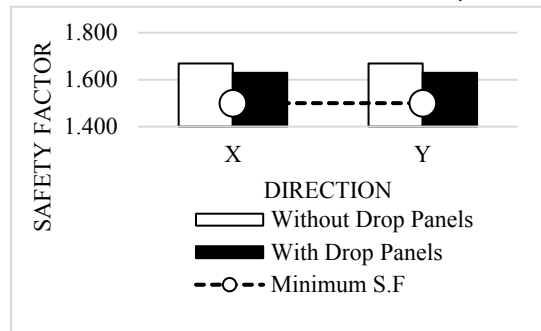


Fig 10. Comparison on Sliding

In Fig. 9 and 10, the building without drop panels has slightly higher resistance to overturning and sliding in both directions than the building with drop panels. This is because the former has larger weight due to uniformly thicker slabs throughout the spans than the latter, slabs of which only have large thickness in the areas of drop panels, comprising at the difference in slab weight of 324 kips. The overturning and sliding S.F values of the former are 9% and 2% respectively greater than that of the latter as overall building in X-direction.

4.4 Comparison on Punching Shear

According to fig. 11 the building without drop panels have smaller resistance to punching shear failure than the buildings with drop panels since drop panels provide additional shear strength around the column. The punching shear ratio of the former is 27% greater than that of the latter at stair roof.

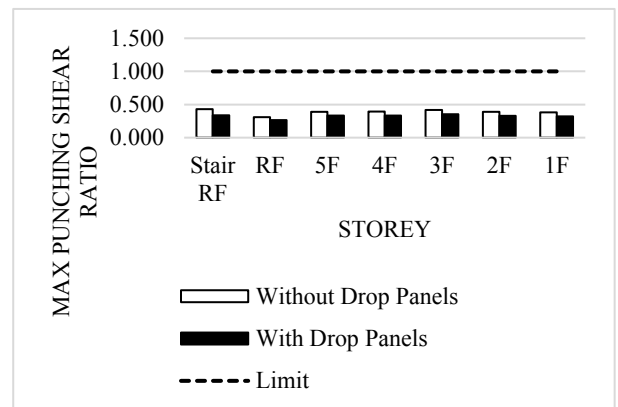


Fig 11. Comparison on Punching Shear

4.5 Comparison on Soft Storey

Figure 4.12 and figure 4.13 illustrate that both buildings have no soft storey effects.

As for the directions, both buildings have higher storey stiffness in Y-direction than in X-direction. As for the two buildings, the building without drop panels has moderately weaker storey stiffness than the building with drop panels. In 70% storey stiffness limitation, the stiffness value of the former is 4% smaller than that of the latter at fifth floor in X-direction.

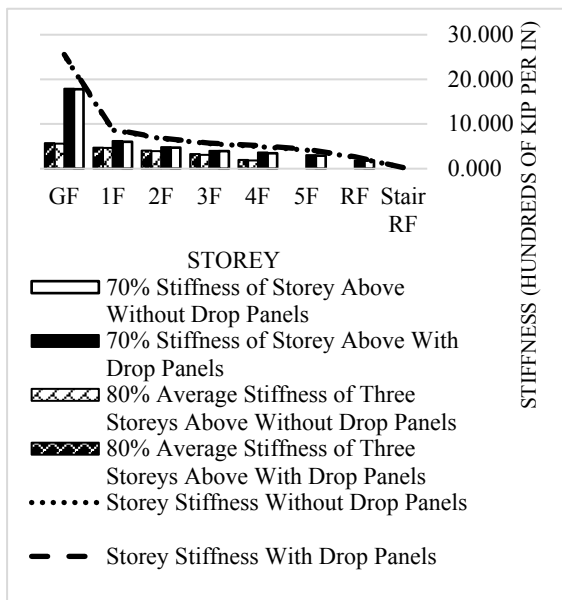


Fig 12. Comparison on Soft Storey in X Direction

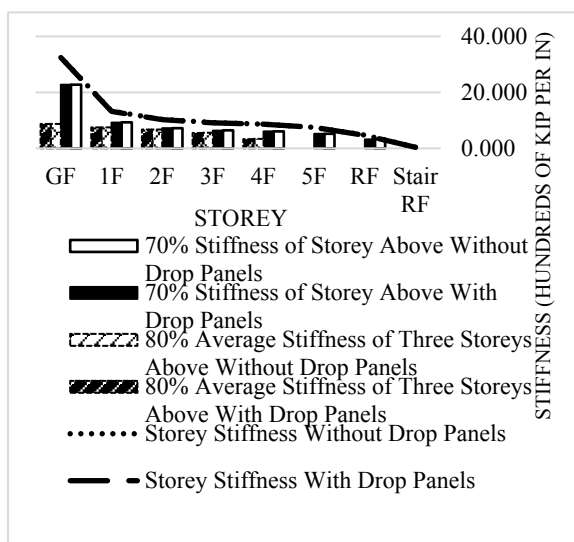


Fig 13. Comparison on Soft Storey in Y Direction

5. CONCLUSION

From the above study, it can be concluded as the following.

(1) The drift ratio in third floor is the maximum in both X direction and Y direction. The drifts without drop panels are larger in both directions than that with drop panels. Therefore, the structural behavior of the building with drop panel is stiffer than that of without drop panel according to drift.

(2) According to the stability coefficient values of the building, the higher the building, the more increase the stability coefficient in both with and without drop panels. The stability coefficients without drop panel are larger in both directions than that of the building with drop panels, apparently being 17% greater at roof in X-direction.

(3) The Torsional irregularity does not occur in both systems and this value is the maximum in roof reasonably. According to the building geometry, maximum-to-average drift ratios in X direction is smaller

than that in Y direction. The building without drop panels is reasonably stronger in resistance to torsional irregularity for both directions than the building with drop panels, with the slightly smaller maximum-to-average drift ratios, obviously being 9% smaller at roof in X-direction.

(4) In the case of overturning moment, that in X direction is smaller than that in Y direction because of the geometry. The building without drop panels have slightly higher resistance to overturning in both directions than the building with drop panels, with the slightly larger S.F values, obviously being 9% greater for overturning in X-direction. The case of sliding is the same manner of overturning moment.

(5) The buildings with both systems do not occur soft storey effect in 70% stiffness case and 80% stiffness case. The stiffness of building without drop panels is nearly equal to that with drop panels in both directions.

ACKNOWLEDGEMENTS

The authors are extremely grateful to the teachers from Department of Civil Engineering in West Yangon Technological University, for their guidance, advice and encourages for completing this paper.

REFERENCES

- [1] ACI Committee 318. 2014. *318-14: Building Code Requirement for Structural Concrete and Commentary*. U.S.A: American Concrete Institute.
- [2] Bijan O Aalami. 2008. *Deflection of Concrete Floor Systems for Serviceability*. India: ADAPT International Pvt. Ltd.
- [3] Harshal Deshpande, Radhika Joshi, Prashant Bangar. 2014. "Design Considerations for Reinforced Concrete Flat Slab Floor System". *International Journal of Scientific and Engineering Research*, vol.5, no.12 (December)
- [4] International Conference of Building Officials. 1997. "Structural Engineering Design Provisions". *Uniform Building Code*, vol.2, U.S.A.
- [5] Lindeburg and McMullin. 2008: *Seismic Design of Building Structure*. 8th ed. U.S.A: Professional Publication. Inc.
- [6] Myanmar Engineering Council. 2016. "Structural Design". *Myanmar National Building Code 2016*, vol.3, Yangon.